NATIONAL CENTRE FOR SCIENTIFIC RESEARCH "DEMOKRITOS"
INSTITUTE OF NUCLEAR & PARTICLE PHYSICS

Activities Report

2020

Institute Of Nuclear and Particle Physics

National Center for Scientific Research "DEMOKRITOS"

Activities Report

2020

Editors:

Dr. C. Markou, Ms. G. Kareli

January 2021

Institute of Nuclear and Particle Physics,
NCSR "Demokritos"
Aghia Paraskevi, 15310, Athens, Greece

http://www.inp.demokritos.gr

Contents

Institute of Nuclear and Particle Physics

Overview

The Institute of Nuclear and Particle Physics (INPP), at NCSR Demokritos, has as its mission the experimental and theoretical research, scientific excellence and innovation in High-Energy Physics, Nuclear Physics and Astro-Particle Physics as well as their applications in line with the National Research and Innovation Strategy for Smart Specialization.

The experimental and theoretical research in High Energy Physics focuses on the study of elementary particles and their interactions. INPP participates in the CMS and ATLAS experiments of the LHC at CERN. The Detector Instrumentation Laboratory (DIL) and the Data Acquisition, Monitoring and Analysis Laboratory (DAMA) of INPP, develop innovative detector technologies and instrumentation along with applications in science and innovation.

Nuclear Physics research focuses on Nuclear Structure, Nuclear Reactions, Nuclear Astrophysics and the study of interactions of X-rays with matter. The INPP hosts a 5.5. MV Tandem accelerator, a unique research infrastructure in Greece that is open to external users from Greece and abroad. The Tandem accelerator laboratory is an interdisciplinary open-access research infrastructure with innovative applications covering the fields of cultural heritage, environment, energy, human health and the development and testing of advanced materials and detectors. The XRF laboratory focuses on cultural heritage, environmental monitoring and biomedicine and offers technology transfer and on-site analytical services to museums, archaeological sites and other institutions.

The Astro-Particle Physics group participates in the development, deployment, data acquisition and data analysis of the kilometer cube underwater neutrino telescope in the Mediterranean, KM3NeT. The INPP hosts the Laboratory of Assembly, Testing and Calibration of the Digital Optical Modules, the basic units of the KM3NeT telescope. The INPP supports also the Deep-Sea Technology and Astro-Particle Physics Research Infrastructure in South-West Peloponnese (Kalamata, Pylos, Methoni).

Dr. C. Markou, Director INPP
tel. +302106503511
email: cmarkou@inp.demokritos.gr

Ms. G. Kareli, Secretary INPP
tel. +302106503512
email: gkarel@inp.demokritos.gr

Web-site: www.inp.demokritos.gr

Organizational Chart

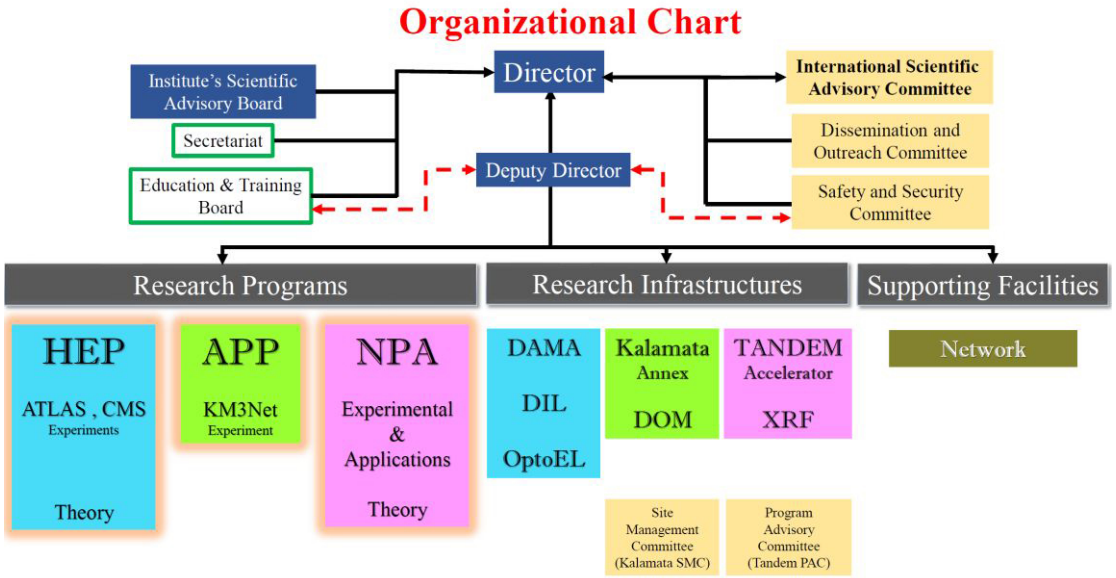

Director:	Dr. C. Markou
Deputy Director:	Dr. M. Axenides
Administration:	G. Kareli, Secretary M. Simantirakis, Administration
Institute Scientific Advisory Board:	T. Geralis (Chair) D. Daskalakis G. Savvidy G. Stavropoulos
International Scientific Advisory Committee:	Prof. C. Bachas Prof. A. Bracco Prof. D. Charlton Prof. Y. Karyotakis Prof. K. Kokkotas Prof. M. Lewitowicz Prof. F. Linde
High Energy Physics	Dr. T. Geralis: HEP-ATLAS & DAMA Dr. D. Loukas: HEP-CMS & DIL Dr. G. Savvidy: HEP-Theory
Nuclear Physics & Applications	Dr. D. Bonatsos: Nuclear Structure Theory Dr. S. Harissopulos: NPA-Experimental Nuclear Physics & Applications – Tandem Dr. A. Karydas: XRF Laboratory & Applications
Astroparticle Physics	Dr. C. Markou: APP-KM3NeT

Personnel

The lists below reflect the INPP personnel as of the 31st of December 2020.

Researchers

Dr. Georgios **ANAGNOSTOU**	Senior Researcher	Exp. High-Energy Physics	anagnog@inp.demokritos.gr
Dr. Minos **AXENIDES**	Director of Research	Theoretical Particle & Astroparticle Physics	axenides@inp.demokritos.gr
Dr. Michail **AXIOTIS**	Researcher	Exp. Nuclear Physics	axiotis@inp.demokritos.gr
Dr. Dionysios **BONATSOS**	Director of Research	Theoretical Nuclear Physics	bonat@inp.demokritos.gr
Dr. Georgios **DASKALAKIS**	Director of Research	Exp. High-Energy Physics	daskalakis@inp.demokritos.gr
Dr. Paraskevi **DEMETRIOU**	Senior Researcher	Theoretical Nuclear Physics	vivian@inp.demokritos.gr
Dr. Theodoros **GERALIS**	Director of Research	Exp. High-Energy Physics	geral@inp.demokritos.gr
Dr. Sotirios **HARISSOPULOS**	Director of Research	Exp. Nuclear Physics	sharisop@inp.demokritos.gr
Dr. Andreas **KARYDAS**	Director of Research	Exp. Nuclear Physics	karydas@inp.demokritos.gr
Dr. Aristotelis **KYRIAKIS**	Director of Research	Exp. High-Energy Physics	kyriakis@inp.demokritos.gr
Dr. Anastasios **LAGOYANNIS**	Director of Research	Exp. Nuclear Physics	lagoya@inp.demokritos.gr
Dr. Dimitrios **LOUKAS**	Director of Research	Exp. High-Energy Physics	loukas@inp.demokritos.gr
Dr. Christos **MARKOU**	Director of Research	Exp. High-Energy & Astroparticle Physics	cmarkou@inp.demokritos.gr
Dr. Konstantinos **PAPADOPOULOS**	Director of Research	Theoretical Particle Physics	cgppdo@inp.demokritos.gr
Dr. George **SAVVIDY**	Director of Research	Theoretical Particle Physics	savvidy@inp.demokritos.gr
Dr. Georgios **STAVROPOULOS**	Director of Research	Exp. High-Energy & Astroparticle Physics	stavrop@inp.demokritos.gr
Dr. Ekaterini **TZAMARIUDAKI**	Director of Research	Astroparticle Physics	katerina@inp.demokritos.gr

Special Scientific Officer

Ioannis **KAZAS**	Exp. High-Energy Physics	kazas@inp.demokritos.gr

Other Scientific Personnel

Stavroula **TSAGLI**	Physicist	tsagli@inp.demokritos.gr

INPP Administration

Emmanuel **SIMANTIRAKIS**	Administrator	msiman@inp.demokritos.gr

INPP Secretariat

Georgia **KARELI**	Secretary	gkarel@inp.demokritos.gr

Technicians

Vassilios **ANDREOPOULOS**	Electronics	andreo@inp.demokritos.gr
Panagiotis **BABOULAS**	Technician	baboulas@inp.demokritos.gr
Ioannis **KISKIRAS**	Electronics	kiskiras@inp.demokritos.gr
Emmanuel **TSOPANAKIS**	Workshop technician	mtsop@inp.demokritos.gr
Aggelos **VOUGIOUKAS**	Craftsman	vougioukas@inp.demokritos.gr

Support Personnel

Sophia **BAKOU**	General support	bakou@inp.demokritos.gr

Personnel under fixed term contracts

Miltiadis **ANDRIANIS**	Physicist	A. Lagoyannis	madrian@inp.demokritos.gr
Giorgos **ANDROULAKIS**	Physicist	C. Markou	androulakis@inp.demokritos.gr
Christos **BAGATELAS**	Physicist	C. Markou	bagatelas@inp.demokritos.gr

Constantinos **GEORGANTAS**	Accountant	A. Lagoyannis	georgadas@inp.demokritos.gr
Vasiliki **KANTARELOU**	Physicist	A. Karydas	kantarelou@inp.demokritos.gr
Spyridon **KONITOPOULOS**	Physicist	G. Savvidy	konitopoulos@inp.demokritos.gr
Zoi **KOTSINA**	Physicist	A. Lagoyannis	zkotsina@inp.demokritos.gr
Spyridon **KOUTSOUKOS**	Physicist	C. Markou	koutsoukos@inp.demokritos.gr
Aggelos **LAOUTARIS**	Physicist	A. Lagoyannis	laoutaris@inp.demokritos.gr
Georgios **LINARDOPOULOS**	Physicist	G. Pastras	Linardopoulos@inp.demokritos.gr
Ioannis **MADESIS**	Physicist	A. Lagoyannis	madesis@inp.demokritos.gr
Manousos-Ioannis **MANOUSAKAS**	Physicist	A. Lagoyannis	@inp.demokritos.gr
Maria Andriani **MARTINOU**	Physicist	C. Markou	martinou@inp.demokritos.gr
Ioannis **MITSOULAS**	Physicist	G. Pastras	mitsoulas@inp.demokritos.gr
Stefanos **NANOS**	Physicist	A. Lagoyannis	nanos@inp.demokritos.gr
Garyfalia **PASPALAKI**	Physicist	C. Markou	paspalaki@inp.demokritos.gr
Georgios **PASTRAS**	Physicist	G. Pastras	pastras@inp.demokritos.gr
Archimedes **PAVLIDIS**	Network Engineer	C. Markou	apavlidis@inp.demokritos.gr
Constantinos **PIKOUNIS**	Physicist	C. Markou	pikounis@inp.demokritos.gr
Constantinos **SAVVIDIS**	Physicist	G. Savvidy	ksavvidis@inp.demokritos.gr
Anna **SINOPOULOU**	Physicist	C. Markou	Sinopoulou@inp.demokritos.gr
Anna **STAKIA**	Physicist	C. Markou	@inp.demokritos.gr
Dimitrios **STAVROPOULOS**	Physicist	C. Markou	dstavropoulos@inp.demokritos.gr
Eleni **VAGENA**	Physicist	A. Lagoyannis	vagena@inp.demokritos.gr
Olga **ZORMPA**	Physicist	C. Markou	zormpa@inp.demokritos.gr

Mobility

Funding Programs in 2020

High Energy Physics

High Energy Experimental Physics - ATLAS

Researchers:	Theodoros Geralis (Team Leader)
	Georgios Fanourakis (Researcher Emeritus)
	Georgios Stavropoulos
PhD students:	Maria Myrto Prapa
	Olga Zormpa
Master students:	Foteini Faidra Trantou
Practical work students:	From Univ. of Patras
	Eleni Androutsou
	Dimitrios Giannakopoulos
	Theodora Remoundou
Technicians:	Ioannis Kiskiras

Introduction

The INPP_ATLAS group is a full member of the ATLAS experiment since October 2017. The group activities are within the ATLAS New Small Wheel (NSW) Muon Upgrade project for Phase I and also on the Muon Software related to parallel threading and the detector alignment. The group starts activities on Physics Analysis in preparation for Run3.

NSW is currently the largest Upgrade project among the LHC experiments and will be part of the Muon end cap ATLAS detectors. The NSW is required to cope with the increased luminosity of the LHC of about ($5x10^{34}cm^{-2}sec^{-1}$) and will withstand high occupancies including the HL-LHC. This also affects the Trigger and data acquisition systems (TDAQ) as the decision to select the events of interest (rejection or acceptance) is made every 25 ns. This is a huge challenge, as the 25 ns decision time is too short for such a complex system with millions of detection channels while also considering that high detector performance must be maintained. The aim of the NSW is to reduce the fake triggers by provide tracking and triggering capabilities to allow pointing of the muons from the outer muon detectors (Big wheels) to the interaction point (IP) with a precision of 1 mrad. The final result will be reduced P_T muon thresholds, higher selection purity and lower rates. Two detector technologies were selected, the Micromegas and the sTGCs (small strips Thin Gap Chambers) that can cope with even higher rates than the ones expected (about $20kHz$) and be radiation resistant in the HL-LHC environment.

Fully completed projects in the previous year (2019) are: 1) The testing of a large number of electronic cards (L1DDC for Micromegas and for sTGC subdetectors) and ADDC for the Micromegas Trigger, 2) The official database handling

for recording the whole history of the electronics components, 3) Porting of the whole Muon software to parallel threading mode.

The sTGC Repeater boards - the largest project of the group - started in 2018 and it was completed in 2020 with the commissioning of all the modules. Integration to the NSW continued after 2020, following the progressive integration of Wheel A and Wheel C. Our group has undertaken responsibility of the full sTGC Trigger Commissioning which is advanced but still in progress.

In the activities subsection we describe the following items on which the ATLAS Demokritos team played leading role during 2020:

1. sTGC Repeaters
2. sTGC Trigger Slice setup
3. sTGC Trigger Commissioning
4. sTGC Detector integration
5. Muon and NSW software activities

Activities

sTGC Repeaters

The sTGC Trigger system operation is based on the proper transmission of the data from the Front End (FE) cards (pFEBs and sFEBs) to the Pad Trigger and subsequently to the Routers (electronics hosted in the Rim crate) and the Trigger Processor. The large distance between the FE cards and the Rim crate and the attenuation over these large distances necessitated the building of repeaters cards to reinstate the signals levels. The serial repeaters (SRL1R) restore signals from the pFEBs to the Pad Trigger (4.8 Gbps) while the LVDS repeaters (LVD6R) restore signals between the Pad Trigger and the sFEBs)640 Mbps). In 2019 the design of the repeaters, the design of their host cages which act also as Faraday cages and their cooling were performed. Detailed studies concerned their performance in data integrity as well as the effectiveness of the cooling. In the case of the LVD6Rs active cooling was necessary using a cooling bar that was integrated in the NSW cooling system. A pre-production of 30 SRL1R repeaters and 5 LVD6R repeaters took place in 2019.

Serial Repeaters - Final Production

In 2020 we have launched the final production of the serial repeaters SRL1Rs. NSW requires 768 SRL1Rs for both Wheels, so the final production was 850 boards. At the same time we have ordered copper boxes, designed to operate simultaneously as Faraday cages and passive cooling. Both orders were taken by Greek companies (Prisma SA for the assembly of the boards and Rentron for the copper cages) 1.

Assembly of the SRL1Rs took place in January 2020 as well as the selection of the boost (12 dB) for optimal operation with different cable lengths. The assembly of on SRL1R repeater requires: placing of jumpers for the boost selection, placing

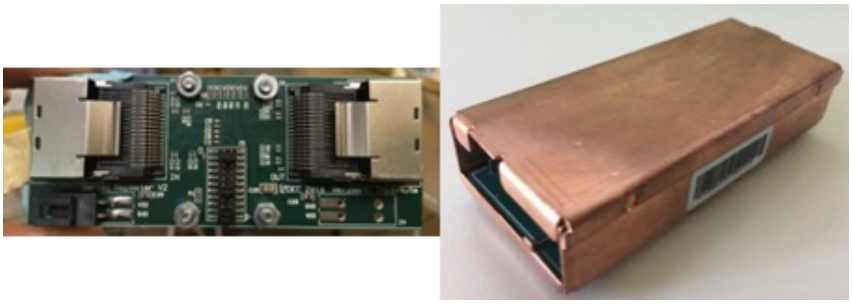

Figure 1: A Serial Repeater SRL1R (left) in its Faraday cage (right)

of thermal pads in contact with the copper box, placing protective kapton foils, enclose in the box. Taken was taken to have no magnetic materials. Labels were produced according to the ATLAS/NSW labeling scheme. The boards were tested in the Test Bench that was developed by our group (PhD Maria Prapa). In 2 is shown the work for the assembly, the Test Bench and 10 SRL1Rs installed at the Vertical Slice setup. During tests only 4 out of the 880 SRL1Rs presented an error, usually related to one channel, thus the yield was higher than 99%.

Figure 2: Assembly work (left), testing (middle) and using the SRL1Rs at the Vertical Slice setup

LVDS Repeaters - Final Production

The production of the LVDS repeaters was performed in two stages. Only half of the LVD6Rs (70 boards) were produced in November 2019, because of delays to purchase the repeater chips but also because it was impossibly to purchase the miniSAS connectors. All aluminum cooling and Faraday cages were though produced in 2019. The rest of the production was possible to perform in February 2020. The assembly of 70 LVD6Rs took place in February 2020. Cooling bars were produced for mounting the LVD6R boards as well as the aluminum Faraday cages. Full production of the LVD6Rs and the aluminum cages took place in Greek companies. Mounting of the LVD6Rs required the placing of thermal pads for a good thermal contact, introduction of spacers, proper spacers for the aluminum cages and proper grounding. The mounting of the remaining 70 LVD6R boards took place in October 2020 and all those devices were the first to be placed in Wheel C.

This time marked the completion of the Repeaters Project by our group. By the time of writing this report, the repeaters are used extensively at the integration

and the commissioning of the sTGC system and no problem has appeared in their operation.

Figure 3: LVD6R cooling bar with four mounted boards (left), one full LVD6R bar with four boards enclosed on the aluminum shielding mounted on Wheel A (middle) and LVD6Rs mounted on Wheel A indicated by red circles

sTGC Trigger Slice setup

In February 2020 our group completed a major task, to build a complete Electronics, Trigger and Readout System corresponding to one full sTGC wedge. The aim was to dispose an autonomous sTGC Trigger Slice system that would allow development, testing and commissioning of the full system. The system was ready just before the lockdown due to the pandemy, and was proven to be extremely useful as development on all activities continued during that period as well, through remote access.

The System corresponds to a fully equipped sTGC wedge:

- Front End boards: 12 sFEBs and 12 pFEBs
- One Rim-Crate
  - 1 Pad Trigger board
  - 1 RimL1DDC board
  - 4 Routers
- 8 L1DDCs boards
- 2 LVD6Rs and 10 SRL1Rs repeaters
- 1 Trigger Processor unit
- 1 Felix system
- 1 Software swROD system

The system is hosted in two racks (see 4), the Analog and the Digital ones. A special mechanical support was machined in order to support the 24 front end cards. All connections were done with exactly the same cable and fiber lengths in order to reproduce an identical system as the on detector system. Almost all the components require cooling: 1) All FE boards were placed on copper pads

and attached to it with thermal pads, 2) The L1DDC were placed in their cooling frame, 3) The LVDS repeaters on their cooling bars and 4) The Rim crate was cooled via the special backplane. A chiller with a custom made distribution system was setup to provide cooling through 3 different circuits. The temperature is kept to its nominal values i.e. temperature no higher than 23^0C. The system components can be powered on and off remotely and a booking system is serving for efficient sharing of the system among different groups. The system that our group has guilt is used by all team of the Trigger group i.e. Univ. of Technion, Weizmann Institute of Science, INFN Rome, University of Michigan, University of Massachusets, Harvard University and our group ATLAS/Demokritos.

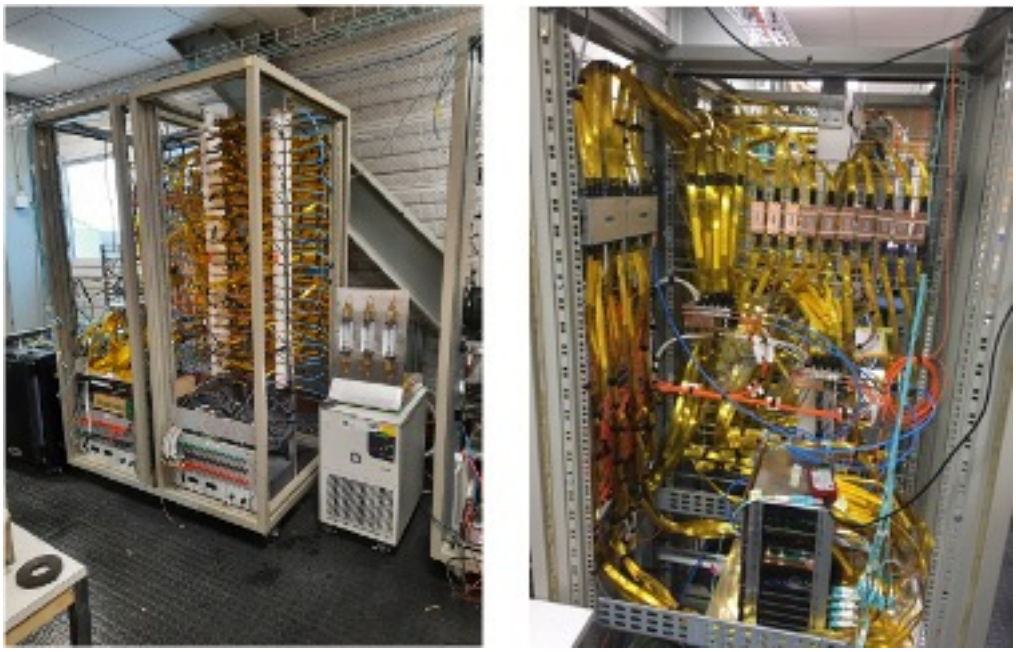

Figure 4: The sTGC Trigger Slice at the Vertical Slice Lab as built by our group

sTGC Trigger Commissioning

NCSR Demokritos group in ATLAS is involved with sTGC TDAQ system. In 2020 four main projects on sTGC Trigger Commissioning, were running in parallel.

- Wheel-A Commissioning
- Validation of sTGC Stage-0 trigger
- Fake Sector Logic
- The Alti pattern generator

In the following schematic 5, NSW trigger electronics are presented. The upper part of this schematic shows sTGC trigger electronics. Four different ASICs (VMM, ROC, TDS and SCA) were designed and manufactured, to produce customized electronic boards for all the stages of the system, from the Front End boards to the data concentrators, the trigger and finally the readout systems.

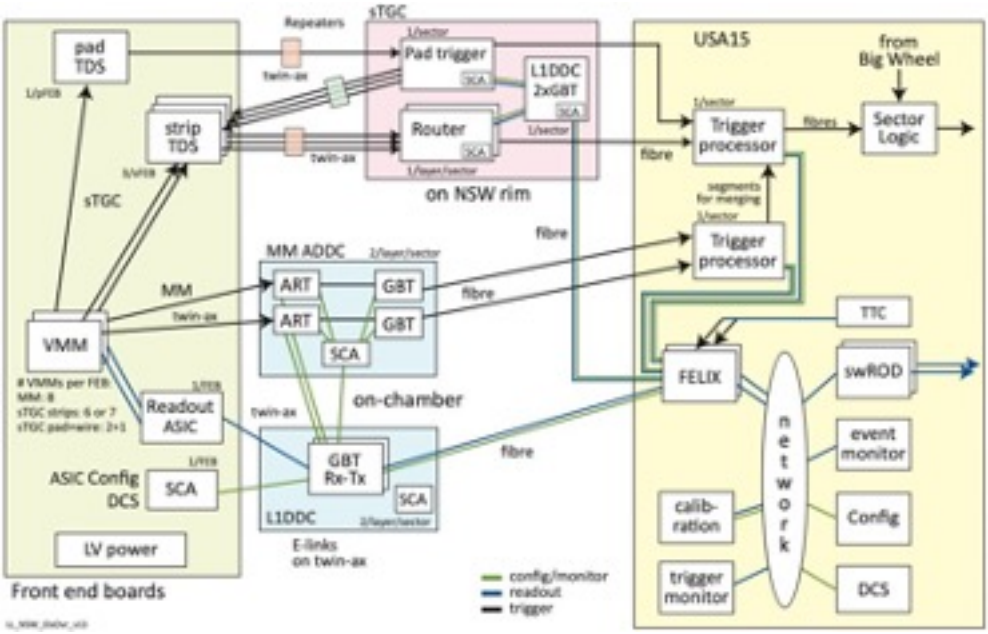

Figure 5: General Schematic of the NSW trigger electronics

Wheel-A Commissioning

Wheel-A Commissioning started in 2020 at CERN Meyrin site, Building 191 (B191) when the detectors started to gradually arrive from the construction sites. Wheel-A and Wheel-C have been installed in this building, before 2020, together with all the accompanying equipment (DAQ computers, TTC computers, cabling etc). In December 2019 the first Small Sector was installed and after this point a long list of tests was developed to validate connections and operation for every sectors. Among those tests, the sTGC trigger team developed tests that could validate the operation of sTGC trigger system. The tests were designed to serve two purposes. Firstly, to check the connectivity of the boards that belong to the trigger path and secondly to test that the data transmission to every path is without errors. The responsibility of NCSR Demokritos group was to develop and conduct these tests in all 16 sectors of Wheel-A. The test list to validate the proper operation of each sector is:

Connectivity Tests:

- PFEB Connectivity (PFEB/PT)
- SFEB Connectivity (PT/SFEB)
- Router Connectivity (QS1 SFEB/Router)
- Router VIOs test (QS1, QS2, QS3 connections)
- TP ILAs test (SFEB/Router/TP)

Data Quality Tests

- PFEB-PT IBERT/Eye Diagram Scans
- SFEB-Router IBERT/Eye Diagram Scans
- Router-TP IBERT/Eye Diagram Scans
- PT-TP IBERT/Eye Diagram Scans

The Connectivity tests were conducted by designing and then running a series of calibrations that tried to simulate the normal flow of the data in the trigger chain. The Data Quality Tests were using the FPGA utilities to test the data transmission by sending/receiving Pseudo-Random Binary Sequence - PRBS data.

Validation of Stage-0 trigger

sTGC Stage-0 trigger is a simplified version of sTGC trigger. It includes a smaller path that allows to get a fast decision on whether there is a valid trigger, meaning an event of interest. Stage-0 includes the pFEBs (pad front-end boards) the Pad Trigger board and the Trigger Processor board. The pFEB boards are receiving data from the sTGC detector's pads, which are larger areas that the detector is split. The pads from one layer are not totally aligned with the ones from the next layers, but staggered. This staggering facilitates the creation of a tower, a possible hit path of a muon., in every layer. Pad Trigger board has a look-up table stored in its FPGA that includes all possible towers. Using that look-up table can decide about whether there is an event of interest, in order to send this information to the Trigger Processor. The validation of Stage-0 was a milestone that was achieved, in 2020 but also a further step had been made. When the Trigger Processor receives the data from the Pad Trigger, meaning an event of interest has been found, it executes its algorithm and produces a pulse that can be used to trigger the rest of the system (remaining trigger electronics or Micromegas detectors). The produced pulse needed adjustments and shaping in order to be used by the TTC system, but this was soon resolved, and this tool became available for further studies.

Fake Sector Logic

The Fake Sector Logic (FSL) design for the ATLAS Muon Trigger system is a Sector Logic emulator that processes data from the detectors and provides information and measurements. This architecture is being developed for the Kintex Ultrascale FPGA on the Trigger Processor board, which is part of the NSW Electronics. Inputs to the FSL consist of merged data from both the sTGC and MM detector FPGAs and are handled by firmware that both supports fiber optic connections and process them to a more compressed format. Outputs are exported via 10G Ethernet to a local Network Interface Card (NIC) via point-to-point connection. Data will be received on the NIC side using a software script and can be further optimized to facilitate and expedite testing procedures.

This design consists of the following parts, as well as any extra logic that ensures the smooth propagation of data between them:

- Input Transceivers and fiber optics connections.
- Processing and compression of data
- 10G Ethernet with UDP implementation- also contains Output Transceivers
- Software to receive and store data from the NIC

The first half of the design has been completed in 2020.

Inputs and fiber optics connections. Input data have a fixed format illustrated in the image 6 and consist of packets hereafter called segment records. Each

segment record contains a double comma character for the serialization of data, data of 4 segments, the sector ID, and Bunch Crossing ID. Segments contain data for their resolution and location in the detector. The most important field in the segment data for the Fake Sector Logic is the $\Delta\theta$ field, which defines if a segment is valid and contains information that will be processed by the logic.

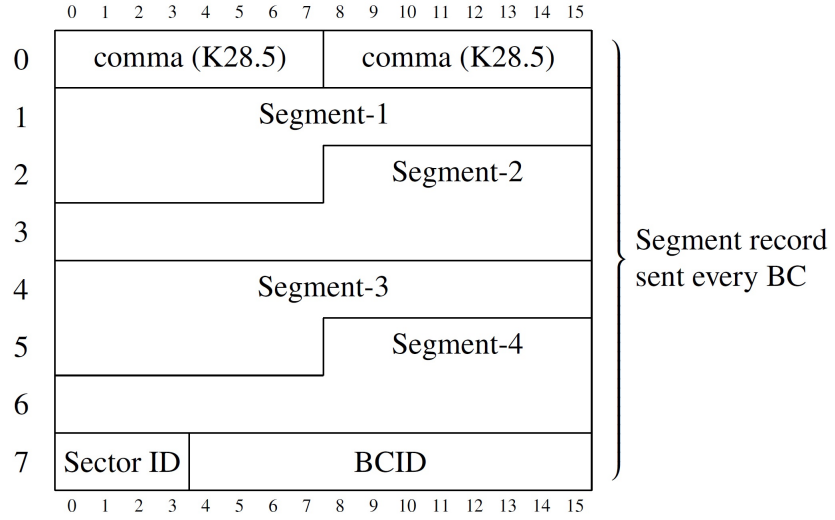

Figure 6: Data format from the NSW Trigger Processor to the Sector Logic

Segment records have been produced in different ways for testing purposes. So far, they appear as inputs following one of two different modes below:

Test Pulse Mode: 1 segment record packet consisting of 4 valid segments comes in per 3563 segment record packets. The rest of the packets are empty or invalid.

Playback Mode: segment record packet contents change per second. This means that regardless of the segment content, the same segment record packet will be input for 1s before changing to a different packet.

The full implementation of the input transceivers with a line rate of 6.4G has been completed in 2020. This part of the design makes full use of the Ultrascale features, provides the best connectivity options on the board while maintaining easy access to additional transceivers and availability of resources.

Processing and compression of data Input data are stored and are processed based on the selected mode of data as well as their content. Invalid segments are identified through $\Delta\theta$ and counted prior to data propagating to the branch of the architecture that is appropriate for the selected type of inputs. The firmware equivalent of a multiplexer is included to combine the simultaneously calculated results of two fibers to the single input of the 10G fiber.

The test pulse mode is based on a compression by three scheme; for every 3 invalid segments, a valid segment with its Sector ID and BCID is exported as output. The playback mode logic processes multiple inputs, compares them to stored previous values and currently exports counter results that indicate the number of identical segment records.

This part of the design has been completed in 2020. Both modes of the de-

sign feature a straightforward architecture of processing layers that can be easily modified to accommodate future testing requirements. The resource consumption is being minimized by taking advantage of the repetitive patterns that occur in the serial inputs and reusing logic and memory elements. Conditional statements and internal validity signals provide a stable data flow among the layers, while concurrently processing multiple fibers.

10G Ethernet The 10G Ethernet implementation uses the UDP/IP and MAC protocol to package and export processed data, effectively turning the FPGA into a NIC. A clock domain crossing FIFO is used to connect the two sides of the design. This part of the architecture consists of several sequential layers of code that adds headers, as well as the transceiver and fiber optics connection. The foundation has been laid in 2020 for this side of the project, in order to introduce the 10G Ethernet core components and to achieve a simplified and 10G compliant version of the UDP.

sTGC Detector integration

Our group has participated with one full time technician for the whole of the year 2020. We list below major works on which we played leading role in design and construction of systems that were necessary for the integration were: 1) The cooling frame for the sTGC L1DDC boards, 2) The Cooling system of the sTGC integration cite, 3) The assembly of the Faraday cages of the sTGC wedges, 4) the sTGC Sectors Assembly and 5) The design and manufacturing of many mechanical parts in the workshop that greatly helped accelerate the completion of the work of the sTGC integration

The cooling system of the sTGC L1DDC boards. sTGC data concentrator boards L1DDC require active cooling. Our group took part in adapting the cooling for a more efficient cooling. Our technician invented a mechanical mold that accelerated the manufacturing and helped build the frames faster. During the 2020 pandemy lockdown about half of the production was performed in Kalamata, in the INPP premises. In total 128 frames were built which are shown in 7.

The Cooling system of the sTGC integration cite. We have participated in the design and have built the whole Cooling system in building 188 at CERN where the sTGC integration of all the Sectors took place. The system was operated for the whole period without any problems providing 5 different lines of cooling circuits for the integration in parallel of two sectors and the full electronics chain. In 7 you can see the whole cooling system.

The assembly of the Faraday cages. The sTGC wedges (half of a sector) are enclosed in Faraday cages in order to reduce externally induced RF noise. We have taken part in the assembly of the Faraday cage which was composed from metallic parts made out of copper. Special care had to be taken for proper soldering and for avoiding leaks of the CO_2 envelop. In 7 you can see the assembly of the Faraday cage.

The sTGC Sectors Assembly. Every Sector is composed by two wedges (4 sTGC layers) and every wedge is split in three quads (Q1, Q2 and Q3). The quad were manufactured in the construction centers in Chile, Canada, Israel and Russia and

were shipped to CERN for assembly. Our technician contributed to the assembly of the whole wedges and Sectors. The work took place in the Clean Room of B180 at CERN. Many intervention allowed the acceleration of the assembly of the sTGC detectors. In 7 you can see the team having assembled one sTGC Sector.

Manufacturing of mechanical parts. Many mechanical parts were manufactured in the machine workshop that allowed faster execution of the assembly operations (see 7).

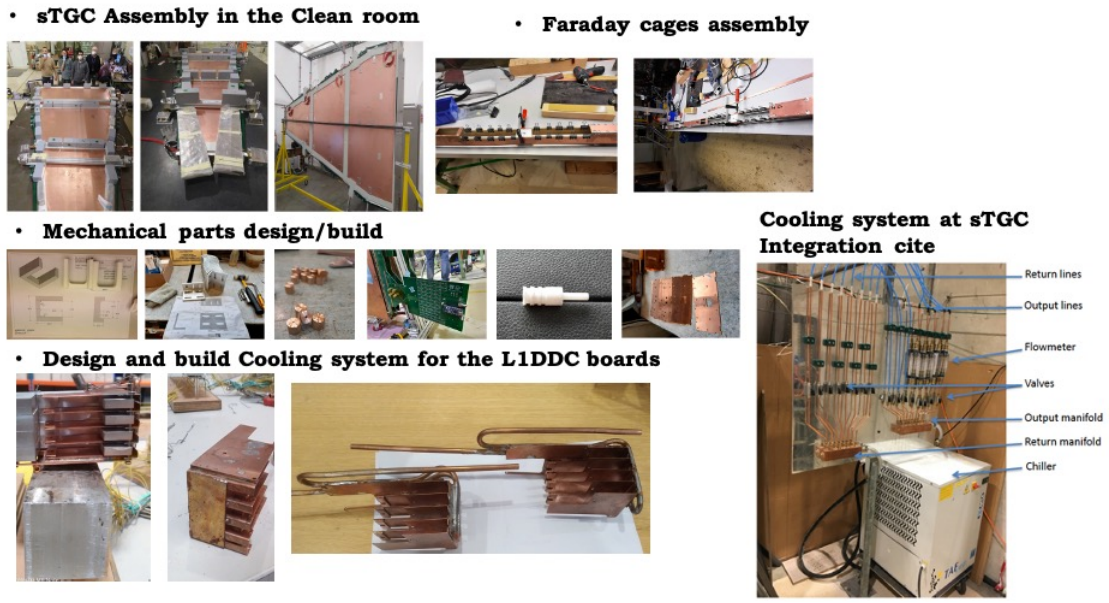

Figure 7: Photos from the integration cite works performed by our group

ATLAS Local Trigger Interface

An upgrade to the current Timing, Trigger and Control (TTC) system at the ATLAS experiment will be the ATLAS Local Trigger Interface. ALTI is a new electronic board, designed to integrate the functionality of the four existing TTC modules and replace them with a single VME module. The primary function of ALTI is to provide the interface between the Central Trigger Processor (CTP) and the TTC optical broadcasting network.

The CTP is part of Level-1 Trigger system at the ATLAS Trigger and Data Acquisition system. It is responsible for making the initial trigger decision (Level 1 trigger accept signal) by identifying interesting particle candidates coming from the Level-1 calorimeter and Level-1 muon trigger systems (8). The L1A trigger signal, along with timing and synchronization signals such as the LHC 40 MHz clock (BC clock), are distributed to the sub-detector electronics via the TTC system.

The ALTI pattern tool

During LS2, no communication between the CTP and ALTI can be established. Therefore, NCSR Demokritos group developed a tool, using Python as

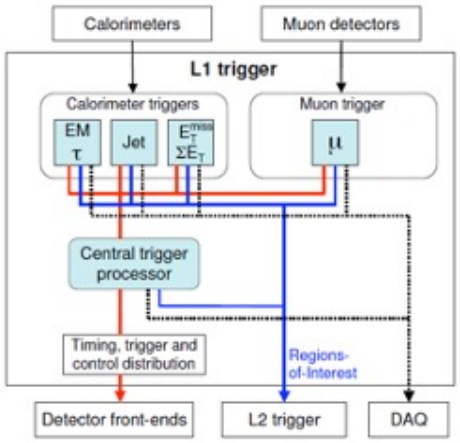

Figure 8: The Level-1 Trigger system.

a programming language and ROOT data analysis framework, in order to drive ALTI. The tool provides the generation of pulse pattern files that implement the TTC information (9). Additionally, it applies important parameters, electronic hardware restrictions, trigger rules and mechanisms on the generation of these patterns which are being used by the CTP in normal operation.

The motivation behind this tool was to utilize ALTI in order simulate real-time trigger conditions, and study the response of the Trigger System for the New Small Wheel muon detector electronics. This procedure facilitated developments related to the Trigger System validation and contributed to the verification of its operation and data readout process.

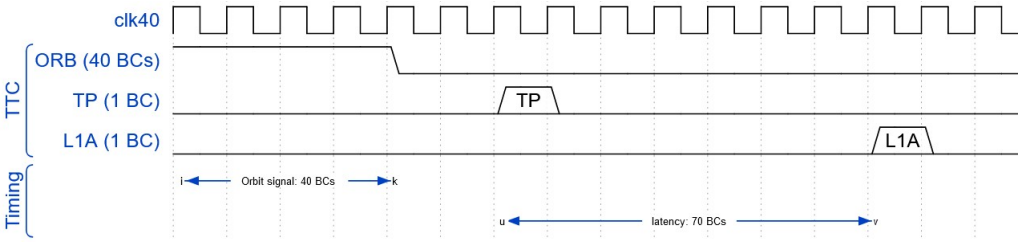

Figure 9: Time diagram of an ALTI pattern file (clock out of scale). An orbit signal represents one LHC turn, followed by a test pulse signal and the L1A signal that corresponds to it 70 Bunch Crossings (BC) later.

Analysis

ALTI was configured with pattern files at different rates, both for clocked and random trigger type. NetIO publish/subscribe system used was used to obtain distributed data from the NSW sTGC trigger path. The required time differences (or distance in BCs) were observed while transmitting TTC signals through ALTI to the individual electronics. The following histogram is produced from sending pulse patterns with random triggers to the sTGC Pad Trigger (Figure 3). It depicts the probability of a bunch crossing to occur, which decreases exponentially over

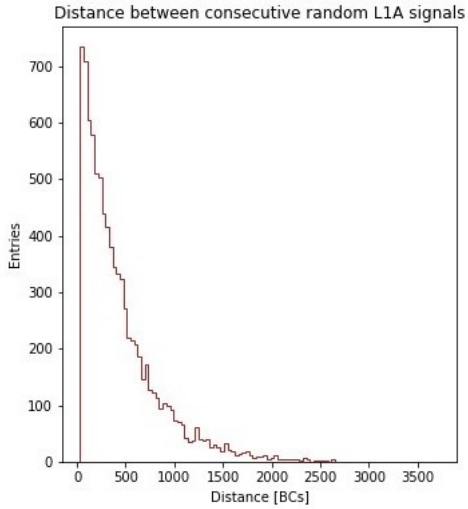

Figure 10: Histogram for random trigger type generated at 100 kHz, 70 BC test pulse – L1A signal latency.

time.

Muon and NSW software activities

The muon spectrometer is made up of several thousand chambers and is the outermost layer of the ATLAS detector. It identifies and measures the momentum of muons that fly out of the collision point. Key to this is a precise understanding of the muon spectrometer's geometry.

Measuring and recording the chambers' as-built geometrical parameters, translated to discrepancies with respect to the nominal (according to design) chamber geometry, is the first step towards precisely understanding the muon spectrometer's geometry.

At small scales, the geometry of the muon spectrometer is almost constantly changing, albeit slowly. Small temperature variations make the chambers and their support structures contract, expand and deform. Further, some of the chambers are mounted on the ATLAS toroid magnets, which themselves can occasionally move and deform.

The muon spectrometer is therefore equipped with an optical alignment system that monitors in real time the positions of chambers relative to each other and to calibrated reference objects in the detector, as well as their deformations. This information can be combined with data from muon tracks in order to fully understand the muon spectrometer's position.

The, precisely specified, muon spectrometer's geometry is implemented into the ATLAS software frame through the Detector Description software. It relies on a database technology and a standard set of geometrical primitives common to all ATLAS subsystems. The Muon Detector Description provides a unique

and coherent geometry source for the simulation and reconstruction algorithms. ATLAS has adopted 3 sets of parameters to describe the disrepancies between the "actual" geometry with respect to the "nominal" one.

1. As built parameters: construction sites measurements translated todiscrepancies w.r.t the nominal (according to design) chamber geometry.
2. Alignment of Stations / A Lines: 6 time dependent parameters meant to describe deviations w.r.t nominal positions.
3. Deformations / B Lines: 11 time dependent parameters meant to describe the deformation effects.

The upgraded NSW of the ATLAS muon system consists of two types of gas detectors (sTGC and MicroMegas), the precise geometry of which has to be introduced into the Muon Detector Description software. The INPP-ATLAS group has undertaken the responsibility to implement the, aforementioned, NSW sets of parameter in the ATLAS offline software. All the necessary tools for storing and retrieving these parameters into the relevant databases have been implemented, tested successfully and included into the official ATLAS software. Furthermore, various tools that correctly calculate the various geometry parameters have been developed and included in the official ATLAS software frame, to be used by other ATLAS packages such as simulation, reconstruction and graphics.

Funding

Some equipment and personnel (PhD) was funded by the DeTANet infrastructures program with an amount of about 50 kEuros for the ATLAS group for the period Feb. 2019 to Feb. 2022. The INPP program ORASY also provided small personnel support. The main support came from the ATLAS NSW project which provided support for 3.5 FTE for the whole of 2020. The table 9 below present the two INPP sources.

Table 9: Funding through the infrastructures DeTANet program and the ORASY within INPP

Prog. ID	Title	Host Institution	Principal Investigator	Starting date	Finishing date	Budget (€)
12312	DeTANet	INPP	T. Geralis	10/02/2019	10/02/2022	125,962.67
	ORASY.	INPP	C. Markou	01/01/2015	31/12/2021	20,000.00

Outreach

Because of the Covid pandemic the Outreach activities were practically suppressed. Our Lab usually participates in many events like the Researcher's Night in which we provide demonstration with Cloud Chambers, exhibition of particle

detectors, microscope inspection of micro pattern detector structures etc. Also we take part in the Master Classes program for high school pupils.

Overview

The year 2020, despite the pandemic problem, has been very productive for our group. We recapitulate the main research activities below:

- Completion of the sTGC Repeaters project with final production and installation in NSW
- Construction of the sTGC Trigger Slice setup, that was used for developments during the pandemic and is still in use
- Demokritos group is the driving force for the sTGC Trigger Commissioning on the Wheels
- Very significant contribution to the sTGC detector integration, providing technical support
- Major contribution to the Muon and NSW software activities
- Very important contribution in the developments for the sTGC Trigger processor like the project of the Fake Sector Logic and also the Alti Pattern generator that are extremely useful tools for the collaboration.

Responsibilities

The members of the ATLAS Demokritos group have gradually undertaken important responsibilities, given the short time we participate as full members in the ATLAS Collaboration. Below we give a list of responsibilities and participation in important bodies within ATLAS:

T. Geralis: Coordinator of the sTGC Trigger Commissioning

T. Geralis: Member of the Muon subdetector Institutes Board

T. Geralis: Member of the NSW Electronics Coordination Group

G. Stavropoulos: Responsible for porting the Muon source code to parallel therading. By the time of writing this report in 2021, **G. Stavropoulos has become Coordinator of all ATLAS Muon Software activities**, which is a major responsibility and achievement for our group.

Presentations in the ATLAS internal meeting in 2020

68 Presentations were given by members of the INPP ATLAS group in internal ATLAS meetings, mainly in the frame of the NSW activity, in the NSW Electronics meetings during 2020, in the Weekly NSW Commissioning meetings and in the Muon Weeks, in the parallel but also in plenary sessions.

ESSnuSB

Researchers:	George Fanourakis
	George Stavropoulos
	Theodoros Geralis
Administration:	George Fanourakis
Employees:	Olga Zormpa
	Maria Myrto Prapa

Introduction

The European Spallation Source Neutrino Super Beam (ESSnuSB or ESSνSB, https://essnusb.eu/) project is a future accelerator-based neutrino oscillation experiment design for CP violation discoveries in the lepton sector. This facility has been proposed after measuring in 2012 a relatively large value of the neutrino mixing angle θ_{13}, opening the possibility to observe for the first time a possible CP violation in the leptonic sector which is the key ingredient to explain the lack of antimatter in the Universe. The measured value of θ_{13} also privileges the 2nd oscillation maximum for the discovery of CP violation instead of the usually used 1st oscillation maximum. The sensitivity at this 2nd oscillation maximum is about three times higher than for the 1st oscillation maximum inducing a lower influence of systematic errors. However, since the neutrino flux is reduced at the 2nd oscillation maximum, a very intense neutrino beam with the appropriate energy is required. The world's most intense pulsed spallation neutron source, the European Spallation Source (ESS), will have a proton linac of 5 MW power and 2 GeV proton kinetic energy. ESSnuSB proposes the upgrade of the ESS proton linac to 10 MW, 2.5 GeV and to use half of the protons to produce a neutrino Super Beam, leaving the ESS neutron program undisturbed. The physics performance of that neutrino Super Beam in conjunction with a megaton underground Water Cherenkov neutrino detector installed at a distance of 360–500 km from ESS is being evaluated. The ESS proton linac upgrades, the accumulator ring needed for proton pulse compression, the target station optimization and the physics potential are included in the study. The ESS neutron facility will be fully ready by 2025 at which moment the upgrades for the neutrino facility could start.

The neutrino (anti-neutrino) oscillation to be studied here is $\nu_\mu \to \nu_e$ ($\bar{\nu}_\mu \to \bar{\nu}_e$). Fig. 11 presents the unoscillated neutrino and anti-neutrino energy distributions which could be obtained by the proposed facility at an arbitrary on-axis distance of 100 km from the neutrino target.These distributions correspond to one year neutrino run (200 days). An almost pure muon neutrino (anti-neutrino) beam is produced with a main contamination of about 0.5% of electron neutrinos (anti-neutrinos). This contribution polluting the primary muon neutrino beam, could be used to measure the electron neutrino cross-section using an appropriate near detector.

Fig. 12 presents the $\nu_\mu \to \nu_e$ oscillation probability at a distance of 540 km for several values of δ_{CP} and for normal and inverted neutrino mass hierarchies. The overlapping grey distribution is the ν_e energy distribution coming from the ν_μ oscillation. It is obvious that the 2nd oscillation maximum is fully covered. From

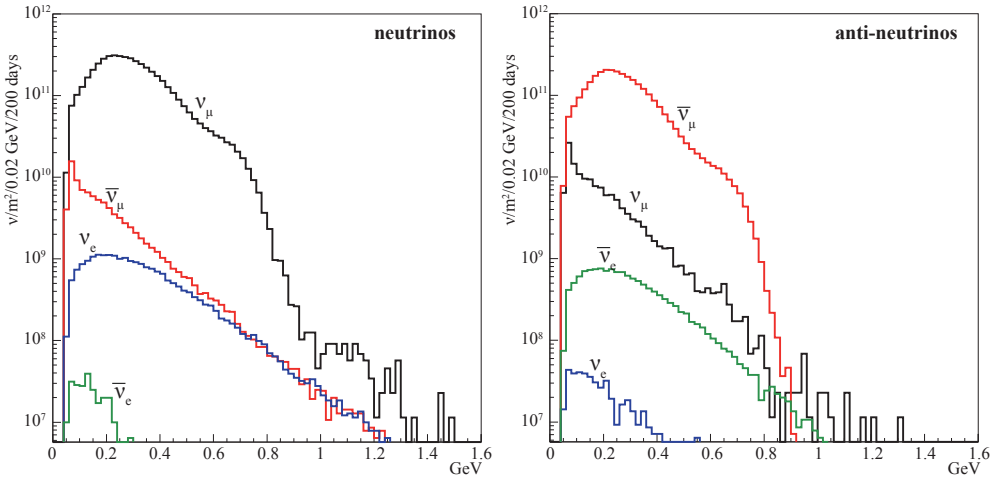

Figure 11: Energy distribution for neutrino (left) and anti-neutrino (right) beam at an arbitrary distance of 100 km from the target station, for 2.5 GeV protons.

this figure it is also seen that the CP violation discovery potential is not affected by the unknown neutrino mass hierarchy. It has to be mentioned that this project is exclusively devoted to CP violation discovery and not to the mass hierarchy determination which is believed to be solved by then by experiments scheduled to start taking data during the next decade.

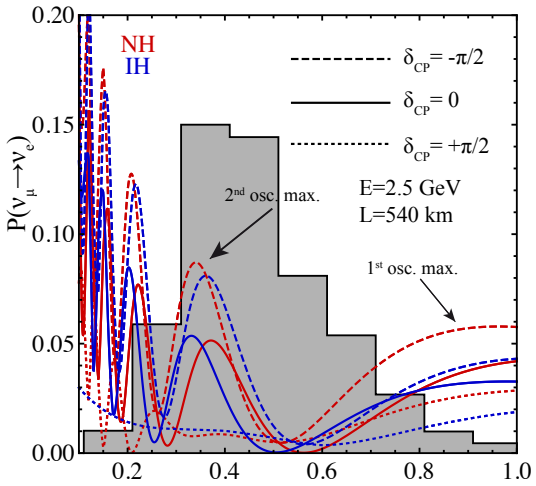

Figure 12: $\nu_\mu \to \nu_e$ oscillation probability as a function of the neutrino energy. The red (blue) lines are for normal hierarchy (inverted). The shaded histogram is the energy distribution of ν_e produced by the ν_μ oscillation and detected by the far detector.

The physics performance strongly depends on the considered systematic uncertainties, which play less a role on the 2nd oscillation maximum thanks to the interference term in the oscillation probability dominating the solar and atmospheric terms.

After 10–years operation, it is expected that about 600 electron neutrinos and antineutrinos will be detected by the far detector. Fig. 13 slows the CP violation discovery significance versus δ_{CP}. Up to 60% of the δ_{CP} values can be covered with a significance of 5 σ. Studies are under way to increase the number of detected neutrinos by further optimising the magnetic horn shape and the far detector

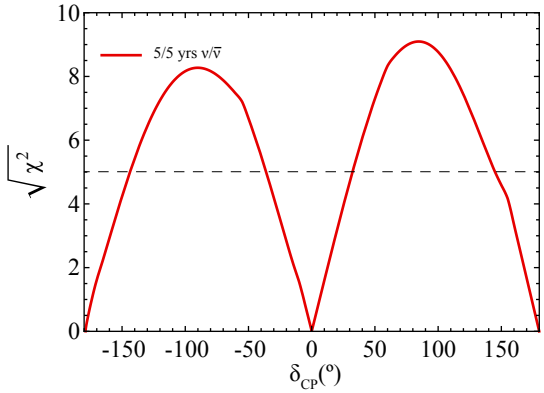

Figure 13: The significance with which CP violation can be discovered as a function of δ_{CP}.

performance. A dedicated working group for the ESSνSB detector designs aim to reduce the systematic uncertainties in the signal/background neutrino flux to below 5%, such that the 5 σ discovery range of δ_{CP} may increase.

Activities

The ESSνSB Demokritos INPP team is part of the Detector Performance and the Physics Reach working groups. Our work has so far been mainly focused on the far detector (FD) studies.

The Detector Performance group has developed the EsbRoot environment for detector simulations and event reconstruction based on the FairRoot framework. However, for the design of water Cherenkov (WC) detectors, envisioned as a near detector (ND) as well as a far detector (FD), an additional open-source simulation package, called WCSim, is being used. WCSim is based on Geant4 and ROOT. A generalised particle source for basic diagnostic tests of the detector geometry and reconstruction algorithms has been used, as well as a Monte-Carlo neutrino event generator GENIE on the estimated neutrino flux from ESS for more realistic event simulations and detector response evaluations. Its outputs have been successfully used as inputs for EsbRoot and WCSim, and the integration of GENIE into EsbRoot is complete. A characterisation of all scattering reaction channels of the neutrinos in active detector materials is in progress. A prospect of constraining the neutrino flux from ESS with measurements of neutrino-electron reaction channels is being explored.

The FD for ESSνSB is a large water cylindrical Cherenkov detector, 78m base diameter and 78m height, based on the MEMPHYS (MEgaton Mass PHYSics) design. Studies on the expected performance of the FD were conducted via appropriately tuned EsbRoot, WCSim and fiTQun environments. Certain reconstruction and analysis strategies such as fiducial volume and timing cuts were implemented. Examples of the results of the analysis of Monte Carlo produced flat neutrino and antineutrino distributions for the geometry used in the T2K experiment are shown below:

To study the energy reconstruction capabilities of the far detector we have used a flat neutrino (antineutrino) beam distribution. The Energy distributions for the

event types of interest and the neutrino beam flavors are presented in Fig. 14.

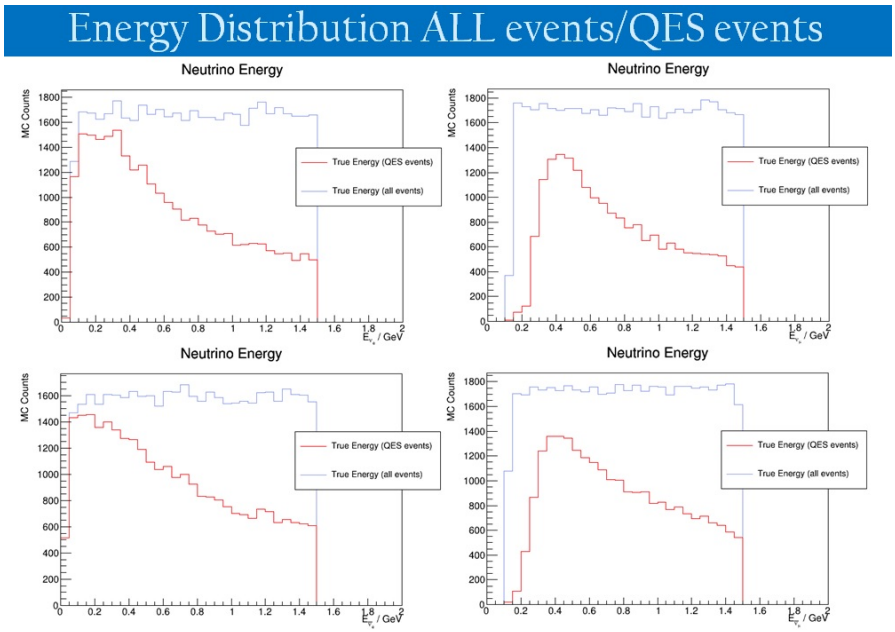

Figure 14: Energy distribution for all types and QES neutrino and antineutrino events.

The results on the migration matrices (reconstructed Energy vs true Energy), which show how well the neutrino (antineutrino) events are reconstructed, for all event and beam types are presented in Fig. 15 and for QES events in Fig. 16.

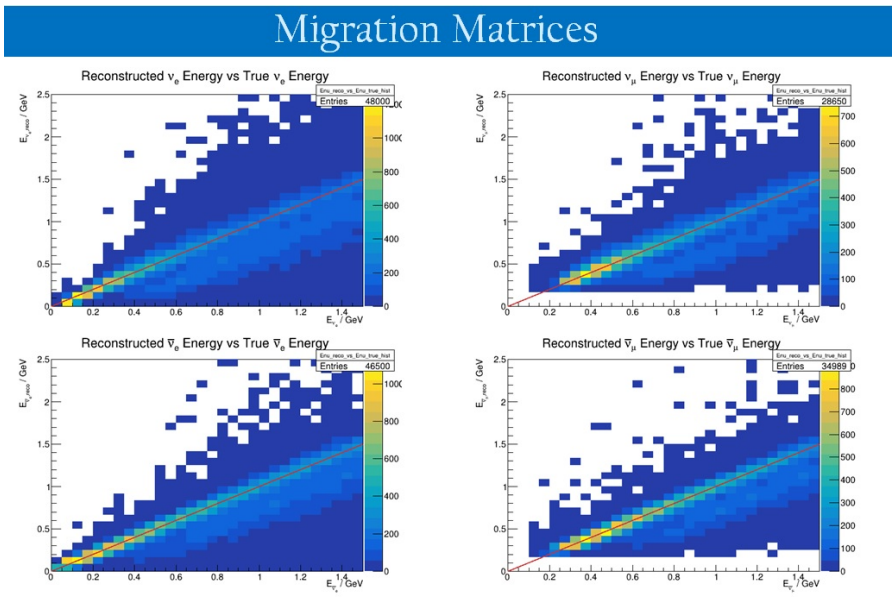

Figure 15: Reconstructed vs true energy distributions for all types of events

The analysis work for the ESSnuSB proposed detector configuration and the related parameter tuning will be in progress until early 2022.

The publications related to the ESSnuSB project work where the INPP group

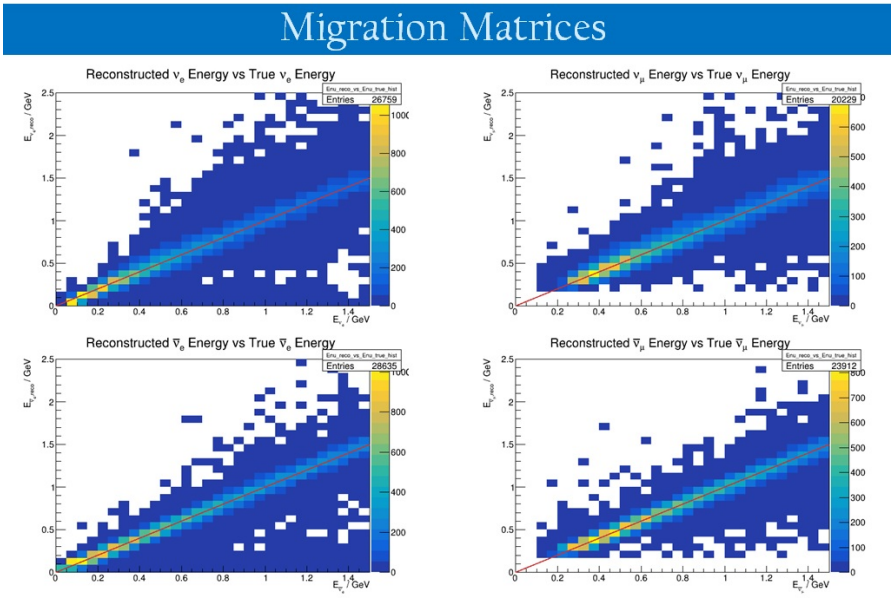

Figure 16: Reconstructed vs true energy distributions for QES events.

has contributed, during the year 2020, include references [1] and [2].

Funding

This project has received funding from the European Union's Horizon 2020 research and innovation program under grant agreement No 777419. INPP group has received a total of 64,953.00 Euros for the 4 years duration of the ESSnuSB project. It has also been supported by the COST Action EuroNuNet *"Combining forces for a novel European facility for neutrino-antineutrino symmetry-violation discovery"*. This action supported travel for meetings and workshops.

Outreach

One of the members of the INPP group (GF) is part of the ESSnuSB Dissemination and Exploitation Board (DEB). DEB's tasks include the organization of participation to conferences, the editing of abstracts, talks and proceeding contributions as well as the public awareness events and materials. DEB's accomplishments include two videos about ESSnuSB, one for general public (https://youtu.be/qAnvftOnAlg) and one for scientist audience (https://https://youtu.be/PwzNzLQh-Dw).

[1] Joochun Park et al. "Status of the detector design studies for ESSνSB". in: *PoS* NuFact2019 (2020), p. 041. DOI: 10.22323/1.369.0041

[2] Joakim Cederkall et al. "The ESSnuSB project". In: *PoS* EPS-HEP2019 (2020), p. 392. DOI: 10.22323/1.364.0392

Overview

The ESSnuSB project is a promising proposal for a next generation neutrino oscillation experiment tuned to the potential discovery of the CP violation in the leptonic sector. Such a discovery will solve one of the most important questions in cosmology: why there is no antimatter in the Universe? The INPP ESSnuSB group has been contributing to the work on the design and studies of the far detector since the beginning of the project. The current results exemplify the superiority of the Physics capabilities of ESSnuSB on the determination of the CP violating phase, over the currently proposed and in preparation long base line neutrino experiments.

High Energy Experimental Physics - CMS

Researchers:	G.Anagnostou
	G.Daskalakis
	A.Kyriakis
	D.Loukas
PhD students:	P.Asenov
	P.Assiouras
	G.Paspalaki
	A.Stakia
Master students:	A. Papadopoulos
Practical work students:	D.Papafilippou
Engineers:	I. Kazas (ELE)

Introduction

In 2020 the INPP CMS group entered in full swing into the preparation of components and modules for the Phase II upgrade of the CMS in the HL-LHC, in parallel with the physics analysis program and maintenance of the CMS apparatus.

The physics program of the CMS experiment aims at answering fundamental questions in particle physics. What is the origin of elementary particle mass? What is the nature of the dark matter we observe in the universe? Is a common framework for the unification of the fundamental forces? Do matter and antimatter have different properties? How strong forces behave under extremes conditions? Until the end of 2018 LHC has delivered 238 fb^{-1} to CMS. This data has yield a vast quantity of physics results summarised by the CMS collaboration in more than 1050 publications. The highlight has been the observation in 2012 of a new particle that has been identified as the Higgs Boson, a cornerstones of the standard model of elementary particles. In addition to this discovery, CMS an ATLAS were able to begin detailed studies of its properties to consolidate that it was indeed the Higgs boson.

Precision Higgs studies and the search for new physics provide a powerful

motivation for higher luminosity. The High Luminosity LHC (HL-LHC) is an upgrade program of the LHC with aim to provide higher peak and integrated luminosity. The scheduled upgrade scenario, refereed as Phase-II as well, is to level the instantaneous luminosity to $5 \times 10^{34} cm^{-2} s^{-1}$, or even to $7 \times 10^{34} cm^{-2} s^{-1}$ in the ultimate performance scenario. This will allow CMS and ATLAS to collect integrated luminosity of the order of 300 fb^{-1} per year and up to 3000 fb^{-1}, or up to 4000 fb^{-1} in the ultimate scenario, for the entire period of 10 years foreseen operation of HL-LHC. The machine will run at a center-of-mass energy of 14 TeV and with a bunch spacing of 25 ns.

The main challenges faced by the experiments at HL-LHC are higher radiation levels and increased pileups. The basic goal of the CMS Phase-II upgrade is to maintain the excellent performance of the detectors in terms of efficiency, resolution, and background rejection for all the physics objects used in the analysis of data. Figure 17 sketches the upgrade of the CMS subsystems.

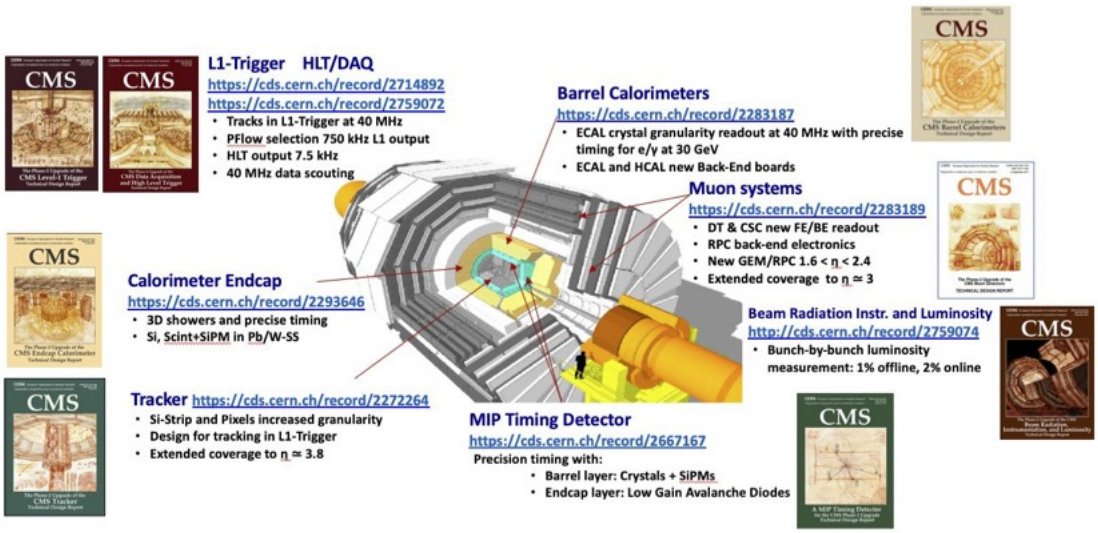

Figure 17: Sketch of the CMS detector with Phase-II upgrade plan

Central to the CMS Phase-II upgrade is the complete replacement of the Silicon Tracker. The new Silicon Tracker must cope with many challenges. In order to be radiation tolerant up to $4000 fb^{-1}$ the CMS collaboration contacted a ten years sensor $R\&D$ program that concluded with the choice of n-on-p senors to p-on- n [3] as the latter proved to exhibit higher radiation resistance. In order to handle the increased pileups, 140-200 expected compared to the current 30-40, increased

[3]CMS Collaboration. "Experimental study of different silicon sensor options for the upgrade of the CMS Outer Tracker". In: *JINST* (2020). DOI: 10.1088/1748-0221/15/04/P04017

granularity of the detector is needed to keep the occupancy bellow 1% and improve the resolutions at high P_t. This issue is addressed with higher segmentation of sensors and an increased latency from $3.2ns$ to $12.5ns$ by increasing the depth of the front end buffers. Improvement in low P_t resolution is achieved by using thinner detectors that reduce the materiel budget. Increased forward acceptance up to 4η is obtained with extension of the pixel detector. A novelty of the new CMS apparatus is the improvement of the trigger system by using data from the outer part of the Tracker for level one (L1) trigger.

Figure 18 shows the layout of the new CMS Tracker. It will extend from the vicinity of the beam pipe up to 1100 mm. The outer part (OT) of the detector that extends beyond 200 mm is made of two types of modules, one type consists of a pair of closed spaces microstrip sensors , the so called $2S$ modules, and the other type consists of a pair of microstrip and macropixel sensors named as PS modules in th CMS terminology. The inner part of the tracker consists of micropixel sensors.

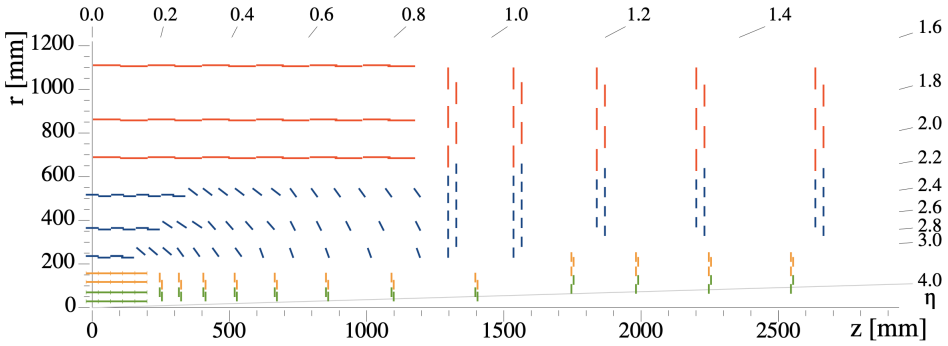

Figure 18: Layout of the CMS Phase-II silicon tracker in $r-z$ view [5]. The radial region below 200 mm is referred to as Inner Tracker and will be instrumented with pixel modules (green and orange colors). In the Outer Tracker, the radial region between 200 and 600 mm is equipped with PS modules (blue lines), while the region beyond 600 mm will be populated with 2S modules (red lines

.

The INPP CMS group joint the CMS Tracker in 2015. The activities of the group were focused on the development of the Outer Tracker and especially on the silicon sensors. The group developed the necessary instrumentation and acquired the status of one among four international centers for the qualification of silicon sensor production provided by Hamamatsu Photonics in Japan. Associated with this activity is an under way program of irradiation studies with ^{60}Co-γ source. Gradually the group extended its activities to the Inner Tracker by assuming the responsibility for the development of firmware and middleware for the readout ASIC of the pixel detector.

Activities

Physics Analysis

The CMS-INPP data analysis group main goal is the deeper understanding of processes and mechanisms described by the Standard Model (SM) of particle physics and the quest for new symmetries and/or new matter in nature. To fulfill that goal the group has developed a twofold strategy: performs SM measurements and at the same time searches for specific topologies that might reveal the existence of supersymmetry or dark matter at LHC. Starting with the SM measurements, the objective is to enhance the experience of the team, gained over the past few years based on measurements in the electroweak sector of SM, by investing in studies in the field of top-quarks physics. The data from proton-proton (pp) collisions produced at the CERN LHC provide an excellent environment to investigate properties of the top quark, in the context of its production and decay, with unprecedented precision. Specifically, the measurements of the W boson helicity fractions in top quark decays, are very sensitive to the Wtb vertex structure. The comparison of the measured W helicity fractions with those estimated from the theory might reveal possible discrepancies from the SM predictions and contribute to a deeper understanding of the underlying physics processes. After the Higgs boson discovery, many theorists argue that a heavy top partner could explain the scale of the Higgs boson mass via loop cancellations. As such, an important extension of the measurements in the top-quark sector of the SM, will be a search for heavy top partners, exploring the $pp \rightarrow T^{'}T^{'} \rightarrow bbWW$ process. A new method was motivated/inspired from CMS-INPP analysis team as a new/different way to search for anything decaying like dilepton top-pairs. The CMS-INPP data analysis group also participated in the development of a methodology, called the Tag Rate Function, which allows to significantly reduce statistical uncertainties of the distributions of $\mathrm{t}^{-}\mathrm{t}$ events with high b-tagged multiplicities utilising the ones with lower b-tagged multiplicities. This approach has a significant impact on the systematic uncertainties of the $t^{-}tH$, $H \rightarrow b^{-}b$ measurement in the dileptonic and fully-hadronic channels. Our research program includes an extension of the above-mentioned analysis at the simulation level in order to study the increase in precision of the proposed Standard Model measurements as well as the extrapolation of the limits in searches for new physics at HL-LHC.

CMS Analysis Note: CMS AN-2020/205

Top Physics, G. Daskalakis, A.Stakia

Short description: We report a measurement of the W-boson helicity fractions from top quark decays, based on a data sample corresponding to an integrated luminosity of $137 fb^{-1}$ of proton-proton collisions at a centre-of-mass energy of $13 TeV$, collected in 2016-2018 by the CMS experiment at the LHC. The measurement uses the semileptonic decays of the tt pairs and the single top production (tW and t-channel). The results are consistent with standard model expectations, see Fig. 19.

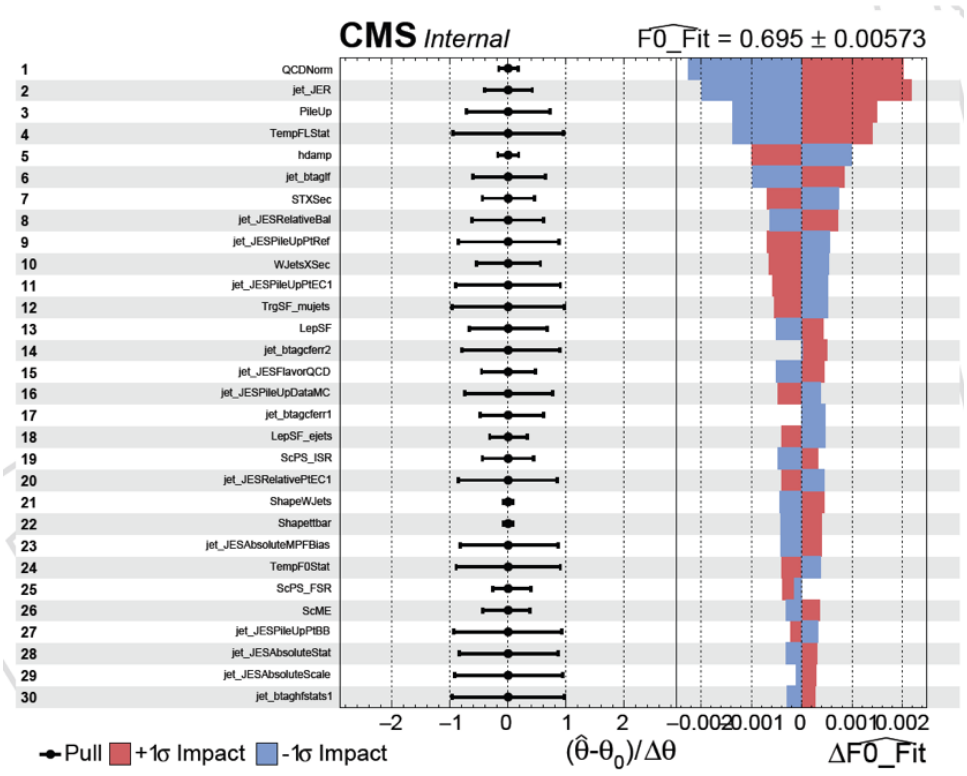

Figure 19: EXPECTED Impact plot for the F0 parameter of interest using the 2018 dataset

CMS Analysis Note: CMS AN-2020/047

Higgs Physics, G.Anagnostou, G. Daskalakis,

Short description: In this note we describe a methodology, called the Tag Rate Function, which allows us to significantly reduce statistical uncertainties of the distributions of $t^{-}t$ events with high b-tagged multiplicities utilising the ones with lower b-tagged multiplicities. This method is using per event weights, derived by parametrised b-tagging probabilities, in order to predict the rate and shape of several distributions in events with higher b-tag multiplicities starting from the ones with lower b-tagged multiplicities. The prediction of kinematic, topological, but also higher-level variables, like a BDT output, is examined and shown. The impact this approach has on the systematic uncertainties of the $pp \to T'T' \to bbWW$ measurement in the di-leptonic and fully-hadronic channels, related with the limited statistics of the simulated samples, is briefly mentioned. In addition, we present a method to approximate the MEM discriminant for events with low b-tag multiplicities, since its computation for those is very computer intensive and hence is completely absent. This variable is important for the BDT estimation, and its approximation is implemented using two complementary approached: a Look-Up-Table and a multivariate regression technique using the higher b-tagged multiplicity events for which MEM is provided, see Fig. 20.

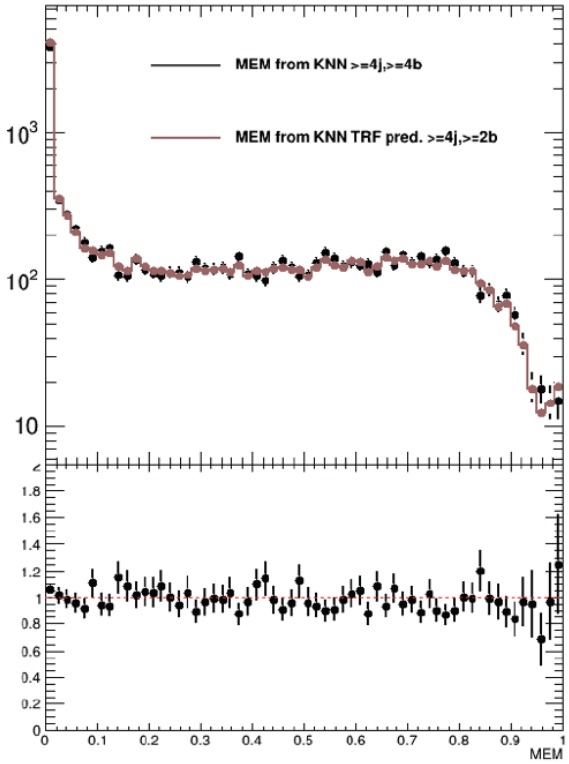

Figure 20: Closure of the TRF predicted MEM from events with at least 2 b-tagged jets with the one for events with at least 4 b-tagged jets

Trigger Manu development

A.Stakia

Anna Stakia, as part of her service work to the CMS experiment, studied the "acceptance" of L1T seeds with respect to the related High Level Trigger paths. This consists of calculating the fraction of events passing an HLT path triggered uniquely by a particular L1 seed, compared to those events passing the same HLT path also triggered by other L1T seeds. A study of the L1T algorithms performance was conducted, estimating how often an event selected by an unprescaled L1T seed is recorded. Those studies concluded in the development of an L1T+HLT acceptance software tool, which at a first stage provided the L1T+HLT acceptance results obtained from NanoAOD input samples; the existing part of code was tested and fixed, and new parts of code were developed for this purpose, these being part of a streamlined, user-friendly workflow. At a second stage, the full set of L1T+HLT acceptance results were to be obtained starting from L1Ntuples, via modifying and upgrading the code to work in such case.

Reviews, Committees

Committees:

Georgios Daskalakis was the chairman of ARC for the publication: EXO-19-

017: ‘Search for new physics in lepton plus MET final state‘

Georgios Anagnostou was ARC member for the publication: B2G-19-004: ‘Search for single production of a vector-like T quark decaying to a top quark and a Z boson in the jets plus missing transverse momentum final state at $\sqrt{s} = 13\ TeV$.

Reviews: “Search for heavy Majorana neutrinos in the same-sigh dilepton channel in proton-proton collision at $\sqrt{s} = 13\ TeV$, CMS Collaboration, CMS Paper EXO-17-028.

Search in the 2-Dimensiona l mass space for final states with 2 invisible particles

G. Anagnostou

A phenomenological study for final states with two invisible particles is performed. A new element is that massive invisible particles are now included in the 2-Dimensional mass reconstruction. This allows topologies with dark matter candidates such as stop quark pairs to be reconstructed Figure 21. The method is applicable at LHC dark matter searches in terms of mass variables instead of missing energy related observables. The main work for these results was performed during 2020 https://arxiv.org/pdf/2009.10032.pdf although the final publication was accepted later [6].

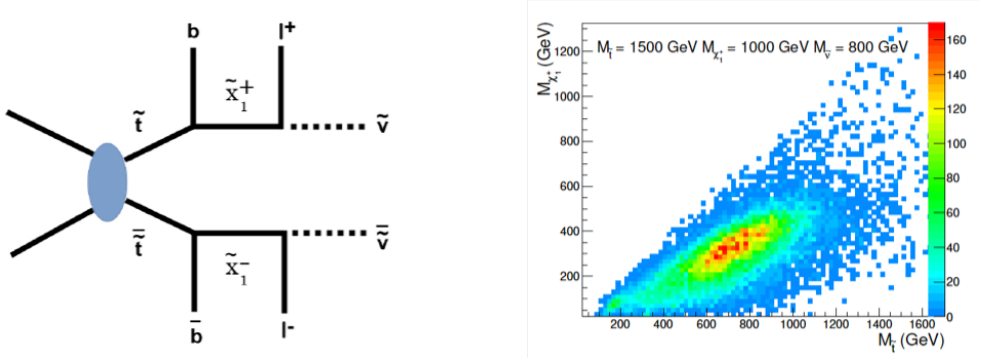

Figure 21: Left: Topologies with dark matter candidates such as stop quark pairs, Right: A pair produced stop quark topology with two invisible particles (see left) as well as reconstructed signal distributions for stop pair production with $M_{stop} = 1500\ GeV$, $M\mathrm{x}_1 = 1000\ GeV$, $Ms_\nu = 800\ GeV$ together with the expected background processes corresponding to an integrated luminosity of 50 fb^{-1} at 13 TeV

gauge mediated supersymmetry breaking

A.Kyriakis

[6] Anagnostou G. “Searching in 2-Dimensional mass space for final states with 2 invisible particles”. In: *J. High Energ. Phys. 2021, 112* (2021). DOI: https://doi.org/10.1007/JHEP07(2021)112

A search has been done for gauge mediated supersymmetry breaking in events that involve photons and large missing transverse momentum. For this analysis used pp collision data at the center of mass energy $\sqrt{s} = 13$ TeV, collected during 2016 with the Compact Muon Solenoid (CMS) detector at CERN LHC and correspond to a total integrated luminosity of $35.9 fb^{-1}$.For the interpretation of the results a gauge mediated supersymmetry scenario (GMSB) was assumed. Supersymmetry is a popular extension of the standard model (SM) of particle physics. For the analysis, a gauge mediated supersymmetry scenario (GMSB) was assumed. In GMSB models, the lightest supersymmetric particle is the gravitino, and the next-to-lightest supersymmetric particle is often taken to be the neutralino. The conservation of R parity implies that the gravitino is stable and thus, it can not be detected. The resulting imbalance in the total observed transverse momentum is referred to as missing transverse momentum , defined as the negative vector sum of the transverse momenta of all visible particles in an event. Its magnitude is referred to as P^T_{miss}. If the NLSP is bino-like, its primary decay will be to a gravitino and a photon, resulting in final states with significant P^T_{miss} and one or more photons. The results were used to set cross section limits on gluino (Figure 22) and squark (Figure **??**) pair production in this framework. Gluino masses below 1.86 TeV and squark masses below 1.59 TeV are excluded at a 95% confidence level.

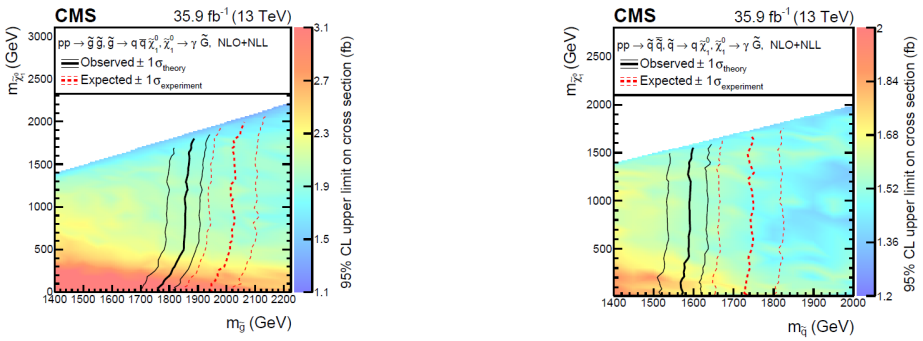

Figure 22: Left: Cross section limits on gluino below 1.86 TeV Right: Cross section limits on squark below 1.59 TeV.

CMS Tracker

P.Assiouras, P. Asenov, A.Kyriakis, I.Kazas, A.Papadopoulos, D.Loukas

During 2020 the activities of the INPP CMS group included: Process Quality Control, Irradiation studies, Development of Inner Tracker firmware and middlware and as a byproduct participation to the MuonE experiment [7]. Intensive activity on TCAD simulations is going on, mainly by Panagiotis Assiouas [8]

[7] Abbiendi. "Status of the MUonE experiment," in: *PoS.* (2021). DOI: https://doi.org/10.22323/1.390.0223

[8] A. Kyriakis P. Assiouras P. Asenov and D. Loukas. "Fast calculation of capacitances in silicon sensors with 3D and 2D numerical solutions of the Laplace's equation and comparison with experimental data and TCAD simulations". In: *J. Inst. 15 P11034* (2020). DOI: https://doi.org/10.1088/1748-0221/15/11/P11034

Process Quality Control at INPP

CMS has developed a quality assurance plan to ensure the full compliance of all sensors with the technical specifications and to monitor their production procedure and fabrication stability. Process quality control is contacted to dedicated test structures produced in the same wafer as the silicon sensors that will be installed in the CMS experiment, thus, sharing the same properties and materials. These test structures provide access to important parameters about the fabrication quality of the sensors, including parameters that are not directly accessible on the sensors and together with the sensor quality control, consist one of the two main procedures of the quality assurance plan of the Outer Tracker silicon sensors for the Phase-2 upgrade. The procedure of the process quality control on the production phase, relies on a test structure set which provides access to all relevant process parameters. Within the set, test structures are connected to 20 contact pads that allow automated measurements to be made by using a 20-needle probe card, but also it can be operated by using individual probe needles. Test structures are separated in two subsets: the quick subset which allows the most important parameters to be measured and the extended which provides the possibility for a more detailed analysis. In this work the process quality control procedure and the related test structure set is described along with the extraction procedure of the relevant process parameters. First results from the pre-production phase are presented as well.

Test Structures

The wafer layout for CMS tracker PS-s, 2S and PSp sensors includes test structures for measurements using manual probes and dedicated test structures that are arranged around an array of 20 contact pads that are equally spaced horizontally and vertically. This array of contact pads is called "flute" and it allows automated measurements to be made, by using a 20-needle probe card and a switching matrix.

Figure 23 shows one diced part of the wafer, called "Halfmoon", in which the test structure sets are constructed. Each halfmoon contains 2 sets of 4 main flutes (labeled "PQC1–PQC4") in each side that are used in the usual procedure of the process quality control. There are also 11 additional flutes in each set that can provide the possibility for in-depth analysis if irregularities are found during a standard PQC measurement, as well as standard test structures like MOS capacitors and diodes that can be measured manually with probes. Figure 24, shows a close-up of one test structure set and its components. The main flutes are separated in:

- Quick flutes: They allow a fast evaluation of the most important parameters, consisting of:
  - PQC1: It includes a quarter-sized diode ($1.25 \times 1.25\ mm$), from which the full depletion voltage and substrate resistivity are measured, a quarter-sized MOS capacitor ($1.29 \times 1.29\ mm$) for flat band voltage and fixed oxide charge concentration measurements, capacitors to evaluate the thickness of the dielectric, van der Pauw crosses [9] to measure the sheet

[9] Dieter K. Schroder. "Semiconductor Material and Device Characterization, 3rd Edition".

resistances of polysilicon, n+ implant and p-stop, and a field-effect transistor to assess the inter-channel properties.

  - PQC2: It provides a gate-controlled diode [10] which allows to access surface recombination velocity and interface trap density, a polysilicon resistor with the same dimensions as a standard bias resistor, two line width structures of n+ and p-stop implants as an addition to the van der Pauw structures of the first flute, and a dedicated structure to measure the dielectric breakdown voltage. This flute acts as an extension to the first flute to allow a complete overview of the most relevant process parameters.

- Extended flutes: In addition with the quick flutes, the extended flutes allow a comprehensive evaluation of all relevant process parameters.
  - PQC3: It provides a half-sized diode $2.5 \times 2.5\ mm$, a metal meander with 12,853 squares, a clover-shaped metal van der Pauw structure, and bulk and p+ van der Pauw crosses.
  - PQC4: It includes a gate-controlled diode with a wider gate than the gate-controlled diode in the second flute. Furthermore, the flute includes contact chains and cross bridge Kelvin resistance structures to determine the metal contact quality.

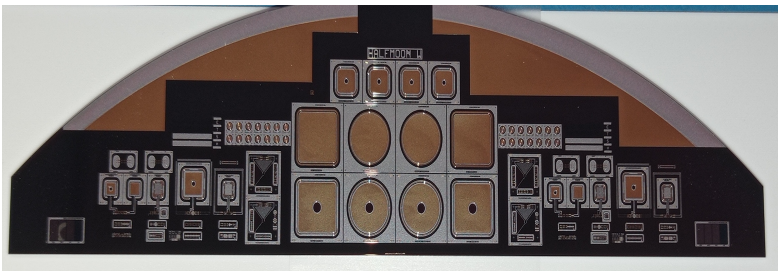

Figure 23: Photo of one halfmoon. Each halfmoon contains 2 sets of 4 main flutes. There are also additional flutes and test structures that can provide a more detailed investigation if it is needed

The PQC setup

Each PQC center has a special probe station, dedicated to test structure measurements. Although the setup in each center may vary, they share some common features and should have some specific requirements. Each setup consists of a prober with an XYZ-stage (or XY-stage with controllable vertical position of the probe card) a jig with integral cooling system and vacuum pipes and which can provide high voltage contact to the backplane of the sensor. The whole probe station setup is inside a light-tight aluminum box enclosing the probe station which

In: • (2005). DOI:

[10] C Becker et al. "Gate-controlled diodes for characterization of the Si–SiO2 interface with respect to surface effects of silicon detectors". In: *Nuclear Instruments and Methods in Physics Research Section A: Accelerators, Spectrometers, Detectors and Associated Equipment* (2000). DOI: https://doi.org/10.1016/S0168-9002(99)01177-8

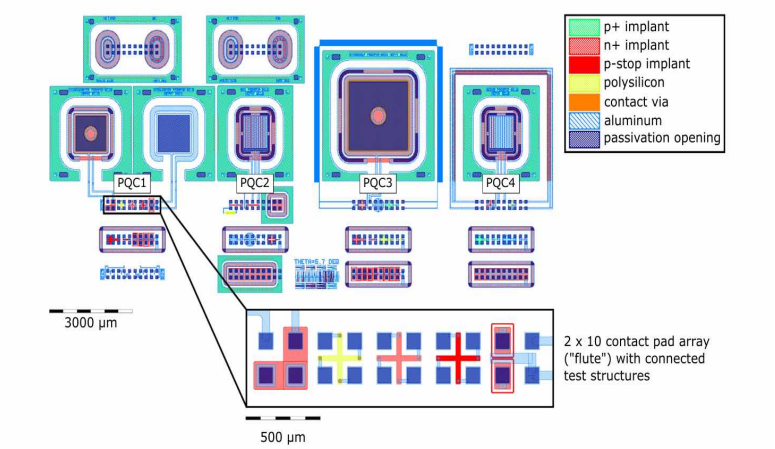

Figure 24: Schematic of the 4 different flutes that exist in each test structure set. They are separated in quick flutes allowing a fast evaluation of most important parameters and extended flutes that provide addition parameters for the quality control of the sensors. The color variation depicts the different materials and implantation with which the wafers are constructed.

provides a dark environment and prevents electromagnetic interference. A dry air compressor is constantly filling the probe station in order to maintain the relative humidity below the 20 %, some resistivity measurements (metal and polysilicon VdP, e.g.) could be performed at 30 %. The air temperature inside the enclosure should be $23 \pm 5\ ^oC$ during the measurement process.

All PQC centers use Keithley 707B six-slot mainframe supporting various cards. The PQC system uses at least one 8 × 12 High-voltage card 7072-HV and one 8 × 12 "low-voltage" Semiconductor card 7072. A 20-needle probe card (figure **??**) is used to contact the PQC flute test structures for performing automated measurements. It consists of a Printed Circuit Board (PCB) that provides all the connections and circuitry and a mount for the probe needles that is fixated to the PCB. The board provides 23 triax LEMO connectors, 20 of which are rooted to the probe needles via the PCB. One connects to a temperature and humidity sensor integrated in the PCB, and the remaining two connectors lead to an RC test circuit consisting of a 100 $M\Omega$ resistor and a 10-pf capacitor. An Atlas Copco air dryer lowers locally on the test structure the humidity bellow 20% RH. Figure 27 shows a photo of the measurement setup.

Example of PQC measurements: The Metal-Oxide-Semiconductor capacitor (MOS)

As an example of the PQC measurement follows the measurement and data analysis procedure for the MOS capacitors.

Metal-oxide-semiconductor capacitor is one of the most useful device in the study of the properties of the Si-SiO_2 interface. The parameters that can be extracted with this device are the fixed oxide charge, oxide trapped charge, mobile oxide charge, interface trapped charge, the oxide capacitance and the oxide thickness. It consists of a SiO_2 layer sandwiched between a semiconductor bulk and a

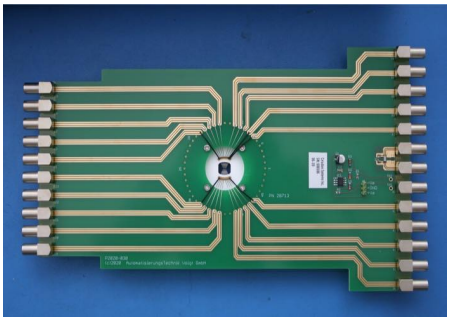

Figure 25: Probe card.

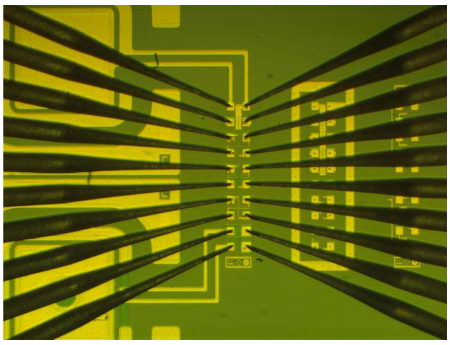

Figure 26: Probe card needls in contact with a flute.

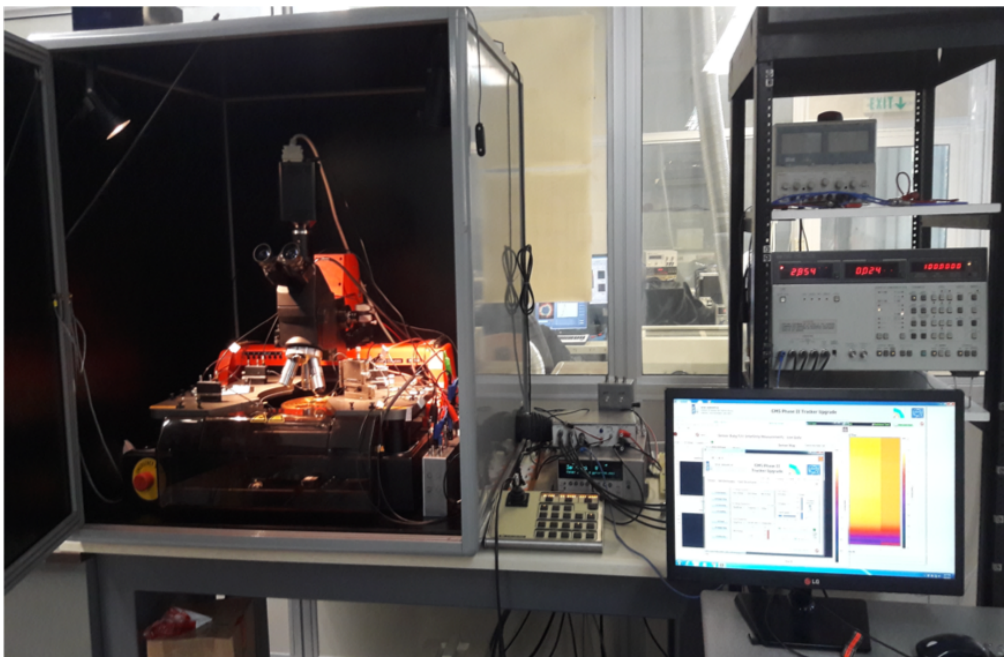

Figure 27: Photo of automatic measurement system at INPP

metal gate electrode. Figure 28 shows the design of the MOS structure of PQC1 flute.

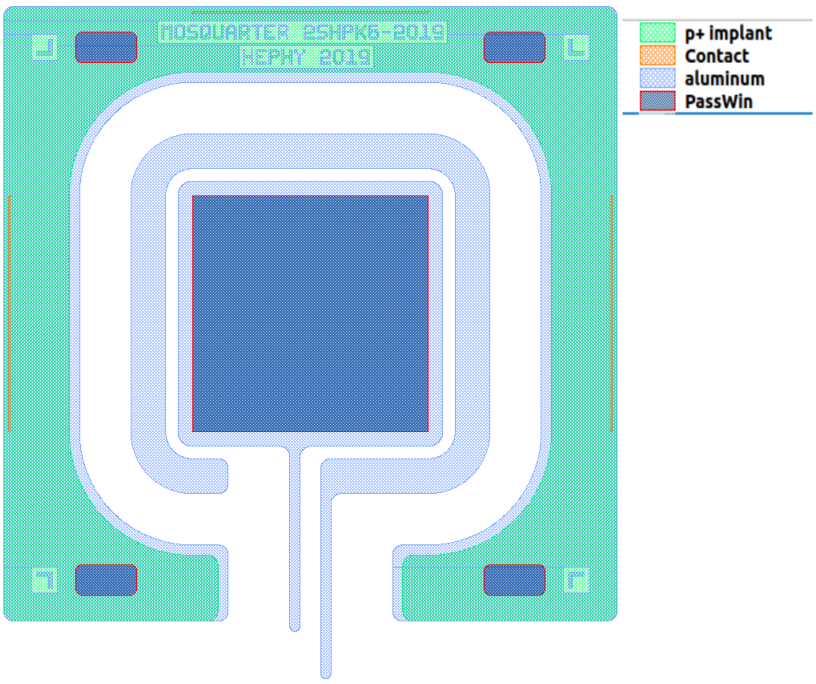

Figure 28: Design of MOS structure in PQC1 flute.

An important parameter in the study of the MOS capacitor is the flat band voltage. The flat band voltage corresponds to the voltage which when applied to the gate electrode the energy bands (Ec and Ev) of the substrate are flat at the Si/SiO_2 interface. If there is no charge present in the oxide or at the oxide-semiconductor interface, the flat band voltage (V_{fb}) simply equals the difference between the gate metal work function, ϕ_m, and the semiconductor work function, ϕ_s ($V_{fb} = \phi_m - \phi_s$), which in an ideal case equals zero ($V_{fb} = 0$). The presence of fixed oxide charges shifts the flat band voltage and this shift of the experimental MOS curve compared to an ideal curve can be used to determine the fixed oxide charge concentration N_{ox} by using the equation 1 , [11].

$$N_{ox} = \frac{C_{ox}/A(\phi_{ms} - V_{fb})}{q} \tag{1}$$

where C_{ox} is the oxide capacitance, A is the gate area of the MOS and q is the elementary charge. In the usual procedure of this measurement the bias voltage is swept from -10 to 5 V and the capacitance is measured by applying an AC pulse at 10 kHZ resulting to the characteristic curve of the MOS capacitor, figure 29.

Three characteristic regions can be identified in figure 29 that corresponds to three different phase of the MOS. In accumulation, majority carriers populate the region beneath the oxide. In this phase the capacitance is equal to the oxide

[11] S.M. Sze and G. Gibbons. "Effect of junction curvature on breakdown voltage in semiconductors". In: *Solid-State Electronics* (1966). DOI: https://doi.org/10.1016/0038-1101(66)90033-5

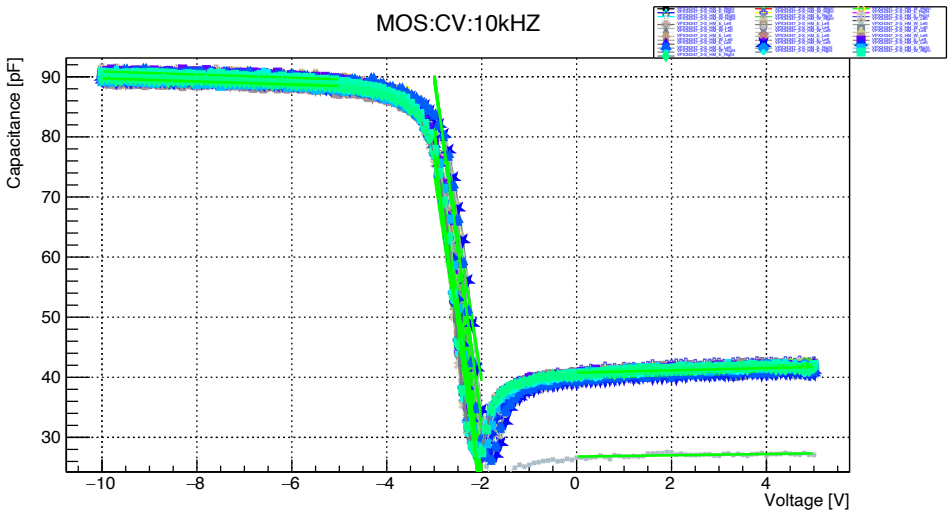

Figure 29: CV measurements performed on MOS capacitors of several wafers from one particular pre-production batch (VPX34347).

capacitance only C_{ox}. As the gate voltage increases and when is equal to the flat band voltage $V_g = V_{fb}$ the region beneath the oxide depletes, which corresponds to an abrupt decrease of the capacitance. The measured capacitance in depletion is given by the oxide capacitance in series with the capacitance of the depleted silicon bulk. In the inversion region, when $V_g \gg V_{fb}$ minority carries accumulate beneath the oxide that stops the further extension of the depleted zone. The capacitance measured in inversion depends on the AC measurement frequency and the sweep rate of the DC gate voltage. At low frequencies (5-100 Hz) electrons are generated in the substrate which enrich the inversion layer, which can follow the variations of the gate charge caused by the AC signal. The charge of the inversion layer exceeds the charge of the depleted region. In this case the depleted area does not affect the capacitance of the device and the total capacitance is equal to that of oxide $C_{inv} = C_{ox}$. At high-frequency (¿ 100 Hz) the inversion charge cannot follow the AC measurement frequency. The capacitance in the high-frequency case remains constant at a minimum value given by the oxide capacitance in series with the capacitance C_d of the space-charge region at maximum depletion width $C_{inv} = C_{ox}C_d/(C_{ox} + C_d)$.

Cobalt-60 gamma irradiation of MOS capacitors

A systematic program of radiation tests with neutrons and charged hadrons is being carried out by the CMS and ATLAS Collaborations in view of the upgrade of the experiments, in order to cope with the higher luminosity at HL-LHC and the associated increase in the pile-up events and radiation fluxes. Our group initiated at Demokritos a complementary radiation study with ^{60}Co-γ photons [12]. The doses are equivalent to those that the outer layers of the silicon tracker systems of the two big LHC experiments will be subjected to. The devices in this study are

[12] P. Asenov et al. "Study of p-type silicon MOS capacitors at HL-LHC radiation levels through irradiation with a cobalt-60 gamma source and a TCAD simulation". In: *JINST 16 P06040* (2021). DOI: https://doi.org/10.1088/1748-0221/16/06/P06040

float-zone oxygenated p-type MOS capacitors. The results of CV measurements on these devices are presented as a function of the total absorbed radiation dose following a specific annealing protocol. The measurements are compared with results from a TCAD simulation.

The samples used for irradiation in this study are float-zone oxygenated silicon n-in-p test structures from thinned 240 μm thick wafers produced by Hamamatsu Photonics K.K. (HPK) . Each test structure contains one square MOS (area = 4 mm × 4 mm).

Cobalt-60 has two characteristic gamma-ray decay modes with energies 1.1732 MeV and 1.3325 MeV, respectively. These energies are much harder than those used in common X-ray irradiation tests. The ^{60}Co source used in our study is a Picker teletherapy unit with a radioactivity of 30 TBq as of March 2012, estimated at approximately 11 TBq by the time the measurements were performed, with a horizontal orientation (Figure 30, left). It was calculated by using FC65-P Ionization Chambers from IBA Dosimetry [13] that the dose rate at irradiation point (40 cm from the source) is 0.96 kGy/h. The irradiation was performed in the secondary standard ionizing radiation laboratory of the Greek Atomic Energy Commission (GAEC), accredited according to ISO 17025 in the field of radiotherapy, and the relevant CMCs (calibration and measurement capabilities) are published in the BIPM database [14]. The electrical measurements for various doses were compared with simulations results obtained with the TCAD sentaurus suite developed by SYNOPSYS. Figure 31 shows comparisons of measurements and simulations for various doses, for more details see [15].

Figure 30: Left: The Cobalt-60 Picker therapy source. Right: The container with the samples in front of the source. The fan and the thermoelectric cooler are visible.

[13] **C**

[14] eds. C.H. Page P. Vigoureux. "The International Bureau of Weights and Measures 1875-1975: NBS Special Publication". In: *National Bureau of Standards* (1975). DOI:

[15] P. Asenov et al. "Study of p-type silicon MOS capacitors at HL-LHC radiation levels through irradiation with a cobalt-60 gamma source and a TCAD simulation". In: *JINST 16 P06040* (2021). DOI: https://doi.org/10.1088/1748-0221/16/06/P06040

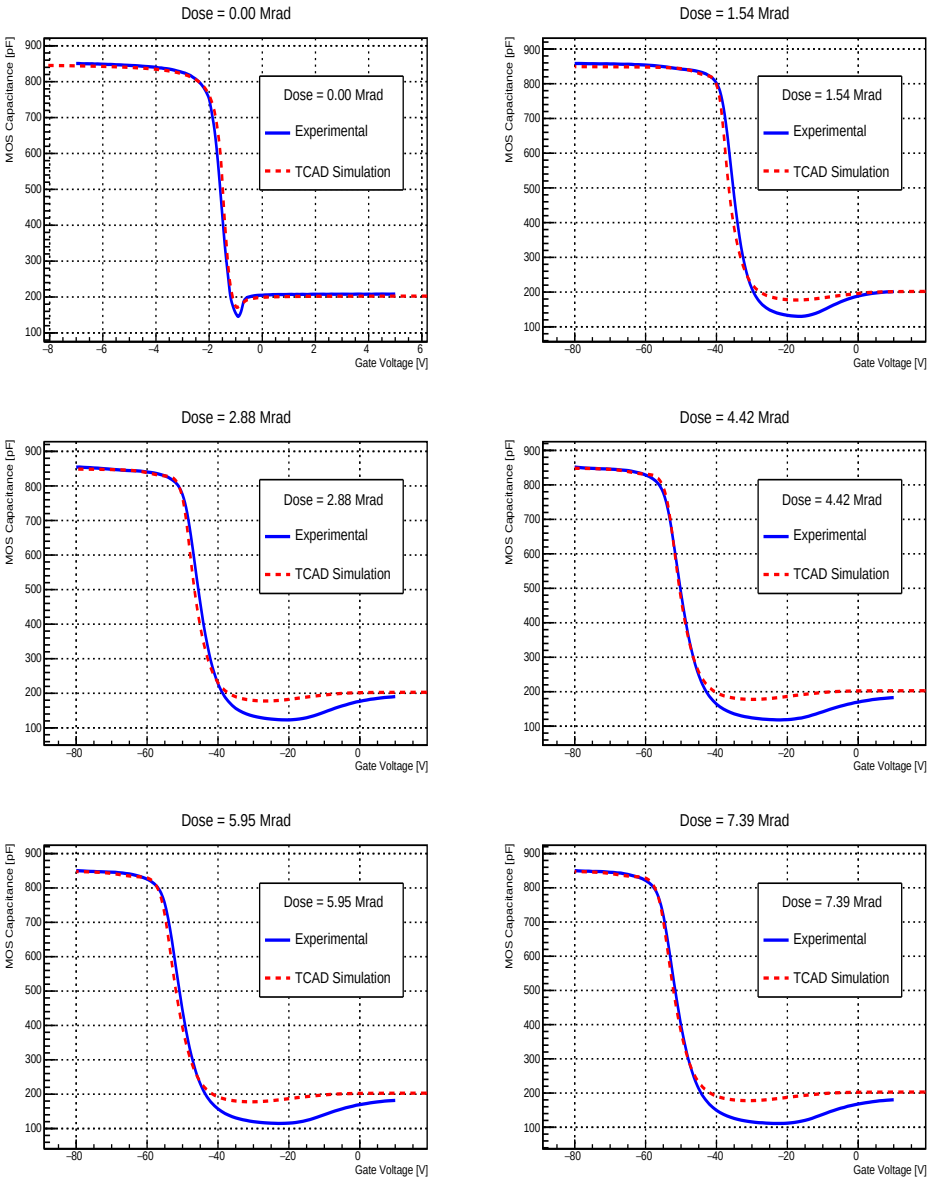

Figure 31: Experimental and TCAD simulated CV curves for a MOS capacitor for various doses; measurement frequency = 10 kHz. The model describes well the experimental data.

Work for the CMS Phase-II Inner Tracker

The Inner Tracker will be equipped with pixel modules. The high-luminosity operation implies extreme challenges for the design of the Inner Tracker in terms of radiation tolerance of sensors and readout electronics, as well as data volume to be stored in the front-end pipelines and sent out at high trigger rates. Thin silicon sensors (of thickness 100–150 mm), segmented into pixel sizes of 25×100 μm^2 or 50×50 μm^2, are expected to exhibit the required radiation tolerance and to deliver the desired performance in terms of detector resolution, occupancy, and two-track separation. Consequently, a readout chip with a small cell size and low detection threshold is required. ATLAS and CMS were carrying out a common development in the framework of the RD53 collaboration [22] and designed a pixel chip with 2500 $\mu m2$ cell size, in 65 nm CMOS technology. With such a configuration the detector resolution is much more robust with respect to radiation damage than the present detector, where the precision relies on the ability to reconstruct the tails of the charge deposit in a 300 mm thick sensor. Figure *** shows the first RD53 prototype, the so called RD53A chip. It has a total of 92×400 pixels arranged in three analogue blocks and common digital block. The FE_SYNC analogue block is based on a single stage design with SAR-like ToT counter using synchronous comparators. The FE_LIN block is a single stage design with current comparator and ToT counter. The FE_DIFF block is relying on a first stage with continuous reset integrator plus DC couple pre-comparator stage, figure 32 . Figure 33 outlines change of operation parameters from Phase-I CMS to Phase-II.

Our group is developing the firmware and middleware for the readout and control of the front end modules of Inner Tracker.Ther readout and control of the future front-end modules of the CMS Tracker, will be performed by the DQAQ, Trigger and Control(DTC) System. The μDTC project was established to perform these tasks in the prototyping and production phases. Common frameworkl for the Outer tracker (OT) and the Inner Tracker IIT) is base on FC7 board and IPBus both developed by CERBN. Figure 34 shows the suite of the DAQ system and the main players.

The MUonE experiment and the CMS Phase-II Tracker

The 2S silicon modules are the building blocks of the Outer Tracker. Fig. **??**The MUonE experiment aims at a completely independent and very precise measurement of the leading hadronic contribution to the muon magnetic moment base on a method proposed in [16].For more details see the MUonE Letter of Intent at https://cds.cern.ch/record/2677471?ln=en. Members of the CMS INPP group joint the MUonE collaboration in the summer of 2020.

The experiment will take place at the CERN SPS aiming to measure the hadronic component of the running electromagnetic coupling $\alpha(t)$, in a momentum transfer (t) region relevant for the calculation of the muon $g-2$ anomaly. The hadronic part of the running can be determined from the precise measurement of

[16] G.Abbiendi et al. "Measuring the leading hadronic contribution to the muon g-2 via μe scattering". In: *The European Physical Journal C77, 139* (2017). DOI: https://doi.org/10.1140/epjc/s10052-017-4633-z

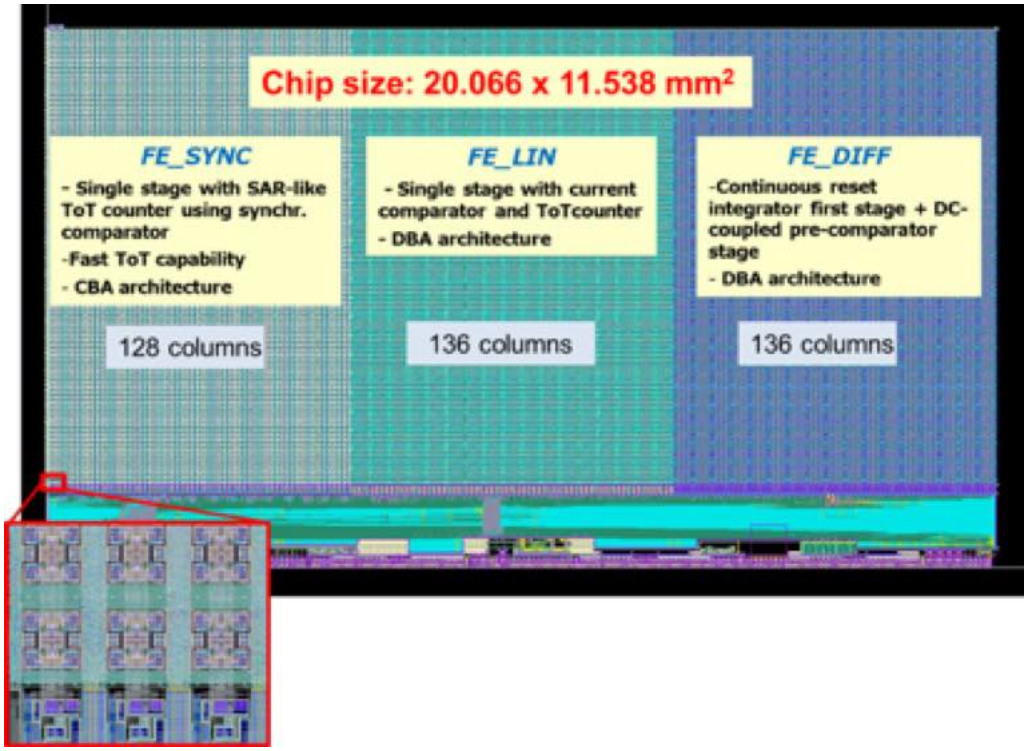

Figure 32: Layout of the RD53 ASIC

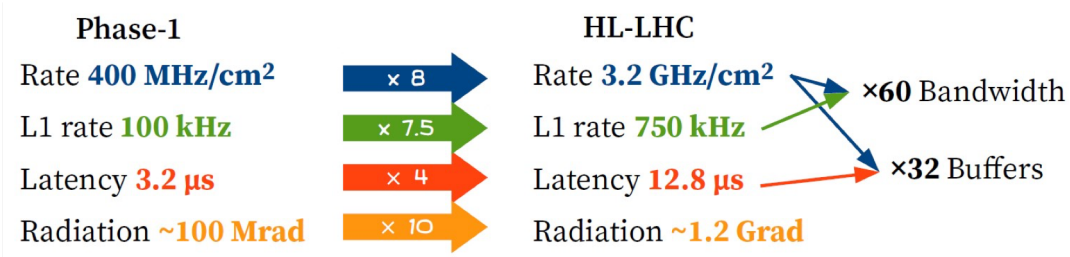

Figure 33: Change of parameters in CMS from Phase-I o Phase-II

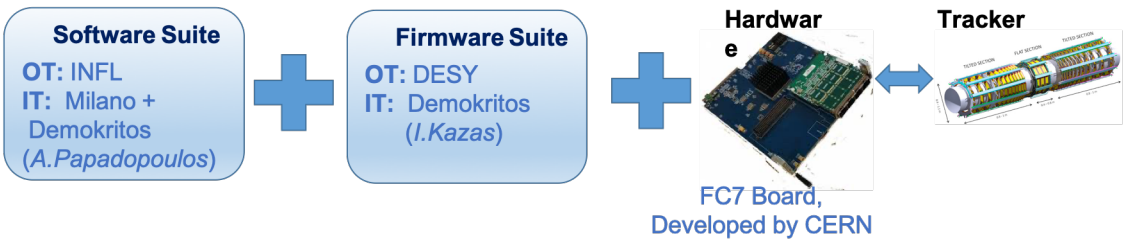

Figure 34: Block diagram of the main blocks in the CMS Phase II DAQ

the shape of the differential cross section for the $\mu e \to \mu e$ elastic process, using high energy muons impinging on electrons at rest in a low-Z target. The measurement does not rely on the absolute knowledge of the luminosity. By using the muon beam of 150 GeV (or higher), with an average rate of $\sim 1.3 \times 10^7$ $\mu\,\mathrm{sec}^{-1}$, currently available at the CERN North Area (the M2 beam), a statistical uncertainty of $\sim 0.3\%$ can be achieved on α_μ^{HLO} after ~ 2 years of data taking. The sensitivity to α_μ^{HLO} is obtained by integrating the effective fine-structure $\Delta\alpha$ in the formula:

$$\alpha_\mu^{HLO} = \frac{\alpha}{\pi}\int^1 dx(1-x)\Delta\alpha_{had}[t(x)], \tag{2}$$

where $\Delta\alpha_{had}(t)$ is a smooth function and is the hadronic contribution to the running of α, evaluated at

$$t(x) = \frac{x^2 m^2{}_\mu}{x-1} < 0, \tag{3}$$

The effect of the contributions of the hadronic vacuum polarization to the $\mu e \to \mu e$ differential cross section is to increase it by a few per mille, mainly in the kinematical region where the outgoing electron angle is below $1 -$ $mrad$. The angles of the scattered electron and muon are kinematically correlated as shown in Fig. 35 (drawn for incoming muon energy of 150 GeV). This constraint is extremely important to select elastic scattering events, rejecting background events from radiative or inelastic processes and to minimize systematic effects in the determination of t.

Our group is developing a Geant4 program in order to compare recent versions of Gean4,t where more accurate electromagnetic processes are included, with older versions. The program is initially developed by P. Asenov and is in constnat evolution, see Figure 36.

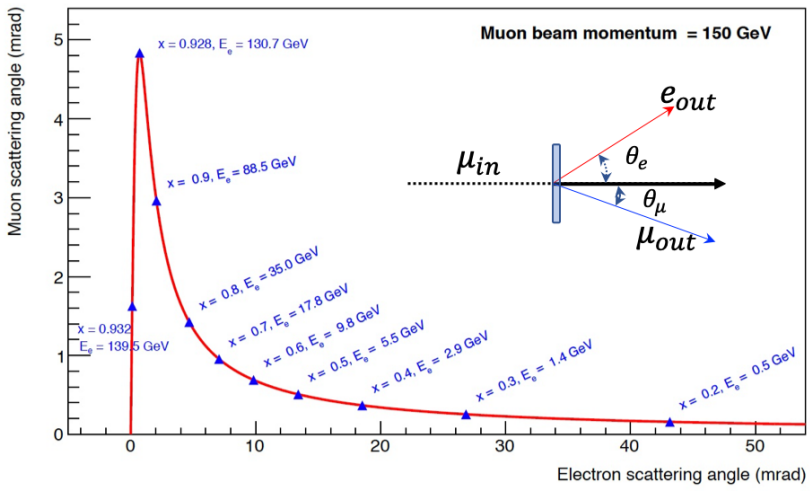

Figure 35: Correlation of muon vs electron angles from kinematical constrains

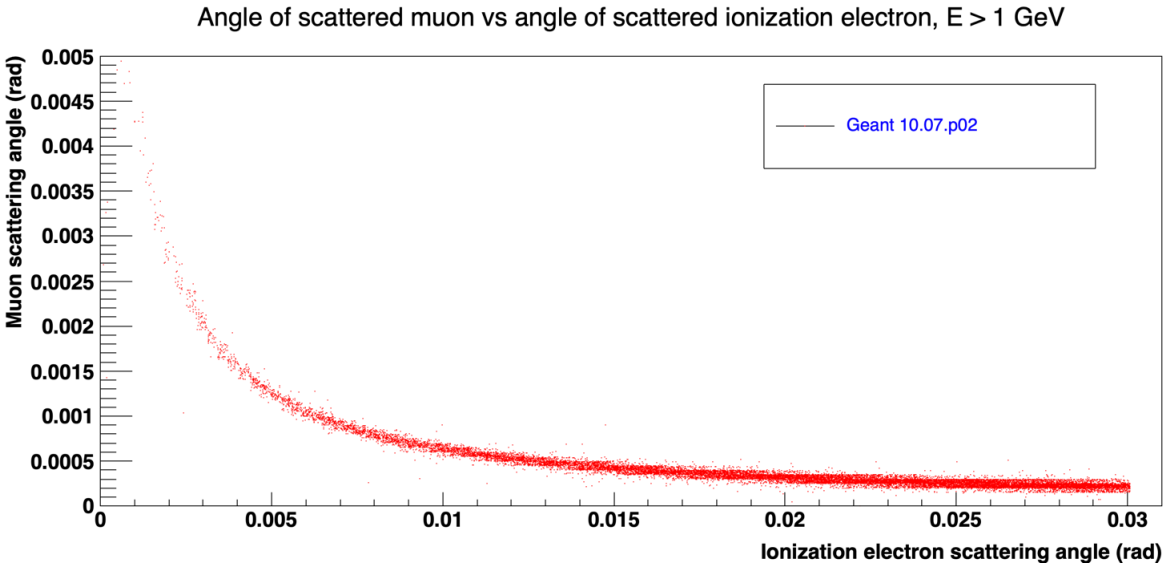

Figure 36: Geant4: Correlation of muon vs electron angles

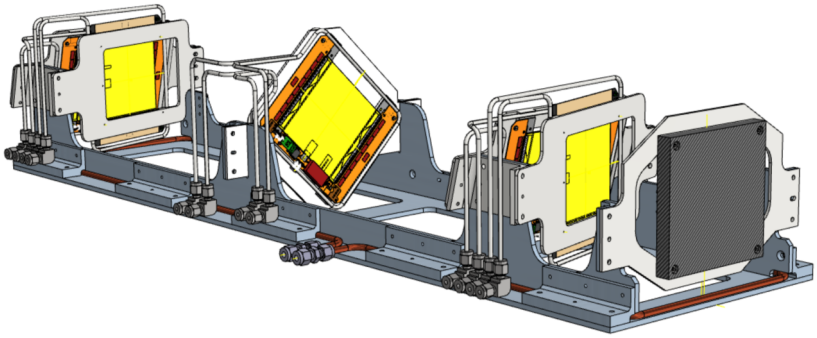

Figure 37: CAD drawing of one MUonE station equipped with three 2S modules

Funding

ESPA : Title: *"New generation of sensors and electronics for the upgrade of the CMS experiment at CERN"*. Duration ,717/03/2020 - 16/07/2021. Budget 4100.41 euro

ELIDEK: Title : *Development of the Phase-II silicon tracker of the CMS experint at CERN* . Duration , 1/11/2019 - 31/5/2021. Budget 17200 euro (P. Assiouras)

ELIDEK : Title ¨: *Silicon Sensors R&D for the HL-LHC* . Duration 5/09/2017 - 31/03/2020. Budget 27900 euro (P.Asenov)

Outreach

Overview

Theoretical High Energy Physics

Researchers:	M. Axenides (Director of research)
	C. Papadopoulos (Director of research)
	G. Savvidy (Researcher emeritus)
Adjunct Scientists:	E. Floratos (Professor emeritus, NKU Athens)
Research Associates:	G. Linardopoulos
	D. Manolopoulos
	I. Mitsoulas
	G. Pastras
PhD students:	D. Canko
	D. Katsinis
	N. Syrrakos
Master students:	N. Tsolis

Introduction

Activities

High Energy Physics - Phenomenology

The research on High Energy Physics - Phenomenology aims to develop innovative methods and algorithms in order to establish an efficient framework for higher order corrections for multi-particle processes including

- amplitude reduction at the integrand level beyond one-loop,
- the evaluation of multi-loop Master Integrals and
- the application of the above-mentioned techniques to scattering processes at the LHC and beyond.

During 2020 the group achieved a major milestone, by completing the analytic representation of all massless planar five-point amplitudes with one off-shell leg [17]. The methodology used is based upon the Simplified Differential Equations Approach (SDE) [18]. We have also studied one-loop pentagon integrals to arbitrary order in the dimensional regulator [19]. The SDE method has been also successfully applied to the canonical basis for the three-loop ladder-box with one external mass off-shell, obtaining subsequently a canonical basis for the massless three-loop ladder-box as well as its solution [20]. We have also studied the reduction of two-loop amplitudes at the *integrand level*, as part of the newly developed software package `HELAC-2LOOP`. All the above-mentioned work is essential in order to obtain high-precision predictions for scattering processes at the LHC, especially for the forthcoming high-luminosity Run.

String theory & quantum gravity

The research agenda of the group includes topics such as: (1) the bridging Quantum Field Theory (QFT) and Quantum Gravity (QGr) in the framework of the AdS/CFT duality, (2) the physics involved in the possible resolution of the black hole information paradox (3) String and M-theory. These topics constitute a very fertile ground of theoretical research on the origins of quantum gravity at the Planck scale. Quantum black holes and cosmological singularities are examples of physical systems where strong gravity effects are manifest and new concepts and principles appear to be at work such as nonlocality and strong chaotic mixing which operate in the framework of the Holographic principle and AdS/CFT correspondence. The group's published proceedings article [21] deals with M2-brane dynamics in the classical limit of the BMN matrix model. The article was the first deliverable in the group's research program "Chaotic dynamics and black holes in BMN theory" (MIS 5047794). Other published articles of the group are [22].

[17] Dhimiter D. Canko, Costas G. Papadopoulos, and Nikolaos Syrrakos. "Analytic representation of all planar two-loop five-point Master Integrals with one off-shell leg". In: *JHEP* 01 (2021), p. 199. DOI: 10.1007/JHEP01(2021)199. arXiv: 2009.13917 [hep-ph]

[18] Costas G. Papadopoulos. "Simplified differential equations approach for Master Integrals". In: *JHEP* 07 (2014), p. 088. DOI: 10.1007/JHEP07(2014)088. arXiv: 1401.6057 [hep-ph]

[19] Nikolaos Syrrakos. "Pentagon integrals to arbitrary order in the dimensional regulator". In: *JHEP* 06 (2021), p. 037. DOI: 10.1007/JHEP06(2021)037. arXiv: 2012.10635 [hep-ph]

[20] Dhimiter D. Canko and Nikolaos Syrrakos. "Resummation methods for Master Integrals". In: *JHEP* 02 (2021), p. 080. DOI: 10.1007/JHEP02(2021)080. arXiv: 2010.06947 [hep-ph]

[21] Minos Axenides et al. "M-theory as a dynamical system generator". In: July 2020. DOI: 10.1007/978-3-030-70795-8. arXiv: 2007.07028 [hep-th]

[22] George Savvidy. "Maximally chaotic dynamical systems". In: *Annals Phys.* 421 (2020), p. 168274. DOI: 10.1016/j.aop.2020.168274; Hrachya Babujian, Rubik Poghossian, and George Savvidy. "Correlation Functions of Quantum Artin System". In: *Universe* 6.7 (2020), p. 91. DOI: 10.3390/universe6070091; Roland Kirschner and George Savvidy. "Parton Distribution Functions and Tensorgluons". In: *Universe* 6.7 (2020), p. 88. DOI: 10.3390/universe6070088; Roland Kirschner and George Savvidy. "Parton Distribution Functions and Tensor Gluons". In: (May 2020). arXiv: 2005.09700 [hep-ph]; George Savvidy. "Discovery of Chromomagnetic Gluon Condensation". In: *PoS* CORFU2019 (2020), p. 162. DOI: 10.22323/1.376.0162; George Savvidy. "Yang-Mills Classical and Quantum Mechanics and Maximally Chaotic Dynamical Systems". In: (Jan. 2020). arXiv: 2001.04902 [hep-th]; George Savvidy. "Maximally Chaotic Dynamical Systems of Anosov–Kolmogorov". In: *Phys. Part. Nucl.* 51.4 (2020), pp. 410–418. DOI: 10.1134/S1063779620040644. arXiv: 2001.01785 [hep-th]; George

Small scale structure of spacetime

The Small Scale Structure of Spacetime (SSSS) project explores the possibility of a discrete spacetime structure in strong gravity environments. It proposes a modular finite quantum mechanical model for the AdS_2 near horizon geometry for the specific class of extremal black holes. The model is holographic and exhibits desirable properties at the Planck scale such as nonlocality and chaotic mixing (fast scrambling).

Boundaries and defects

Boundaries and defects play central roles in quantum field theory (QFT) both as means to make contact with nature and as tools to constrain and understand QFT itself. Boundaries in QFT can be used to model impurities and also the finite extent of sample sizes, while interfaces allow for different phases of matter to interact in a controllable way. More formally, these structures shed light on the structure of QFT by providing new examples of dualities and renormalization group flows. The group's present research focuses on three areas: 1) formal and applied aspects of boundary and defect conformal field theory, from anomalies and c-theorems to topological insulators, 2) supersymmetry and duality, from exact computations of new observables to the construction of new theories, and 3) QFT in curved space and gravity, from holographic computations of entanglement entropy to ideas in quantum information theory. The latest results of the group were in the field of holographic defect CFTs and included the publication of an original research paper [23] which dealt with the solution of two very popular models of holographic dCFTs via proving closed determinant formulas for all their 1-point correlation functions, as well as the proceedings submission [24] which summarized the author's oral presentation in the 2020 Corfu Summer Institute. The research on the physics of boundaries and defects was for the most part funded by the HAppEN project (see below).

Complex systems

The study of Non-linear Chaotic Dynamics and Complex Systems involves both research and teaching. It pertains to the interplay between chaotic dynamics and fundamental interactions. Noteworthy results have been obtained in the very past such as the observation of chaos in Yang Mills theories (G. K. Savvidy) as well as more recently in matrix and membrane dynamics of M-theory. Demokritos has been the hub of the national network of Complex Systems COSA-NaNet which organizes regular seminars on Nonlinear Chaotic Dynamics and Complexity along with a graduate level course on "Special topics on Complex Systems and Applications" in association with the National Technical University of Athens (see

Savvidy. "Extended Kolmogorov Entropy". In: (Apr. 2020). arXiv: 2004.13528 [math.DS]

[23] Marius De Leeuw et al. "Spin Chain Overlaps and the Twisted Yangian". In: *JHEP* 01 (2020), p. 176. DOI: 10.1007/JHEP01(2020)176. arXiv: 1912.09338 [hep-th]

[24] Georgios Linardopoulos. "Solving holographic defects". In: *PoS* CORFU2019 (2020), p. 141. DOI: 10.22323/1.376.0141. arXiv: 2005.02117 [hep-th]

Teaching-Outreach as well as Summer schools for undergraduate University students).

HAppEN program

The aim of the research performed in the program HAPPEN is the understanding of the connection between quantum entanglement and gravity in the framework of the holographic duality. The establishment of this connection requires the study of quantum entanglement in both sides of the duality. More specifically:

- In the bulk theory, entanglement entropy is given by the area of open minimal surfaces in AdS spaces, which are anchored at the AdS boundary. In the HAPPEN program we study the integrable structure of these surfaces and try to construct non-trivial new ones.
- In the field theory side the entanglement entropy is studied. The main focus in the program HAPPEN is the study of entanglement beyond the ground state of the theory.

During 2020, the group achieved several major goals of the program.

A long program for the construction of non-trivial minimal surfaces in AdS space, based on non-linear sigma model techniques Pohlmeyer reduction and the dressing method) was concluded. The construction and the properties of these new minimal surfaces was presented in [25].

The study of these methods for the minimal surface in AdS, revealed more general properties of the non-linear sigma models in symmetric target spaces. More specifically, the application of the dressing method for an arbitrary seed was achieved and the dressed solution was interpreted as a non-linear superposition of solutions within the family of solutions with the same Pohlmeyer counterpart as the seed [26].

Although the dressed minimal surfaces are highly non-trivial, it is not possible to construct with this method the minimal surface which is defined by specific boundary data. For this purpose an alternative description of the minimal surfaces as a geometric flow of the boundary data towards the interior of the AdS space was developed using differential geometry techniques [27]. This method cannot provide the finite terms of the holographic entanglement entropy, nevertheless it provides all divergent terms including the universal logarithmic terms in odd dimensions.

On the side of the field theory, the study of entanglement in thermal states was concluded [28]. The study reveals that the area law holds not for entanglement

[25] Dimitrios Katsinis et al. "Dressed minimal surfaces in AdS_4". In: *JHEP* 11 (2020), p. 128. DOI: 10.1007/JHEP11(2020)128. arXiv: 2007.10922 [hep-th]

[26] Dimitrios Katsinis, Ioannis Mitsoulas, and Georgios Pastras. "The Dressing Method as Non Linear Superposition in Sigma Models". In: *JHEP* 03 (2021), p. 024. DOI: 10.1007/JHEP03(2021)024. arXiv: 2011.04610 [hep-th]

[27] Dimitrios Katsinis, Ioannis Mitsoulas, and Georgios Pastras. "Geometric flow description of minimal surfaces". In: *Phys. Rev. D* 101.8 (2020), p. 086015. DOI: 10.1103/PhysRevD.101.086015. arXiv: 1910.06680 [hep-th]

[28] Dimitrios Katsinis and Georgios Pastras. "An Inverse Mass Expansion for the Mutual Information in Free Scalar QFT at Finite Temperature". In: *JHEP* 02 (2020), p. 091. DOI:

entropy, but for the mutual information. The results include a perturbative analytic calculation of the mutual information, as well as high and low temperature expansions.

Viewing the entangling surface as a defect (both in the bulk and in the boundary of holographic theories), the program also funded the research on Boundaries and Defects that was described in the previous section. The corresponding deliverables were [29].

The MixMax project

The primary objective of the MIXMAX project (2015-2018; H2020-MSCA-RISE-MIXMAX) was a systematic development of the state of the art new generation of Pseudo Random Number Generators based on Kolmogorov-Anosov C-K systems, which demonstrates excellent statistical properties, into a multidisciplinary usable product. This innovative class of RNG was proposed earlier by G. Savvidy in 1986 and by the members of the network and relies on the fundamental discoveries and results of Ergodic theory. It has been recently tested in many platforms and is evaluated as random number generator in the CMS simulation program. The MixMax generator is now included in: ROOT, Geant4/CLHEP as default generator (MixMax was set as default engine since release 2.4.0.0 deployed on November 2017 and in Geant4 since release 10.3), PYTHIA, GSL - GNU Scientific Library, the Extensions/Applications, CMS as default generator (CMS poster). The MIXMAX software has been used in the design of the NASA Solar Neutrino Spacecraft Detector by the group of researchers from NASA and by Wichita State University.

Funding

Teaching

The group offers courses in quantum field theory for graduate and undergraduate students jointly from NTUA and NCSR-Demokritos, training of graduate students for advanced degrees. Seminars and lectures in summer schools organized by Demokritos for university undergraduate students.

Overview

10.1007/JHEP02(2020)091. arXiv: 1907.08508 [hep-th]

[29] Marius De Leeuw et al. "Spin Chain Overlaps and the Twisted Yangian". In: *JHEP* 01 (2020), p. 176. DOI: 10.1007/JHEP01(2020)176. arXiv: 1912.09338 [hep-th]; Georgios Linardopoulos. "Solving holographic defects". In: *PoS* CORFU2019 (2020), p. 141. DOI: 10.22323/1.376.0141. arXiv: 2005.02117 [hep-th]

Table 10: Funding of the Theory Group

Prog. ID	Title	Host Institution	Principal Investigator	Starting date	Finishing date	Budget (€)
	CA16201: Unraveling new physics at the LHC through the precision frontier	IFIC	C. Papadopoulos	2017	2021	
	HFRI: Two-loop Amplitude Calculations Based on Integrand Reduction	NKUA	C. Papadopoulos, D Canko	2019	2022	32,400
E-12390	Operational Program Human Resources Development, Education and Lifelong Learning 2014-2020 in the context of the project 'Higher order corrections in QCD with applications to High Energy experiments at LHC'	INPP	C. Papadopoulos	2020	2022	37,000
E-12300	HFRI: Holographic APPlications of quantum ENtanglement (HAPPEN)	INPP	G. Pastras M. Axenides	2018	2021	182.598,94
E-12390	IKY: Operational Programme Human Resources Development, Education and Lifelong Learning" in the context of the project "Strengthening Human Resources Research Potential via Doctorate Research" (MIS-5000432)	INPP	M. Axenides D. Katsinis	2018	2021	30.000
E-12386	Operational Program Human Resources Development, Education and Lifelong Learning 2014-2020 in the context of the project "Chaotic dynamics and black holes in BMN theory" (MIS 5047794)	INPP	E. Floratos, M. Axenides	2020	2022	45,500

Astroparticle Physics

Researchers:	Dr. Christos Markou (Coordinator)
	Dr. E. Tzamariudaki
PhD students:	A. Sinopoulou
	D. Tzanetatos
	D. Stavropoulos
Master students:	G. Zarpapis
	A. Lygda
	Ph. Katsimalis
	A. Peza
Employees:	G. Androulakis
	C. Bagatelas
	S. Koutsoukos
Technicians:	V. Tsagkli
	A. Vougioukas
	S. Bakou

Introduction

The astroparticle physics group of the Institute of Nuclear and Particle Physics (INPP) is mainly focusing on the detection and subsequent study of neutrinos from cosmic accelerators. The study of cosmic neutrinos offers significant advantages towards answering basic questions about the origin and nature of cosmic rays. Neutrinos, being neutral, are not deflected by interstellar magnetic fields and, unlike protons, are not significantly absorbed by intervening matter. Thus, they point to their sources over all energy ranges and distance scales, and hence are uniquely valuable as cosmic messengers. In addition, the detection of astrophysical high energy neutrinos will shed light on the production mechanism of high energy gamma rays by understanding whether the sources of high energy gamma rays observed by the HESS telescope are due to electromagnetic or hadronic processes.

The INPP astroparticle physics group is a member of the KM3NeT collaboration. KM3NeT [30] is a distributed Research Infrastructure, member of the ESFRI Road Map that will consist of a network of neutrino telescopes in the Mediterranean Sea with user ports for Earth and Sea sciences. Once completed, the telescopes will have detector volumes between megaton and several cubic kilometers of clear sea water. Located in the depths of the Mediterranean Sea, KM3NeT will open a new window on our Universe and will contribute to the understanding of the properties of the elusive neutrino particles. The ARCA (*Astroparticle Research with Cosmics in the Abyss*) telescope, which is located offshore of Sicily, Italy, at a maximum depth of 3450 m, is devoted to the search for neutrinos from distant astrophysical sources, such as superenovae, gamma ray bursts or collid-

[30] S Adrián-Martínez et al. "Letter of intent for KM3NeT 2.0". In: *Journal of Physics G: Nuclear and Particle Physics* 43.8 (June 2016), p. 084001. ISSN: 1361-6471. DOI: 10.1088/0954-3899/43/8/084001. URL: http://dx.doi.org/10.1088/0954-3899/43/8/084001

ing stars. The ORCA (*Oscillation Research with Cosmics in the Abyss*) detector which is located 40 km offshore Toulon, France, at a depth of 2450 m, aims at studying neutrino properties through the precise measurement of neutrino oscillations exploiting neutrinos generated in the Earth's atmosphere. An artistic view of the KM3NeT detectors is shown if Fig. .

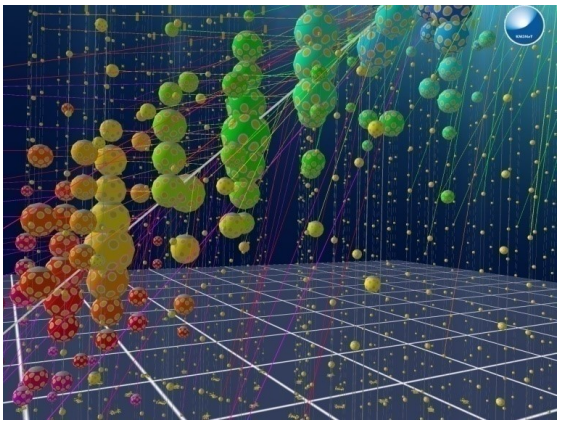

Figure 38: An artist's view of an event as it will be seen by the KM3NeT telescopes

Activities

In 2020 the group has been active in construction, testing and validation of the KM3NeT detectors and individual components, physics analyses and studies, governance and management.

KM3NeT management and governance

Dr. C. Markou served as head of the Institution Board (IB) of KM3NeT (until Fall 2020 when he completed two successive terms as head of the KM3NeT IB which is the maximum allowed). As such, among other duties, he represents the KM3NeT IB to the Resources Review Board, and the Scientific and Technical Advisory Committee of the experiment. Dr. C. Markou and Dr. E. Tzamariudaki are members of the KM3NeT Publication committee. In addition, Dr. Tzamariudaki participates in the Conference committee of the experiment, acts as the Greek-site manager and is a member of the Management Team of the experiment. Dr. E. Tzamariudaki is a member of the Equality, Diversity and Inclusion committee (EDI) of KM3NeT. G. Androulakis is the Quality Assurance / Quality Control manager of KM3NeT, member of the Management Team and the Steering Committee of the experiment.

KM3NeT contruction

Since 2016 a DOM integration, validation and testing facility has been established in the premises of INPP (Fig. 39). The DOM lab has been funded exclusively

through internal funds. It was completed in record time (compared to other similar labs in KM3NeT), and has been operational in late 2016. Ever since, the lab continues with the integration of DOMs.

Figure 39: The DOM Lab at INPP

Currently the lab employs 2 FTE of skilled personnel, with additional help from other group members as the need arises. In 2020 the DOMs of ORCA-DU1 which have been recovered due to an electrical problem and have been sent to the INPP DOM Lab, have been thouroughly tested and were successfully refurbished.

An additional contribution to the collaboration are testing and validation efforts concerning the high-pressure testing of the DOM penetrators which are used for powering the DOMs and for data transfer from the DOMs to the shore station via an electro optical cable. As the penetrators can be a single point of failure for the DOMs, acceptance testing is extremely important. These tests are curried out using a high-pressure testing chamber, capable of sustaining pressure up to 600 bars (Fig. 40). These tests are done for a large fraction of the KM3NeT DOM penetrators (120 penetrators during 2020), as the only other similar facility is in NIKHEF, Amsterdam.

The group has also undertaken the calibration of the DOM compasses which are mounted on the central logic boards (CLBs). These tests are done for the KM3NeT collaboration only in the premises of INPP. More than 100 compasses were calibrated in INPP during 2020.

In order to improve and standardize the calibration procedure, a fully automated gimbal was designed and put in operation at the INPP in N.C.S.R. "Demokritos" (project of the interim student Ph. Katsimalis). All parts are 3D printable or standard commercial components (Fig. 41). The rotations along all 3 axes are performed automatically via Arduino controlled stepper motors with pre-defined angular speed and breaks between successive rotations, eliminating the human error factor in the final calibration quality.

Figure 40: Pressure testing of the penetrators

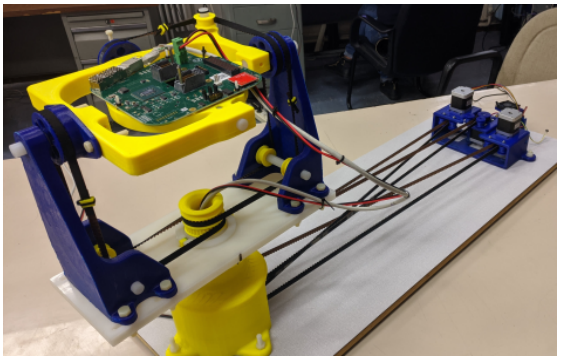

Figure 41: The fully automated gimbal designed in INPP

Physics analyses

Several group members have been active in physics analyses, focusing mainly to the analysis of the data from the first DUs of the ARCA and ORCA detectors. Most of these analyses were carried out either in the context of Ph.D. and M.Sc. theses or refer to interim projects. These are briefly outlined below.

"Analysis of the data collected with the first detection units of the under construction KM3NeT/ARCA detector"

Anna Sinopoulou, PhD Candidate, Supervisors: E. Tzamariudaki, C. Markou

This analysis focuses on optimizing requirements in order to isolate well reconstructed events and in addition, on finding suitable selection criteria for suppressing the background from atmospheric muons and identifying atmospheric neutrino candidates.

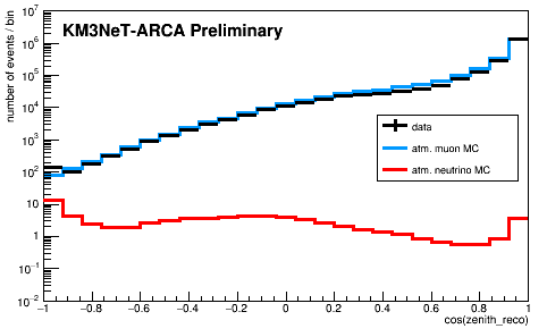

Figure 42: Distribution of the cosine of the zenith angle for all reconstructed events.

The distribution of the cosine of the zenith angle for all reconstructed events for the ARCA detector configurations with 1 and 2 detection units (DUs) is shown in Fig. 42. The requirements applied on the reconstruction level of the data are based in the detector's physics and geometry. Concerning the physics background, a minimum number of DOMs with hits in time with the reconstructed track was required. Time correlation between the hits plays a really important role at the event "accurate" reconstruction and therefore, a requirement on the minimum percentage of noise hits is also applied. Concerning the geometry of the detector at this early stage of the 1/2 DUs, the minimum track length required in order to "safely" reconstruct the event was used. In addition, the percentage of the PMTs with signal hits over all the PMT hits was investigated and a minimum acceptance value was set. This requirement is also improving the track reconstruction efficiency. Requirements concerning the reconstruction quality parameters have also been investigated and acceptance values have been set and used. All the steps of this analysis where tested in the data, atmospheric muon and atmospheric neutrino samples in order to investigate their performance and to prove their efficiency. The distribution of the cosine of the zenith angle for events that fulfill the selection criteria is shown in Fig. 43.

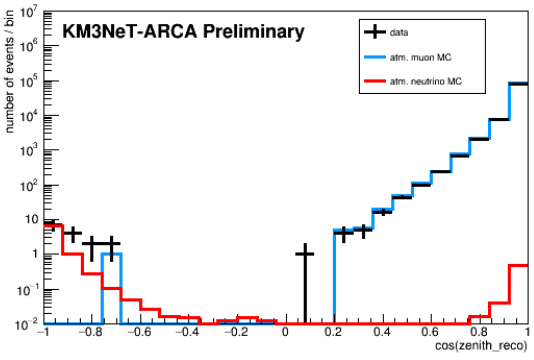

Figure 43: Distribution of the cosine of the zenith angle for events surviving the neutrino selection criteria.

Example event displays of neutrino candidates are shown in Fig. 44 and Fig. 45, where the height of the DOM hit is shown as a function of the measured

hit time, for the KM3NeT/ARCA detector configuration with one and two DUs, respectively. The height is given with respect to the lowest DOM. All DOMs with hits are represented by blue circles while DOMs with triggered hits are shown with red circles. The magenta line shows, for direct Cherenkov photons, the arrival time to the DOM as expected from the muon track reconstruction.

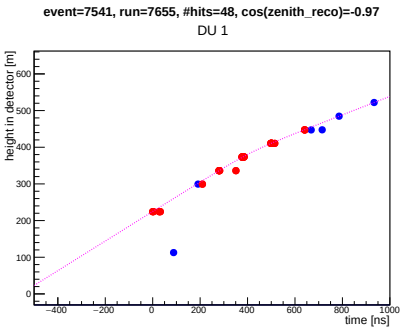

Figure 44: Height in the detector vs the time of the recorded PMT hits seen in both DUs of ARCA1 for an upgoing neutrino candidate.

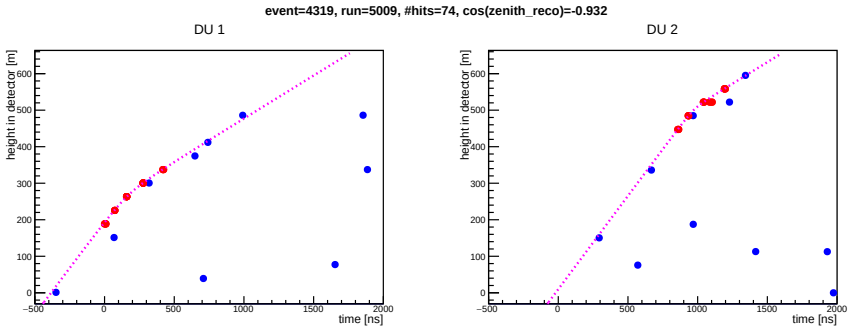

Figure 45: Height in the detector vs the time of the recorded PMT hits seen in both DUs of ARCA2 for an upgoing neutrino candidate.

In the final sample a powerful rejection of atmospheric muons misreconstructed as upgoing has been achieved as only one atmospheric muon event reconstructed with an upgoing track direction survives the final selection. 15 neutrino candidates have been found with $cos(\text{zen}) < 0$, while 8.1 were expected from the atmospheric neutrino MC in 260 days of total livetime. The energy spectrum of the upward going MC simulated neutrino events satisfying the final selection criteria is shown in Fig. 46, where a detection energy threshold of 200 GeV is observed.

A zenith angle resolution of 1.4° and 1.1° is obtained respectively for ARCA1 and ARCA2, for all reconstructed events. After the selection requirements applied, the corresponding muon zenith angle resolutions are 1° and 0.7° respectively (Fig. 47).

The aim of the analysis was to show that the detection of atmospheric neutrinos already with 1% of the full ARCA detector is possible, along with a powerful

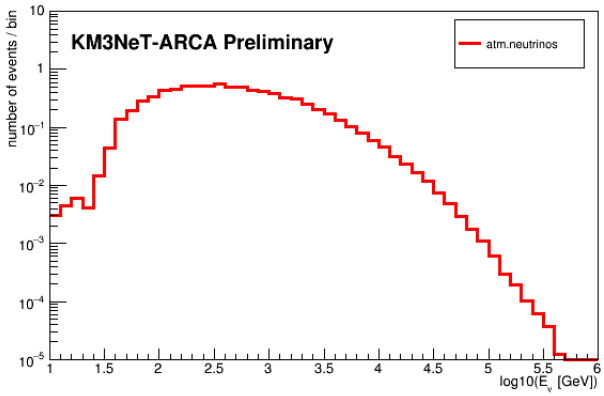

Figure 46: Energy spectrum of the upward going MC simulated neutrino events satisfying the final selection criteria.

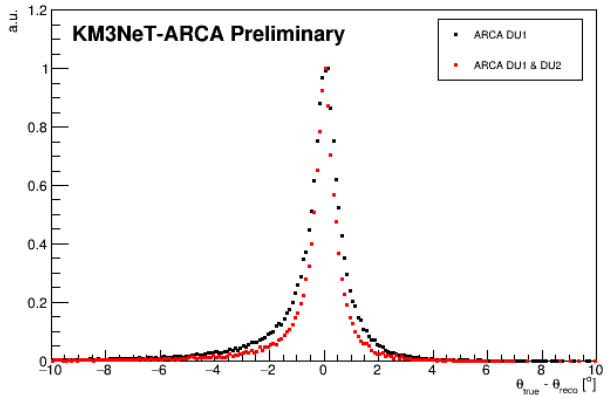

Figure 47: Zenith angle resolution for events surviving the selection criteria, separately for the two ARCA detector configurations studied.

reduction of the atmospheric muon contribution. Furthermore, a good data/MC agreement verifies the KM3NeT technology, the detector understanding and detector calibration illustrating the capability of the future KM3NeT detectors.

The results have been presented as a poster in the XXIX INTERNATIONAL CONFERENCE ON NEUTRINO PHYSICS-Neutrino2020. During the last months of the year Anna worked on the new official MC production for the full KM3NeT/ARCA detector and she started investigating variables for rejecting the atmospheric muon background.

"Analysis of the data collected with the 4 detection units of the under construction KM3NeT/ORCA detector"

D. Stavropoulos, PhD Candidate, Supervisors: E. Tzamariudaki, C. Markou

The KM3NeT/ORCA detector operated with four Detection Units (ORCA4) in the time period between 23/07/2019 and 25/01/2020. Two additional detection units (DUs) were then deployed leading to a detector configuration with six DUs. The data collected with the ORCA4 detector configuration were analysed and a

run selection was made in order to ensure the quality of the data to be processed through the reconstruction algorithms. The fraction of the information discarded as a result of high bioluminescence activity is presented in Fig. 48 for all ORCA4 runs. Runs with very high trigger rates due to bioluminescence have been rejected from the analysis (red markers) while runs with lower values are kept (blue) for further analysis. The average detector trigger rate as a function of the run number is shown in Fig. 49.

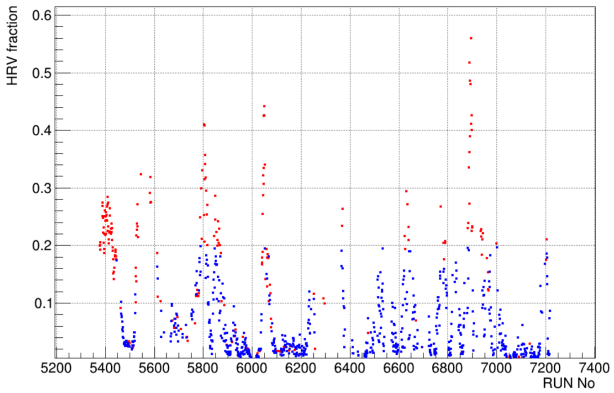

Figure 48: The fraction of the information discarded as a result of high bioluminescence activity for all ORCA4 runs. The selected runs are shown in blue and the rejected runs in red.

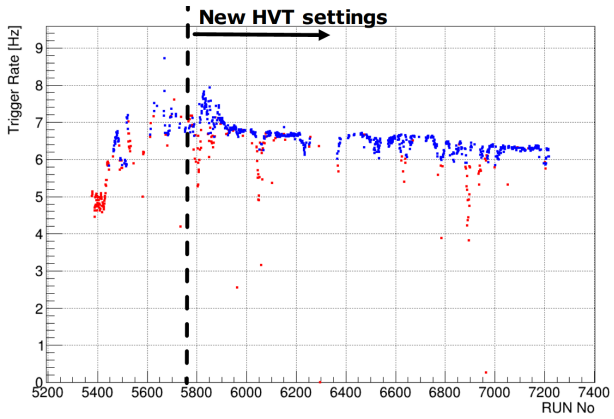

Figure 49: The event trigger rate of the detector as a function of the run number. The selected runs are shown in blue and the rejected runs in red.

The data selection corresponds to a livetime equivalent to 141 days. The data were reconstructed under the track hypothesis using algorithms developed and implemented by the KM3NeT collaboration. Concerning the simulation, Monte Carlo-based software programs were used to simulate atmospheric neutrino and antineutrino events of each flavour (signal), as well as atmospheric muon and random noise events (background). In order to identify the signal events, selection criteria were chosen by studying the reconstruction quality parameters, the topology of hits in the event, as well as the position of the reconstructed vertex. Applying these criteria to the data results in 267 events, while 273.2 events are

expected from the simulation. The results are presented in Fig. 50, where the distribution of the cosine of reconstructed zenith is presented for all events (dashed lines) and for the selected events (solid lines).

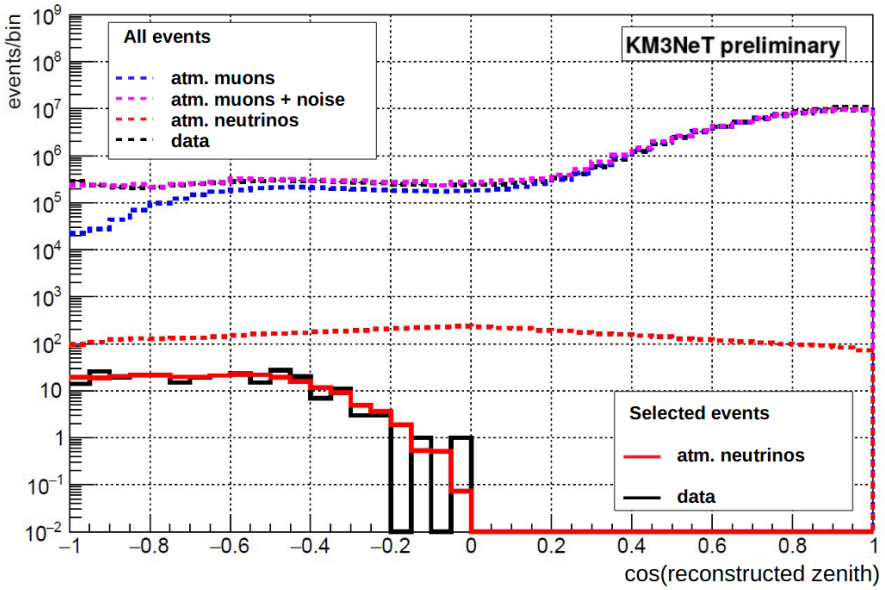

Figure 50: Distribution of the cosine of the reconstructed zenith angle for all ORCA4 data and simulated events (dashed lines) and for the selected data and simulated events (solid lines)

This analysis was presented in The 29th International Conference on Neutrino Physics – Neutrino2020 (10.5281/zenodo.4122661).

"Acoustic detection of neutrino signals"

V. Tsourapis, Ph.D. student. Supervisor: C. Markou

Vasilis Tsourapis, a new PhD student, joined our team in October 2020. During that early period he became familiar with the studies already carried out within our group on the acoustic detection of neutrino signals. In addition, he also started using the ACORNE and CORSIKA software packages which are needed to produce a fully fledged simulation on acoustic detection.

"Monitoring of the PMT rate to identify *problematic* PMTs"

A. Lygda, interim student. Supervisor: E. Tzamariudaki

During 2019, D. Stavropoulos had studied the long-term performance of the ARCA detector by analysing data from the first detection units deployed off shore Sicily. The purpose of this analysis was to evaluate the sedimentation effect and its impact on the detection rates of the PMTs of the upper hemisphere of the DOMs and to monitor the mean PMT single rates to study the detector functionality and verify its description by the MC simulation.

A. Lygda has used the analysis of D. Stavropoulos as a starting point and has deveoped tools to automize the identification of "*problematic*" PMTs by monitoring the PMT rates. The term "*problematic*" here includes not functional PMTs, PMTs with improper HV settings (PMTs set on a too-high High Voltage) as well as PMTs with low rate (< 2 kHz) (Fig. 51). The analysis provides information on the functionality of the PMTs on a run-by-run basis. This information is very useful for the run-by-run MC simulation of the detector response, but also for identifying problematic PMTs and, if it is possible, for taking corrective measures (i.e. for PMTs identified as set on too-high HV).

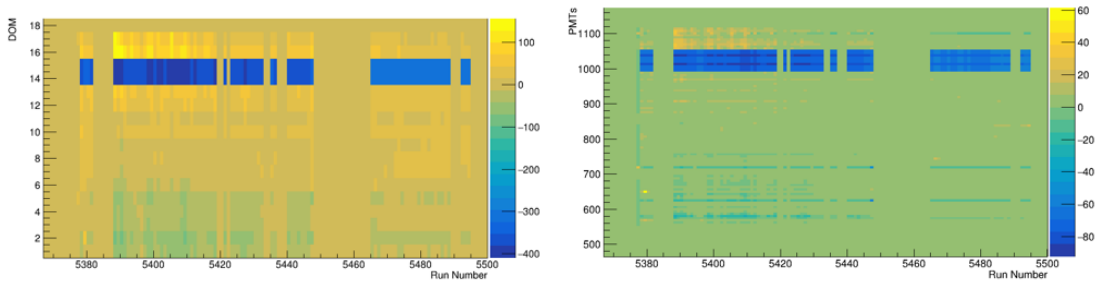

Figure 51: Left: Mean PMT rate for all DOMs of DU2 of the ORCA detector for the running period studied. Right: The difference of the rate of each PMT from the mean PMT rate is shown for all PMTs of DU2 of the ORCA detector for the running period studied

"Analysis of acoustic pulses produced by high energy neutrinos"

A. Peza, interim student. Supervisor: C. Markou

During her internship, Alexandra Peza carried out an analysis of acoustic pulses produced by high energy neutrinos. The main goal of the analysis was to separate the incoming signal from the background and, in doing so, the advanced mathematical method of wavelet transformation was used. More specific, the Wavelet transformation is a transformation between time and frequency, which aims to find temporally located frequencies of interest. The frequencies of interest may have come from sudden, short-lived, low-energy events that would have been overlooked during the Fourier transformation. The Gaussian Wavelet Transform has been used for the analysis. The goal is to compare different types of wavelets which could possibly result in improving the detection potential (resulting to a better and clearer detection). Using the Gaussian Wavelet Transform for a sound file, the 3 wavelets with the most satisfying results were the following ones:

Before adding the neutrino pulse to the background , a constant number C has been used in order to determine which is the minimum C value, for which the pulse is seperated from the noise. The pulse shape is added to the background multiplying with a constant C to adjust the relative (comparing to the background) magnitude of the pulse. The quantity max−min = maximum − minimum coefficient is used for the signal classification. If no pulse is inserted, the noise after the wavelet transform is "uniform". Due to that, the maximum value of the coefficients will not differ much from the minimum. In the case a pulse is added,

the uniformity is damaged, so the maximum - minimum value will differ; if no diffirence is observed then the wavelets can not distinguish the pulse. Therefore, the Max-Min coefficient makes it possible to find in which value of C, or more precisely up to which minimum or maximum value of C, the wavelet can detect the pulse. As in a fourier transformation, wavelet transformation also returns coefficients, but the difference compared to the fourier transformation is that the coefficients are frequency and time dependended.

The difference for max−min for different values is shown in Fig. as a function of C for different values of the frequency.

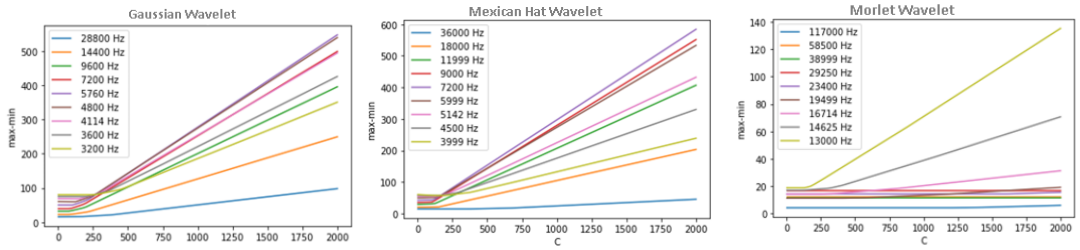

In order to test and verify these results the procedure was repeated for more sound files and the results, which were used to evaluate the different wavelets for the detection of acoustic pulses, are shown in Figures ...

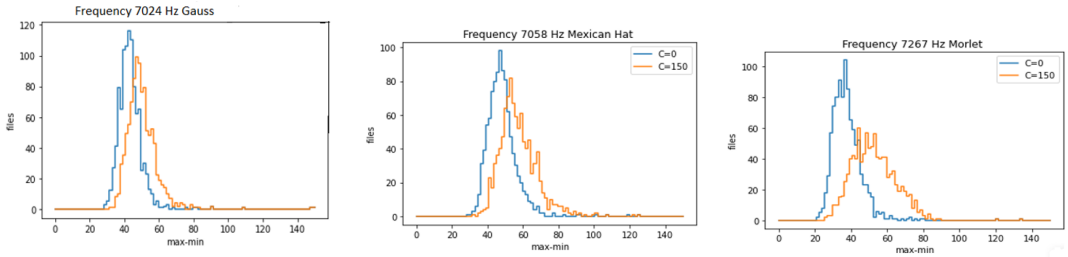

The difference max-min is quoted for each sound file. The analysis focuses on identifying wavelets for which the difference between max and min for the case of no signal (C=0 means only noise) small compared to the case when a neutrino pulse is added.

Quality Assurance and Quality Control (QA/QC) for KM3NeT

The distributed organization of KM3NeT production induces some special characteristics in the construction of the detector: there are two installation sites, integration of detection units is distributed over more than ten integration sites, qualification and acceptance testing of components is performed in several testing facilities around Europe and procurement of components is done centrally by individual institutes-budget holders. Under this framework, ensuring a uniformity in the production quality and traceability of all those components that travel continuously between European institutes are challenging tasks, requiring a robust QA/QC system.

The quality group of KM3NeT is one of the largest technical groups of KM3NeT. It is coordinated by G. Androulakis, who is interfacing between KM3NeT production and governing bodies in order to monitor and improve the quality of the

detector. The scope of KM3NeT QA/QC spans all stages of commisioning of the detector, from integration, testing, installation of detection units and operation, to calibration and embedded software. In particular, the KM3NeT QA/QC group is responsible for

- KM3NeT-wide management of non-conformities;
- administration of design changes and validation thereof;
- ensuring traceability of components travelling between tens of sites and getting integrated

and contributes to

- reliability studies and identification of critical failure modes of subsystems;
- risk analysis;
- organisation of KM3NeT documentation;
- definition of the central DB structure

The QA/QC manager is responsible for reporting to oversight committees such as the KM3NeT Institute board (IB), Scientific and Technical Advisory Committee (STAC) and the Resource review Board (RRB). By the KM3NeT organogram, G. Androulakis in his capacity as QA/QC manager is de facto a member of the Project Steering Committee as well as the Management Team, thus strengthening INPP's involvement in the decision making of KM3NeT.

KM3NeT-INFRADEV

In 2017 the KM3NeT-INFRADEV project started, funded by H2020 for a period of 3 years. In the context of this project, Dr. E. Tzamariudaki is the coordinator of Workpackage 9, on "Technology transfer" and Dr. C. Markou is the coordinator of Workpackage 10 on "Zero carbon footprint". Members of the group are also involved in most other WPs of the project. Several WPs, among which WP4 and WP9 have been extended to the end of 2020.

"Measurement of the optical parameters of water"

S. Koutsoukos, G. Zarpapis, A. Vougioukas, E. Tzamariudaki, C. Markou

Commercially available instruments are not well suited for measurements of the optical parameters of the deployment sites as the small length optical base of such instruments requires an increased accuracy of the light intensity measurement. In order to obtain a reliable measurement of the water transparency, an open geometry light measuring system, the Long Arm Marine Spectrophotometer (LAMS), was constructed and was used to measure the transmission length in deep sea during the sea campaigns in 2008 and 2009 ([31]). In the context of Technology transfer (WP 9 of the KM3NeT-INFRADEV project), a new version of the LAMS device is being constructed, keeping the same idea of measuring the transmission length, but simplifying the process by performing in a single deployment, simultaneous measurements at three different distances between emitter and receiver (Fig. 52) instead of three deployments needed for the original LAMS. In this way, the total measurement time can be reduced to just a few (6) hours, the time

[31] E. G. Anassontzis et al. "Water transparency measurements in the deep Ionian Sea". In: *Astropart. Phys.* 34 (2010), pp. 187–197. DOI: 10.1016/j.astropartphys.2010.06.008

being dominated by the time required to deploy and recover the system at the intended water depth. Since the design and operation of the old version of LAMS was successful, it was decided that the changes of the redesigned system be limited to those necessary and cannot be avoided (due to the lack of components which are no longer in production for example), or to small changes that would greatly improve the efficiency of the measurement. The new system will also record data from an external pressure sensor in order to register the depth of the system during deployment.

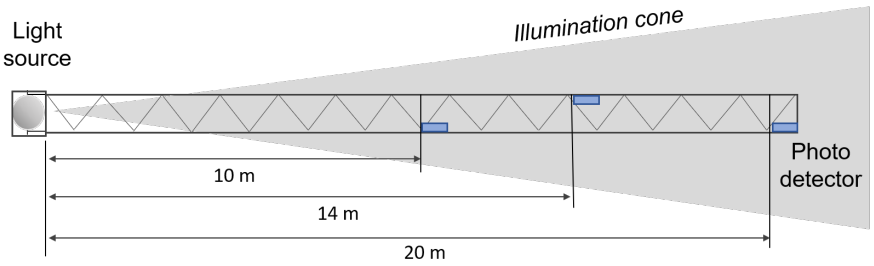

Figure 52: Rough schematic showing the placement of light receivers and the light source

The light emitter and the support structure (without the 2m long steel arm) of the original LAMS device are utilised, while three autonomous receiver units have been redesigned. In order to perform the three light intensity measurements simultaneously, the light sensor modules need to be smaller in size compared to the original LAMS, and to be mounted on the inside of the metal support at distances of 10m, 16m and 20m away from the light source. Custom made cylindrical steel casings have been constructed to house the new receivers. The new pressure steel casings are placed diagonally inside the frame at 10m, 16m and 20m mounted securely at the corners of the square cross section titanium frame, all facing the light emitter.

In 2020 the stainless steel pressure casings which house the electronics and battery packs have been pressure tested. Also, the internal support structures that hold the boards and batteries and all associated cabling have been finalized and tested. Extensive tests have been carried out during the system integration to check the functionality and stability of the system. A snapshot of typical cycles of LAMS data (obtained in the LAMS assembly area) from a configuration with optical path of 10m is shown in Fig. 53.

"Report on implementation and user tests of virtual education centre and on training workshops"

D. Stavropoulos, Ph.D. candidate

The KM3NeT Research Infrastructure will, over a period of at least a decade, produce a large amount of unique scientific data that are to be made available to the scientific communities concerned and to the broader general public. This requires the set-up of tools, procedures, documentation and rules to provide this service. Training on how to handle and analyse the data is essential for external usage. This training is provided through the KM3NeT Virtual Education Centre (edu.km3net.de). The tutorials prepared for this training have been im-

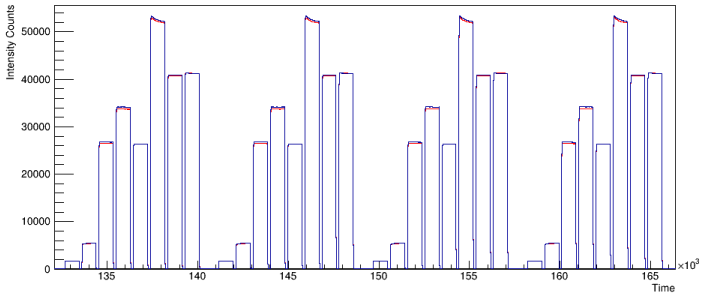

Figure 53: A snapshot of typical cycles of LAMS data (obtained in the LAMS assembly area) from a configuration with optical path of 10m is shown. The photodiode response is given in ADC counts.

plemented in the context of the "Open access to KM3NeT data" work package of the KM3NeT-INFRADEV. These tutorials are in the form of videos. They introduce several ways of accessing the KM3NeT open data, how to implement simple statistical analysis as well as combined analysis between the KM3NeT open data and open data provided by other experiments. For each tutorial, the user is suggested to practice hands-on with an exercise related on the material in which he/she has been introduced to. More details about this work can be found at https://www.km3net.org/wp-content/uploads/2021/03/D4.11-KM3NeT-Virtual-education-centre.pdf

Funding

Outreach

Our Institute participated in the organisation of the drawing contest "Draw me a neutrino", launched by the KM3NeT Collaboration. Participants in this contest were invited to a send a drawing of (their interpretation of) a neutrino. There were no restrictions on the drawing technique and the invitation was published in the KM3NeT pages and in the social media, introducing neutrinos to the general public and describing the physics goals of KM3NeT. The contest addressed different age groups, with the drawing of a different neutrino species assigned to each age group (primary school, highschool, and adults). The contest was very successful, with more than 500 drawings submitted from 16 defferent countries. The winning drawings were announced in an online ceremony which was attended by a large audience from all participating countries. A dedicated KM3NeT Virtual Neutrino Art Centre hosts a selection of these drawings. The contest logo is shown in Fig. 54 and the winning drawings are shown in Figs. 55, 56 and 57.

Overview

Figure 54: Logo of the "Draw me a neutrino" contest.


Figure 55: The winning drawings in the electron-neutrino category (left: by Amalia Kosmatou, Greece and right: by Chahna Jain, India

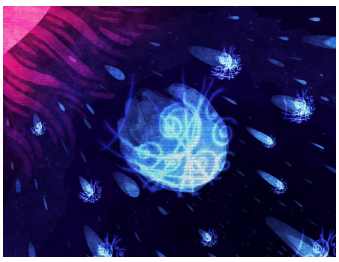
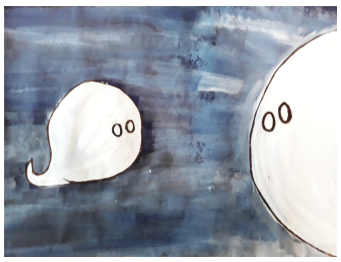

Figure 56: The winning drawings in the muon-neutrino category (left: by Mariam Darjania, Georgia and right: by Aadishri V. Kher, India

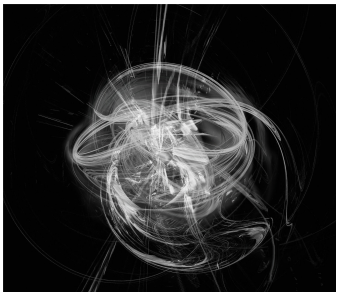
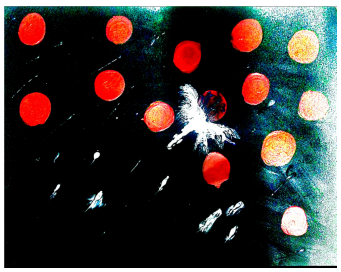

Figure 57: The winning drawings in the tau-neutrino category (left: by Evangelos Zacharopoulos, Greece and right: by Vs. sai Karthik, India

Nuclear Physics and Applications

Theoretical Nuclear Physics

Researchers:	Dennis Bonatsos
Research Associates:	Ioannis Assimakis
	Konstantinos Karakatsanis
	Andriana Martinou
PhD students:	Smaragda Sarantopoulou
	Hadi Sobhani
Master students:	Spyridon Peroulis

Introduction

The knowledge of nuclear structure is the basis for the evolution of new technology. For instance the discovery of new metastable (long living) nuclear states can lead to new nuclear medicines. Unstable nuclei can be used in the construction of nuclear batteries, to solve the problem of energy storage. But nuclear structure is also the basis for the discovery of new physics. The detection of dark matter relies on the calculation of the "nuclear form factors", which derive from nuclear structure. The theoretical calculation of the abundances of chemical elements in the universe can be used to approve or reject cosmological models. Such calculations rely on the firm knowledge of the nuclear structure. Physics beyond the Standard Model can emerge if the neutrino-less double beta decay is realized. The calculations for such a reaction very much depend upon the nuclear structure.

The most well-established (and actually Nobel Prized) theoretical model for the study of Nuclear Structure is the Nuclear Shell Model. Computer codes, based on the Nuclear Shell Model, have been developed by various researchers worldwide, to deliver theoretical predictions about the nuclear structure observables. But since the nucleus is a many-body system consisting by protons and neutrons, which interact through a yet unknown force, the so called "strong force", even super-computers fail to run these codes for medium mass and heavy nuclei.

Therefore the nuclear physics society is developing the Algebraic Nuclear Models, in its effort to cut back the computational work. The algebraic version of the Nuclear Shell Model, namely the Shell Model SU(3) symmetry, was introduced by J. P. Elliott in 1958 [32], but unfortunately it was meant to be applied only in light nuclei. Various attempts [33] had been made since then to extend this symmetry in medium mass and heavy nuclei, in which the computational work is more demanding.

The research group of Nuclear Theory in I.N.P.P. Demokritos has developed its

[32] J. P. Elliott. "Collective motion in the nuclear shell model. I. Classification schemes for states of mixed configurations". In: *Proceedings of the Royal Society of London. Series A. Mathematical and Physical Sciences* 245.1240 (May 1958), pp. 128–145. DOI: 10.1098/rspa.1958.0072

[33] József Cseh. "Some new chapters of the long history of SU(3)". In: *EPJ Web of Conferences* 194 (2018). Ed. by N. Arsenyev et al., p. 05001. DOI: 10.1051/epjconf/201819405001

own theory, the proxy-SU(3) symmetry, which actually extends the Shell Model SU(3) Symmetry in medium mass and heavy nuclei. The model was introduced in 2017 in Ref. [34] and gave immediately parameter free calculations about the nuclear shape in Ref. [35]. In Ref. [36] Bonatsos explained why the protons and neutrons have to occupy the valence nuclear shell with a specific order, forming the highest weight SU(3) irreducible representation (irrep). With the use of the highest weight irrep one may predict correctly the critical nuclei in the prolate-oblate nuclear shape transition.

Potentially in the future, the proxy-SU(3) symmetry can be used for the calculation of literally every nuclear observable. For instance the life-times of long living nuclear states (metastable or isotopic states), which are important for nuclear medicines and nuclear batteries, can be predicted. Realistic calculations can also be performed about: a) the nuclear spectrum and b) the nuclear binding energies, which are vital for the knowledge of nuclear stability, for the energy amount which is stored in a nucleus and for the nuclear astrophysical processes. The yet unsolved riddle of nuclear structure, the phenomenon of " shape coexistence", in which the nucleus has two distinct shapes in low energies, can also be unveiled within the Shell Model SU(3) symmetry. The proxy-SU(3) symmetry is being mathematically and physically constructed upon *coherent nuclear states*. Such states are rare in nature and are absolutely necessary for the construction of quantum computers. Those mentioned above are only few of the vast future applications of the proxy-SU(3) symmetry.

Activities

Despite the fact that the year 2020 was the year of the pandemic and of worldwide lock-downs, it was a very productive year for the Nuclear Theory group in the I.N.P.P. The group published 6 articles in peer review journals during 2020 and opened up the proxy-SU(3) symmetry to national and international collaborators.

In Ref. [37] Bonatsos along with international collaborators from Iran, China and the U.S.A studied the nuclear wave-functions and the energies of the critical point among the vibrational and the γ-unstable nuclei. Vibrational nuclei are considered to be near-spherical, while γ-unstable nuclei look like an unstable liquid drop, which can easily go from axially symmetric shapes into triaxial ones.

Afterwards in Ref. [38] Bonatsos along with collaborators from Iran studied

[34] Dennis Bonatsos et al. "Proxy-SU(3) symmetry in heavy deformed nuclei". In: *Physical Review C* 95.6 (June 2017). DOI: 10.1103/physrevc.95.064325

[35] Dennis Bonatsos et al. "Analytic predictions for nuclear shapes, prolate dominance, and the prolate-oblate shape transition in the proxy-SU(3) model". In: *Physical Review C* 95.6 (June 2017). DOI: 10.1103/physrevc.95.064326

[36] Dennis Bonatsos. "Prolate over oblate dominance in deformed nuclei as a consequence of the SU(3) symmetry and the Pauli principle". In: *European Physical Journal A* 53.7 (July 2017), p. 148. DOI: 10.1140/epja/i2017-12346-x

[37] Hadi Sobhani et al. "Analytical study of the γ-unstable Bohr Hamiltonian with quasi-exactly solvable decatic potential". In: *The European Physical Journal A* 56.2 (Feb. 2020). DOI: 10.1140/epja/s10050-020-00048-5

[38] Dennis Bonatsos, Hadi Sobhani, and Hassan Hassanabadi. "Shell model structure of proxy-SU(3) pairs of orbitals". In: *The European Physical Journal Plus* 135.9 (Sept. 2020). DOI:

the single nucleon orbitals that must replace one another, in order to restore the Shell Model SU(3) symmetry and thus create the proxy-SU(3) symmetry [39] in medium mass and heavy nuclei. The orbitals were viewed in the framework of a) the Deformed Shell Model (Nilsson Model) and b) the Shell Model. The outcome of this study was that each Nilsson orbital corresponds to a single shell model eigenvector. Therefore very simple replacements of orbitals have to take place, within the Shell Model, so as to elaborate the proxy-SU(3) symmetry in heavy nuclei.

Almost simultaneously the Nuclear Theory group along with collaborators from Bulgaria and Hungary published the article [40], in which they established both physically and mathematically the proxy-SU(3) symmetry by introducing a unitary transformation among the single-nucleon orbitals, which replace one another in the proxy-SU(3) symmetry. The idea and the implementation has been achieved by constructing a computer code in Mathematica. The significance of this achievement was that for the first time there has been an extension of the Shell Model SU(3) symmetry, which treated together the intruder along with the normal parity orbitals in the valence shell corroborated by a unitary transformation. The nuclear physics society had been trying [41] to invent such an extension of the Shell Model SU(3) symmetry since 1972 [42].

Later on, the collaboration of the Nuclear Theory group in the I.N.P.P. with the Iranian, Chinese and American colleagues resulted to another publication [43], in which the critical point among the vibrational and the γ-unstable odd-mass nuclei was studied. This work was the follow-up of Ref. [44] and concerned calculations for the energies and electric transition probabilities (B(E2) values) of the ^{187,189,191,193,195}Ir isotopes.

The next to come was Ref. [45], in which the Nuclear Theory group of I.N.P.P. proved that the highest weight irreps should be used in the framework of another (older) extension of the Shell Model SU(3) symmetry, namely the pseudo-SU(3) [46], in order to predict correctly the prolate-oblate nuclear shape transition. This

10.1140/epjp/s13360-020-00749-2

[39] Dennis Bonatsos et al. "Proxy-SU(3) symmetry in heavy deformed nuclei". In: *Physical Review C* 95.6 (June 2017). DOI: 10.1103/physrevc.95.064325

[40] Andriana Martinou et al. "Proxy SU(3) symmetry in the Shell Model basis". In: *European Physical Journal A* 56.9 (2020), p. 239. DOI: 10.1140/epja/s10050-020-00239-0

[41] József Cseh. "Some new chapters of the long history of SU(3)". In: *EPJ Web of Conferences* 194 (2018). Ed. by N. Arsenyev et al., p. 05001. DOI: 10.1051/epjconf/201819405001

[42] R.D.Ratna Raju, J.P. Draayer, and K.T. Hecht. "Search for a coupling scheme in heavy deformed nuclei: The pseudo SU(3) model". In: *Nuclear Physics A* 202.3 (Mar. 1973), pp. 433–466. DOI: 10.1016/0375-9474(73)90635-0

[43] Hadi Sobhani et al. "γ-Unstable Bohr Hamiltonian with sextic potential for odd-A nuclei". In: *Nuclear Physics A* 1002 (Oct. 2020), p. 121956. DOI: 10.1016/j.nuclphysa.2020.121956

[44] Hadi Sobhani et al. "Analytical study of the γ-unstable Bohr Hamiltonian with quasi-exactly solvable decatic potential". In: *The European Physical Journal A* 56.2 (Feb. 2020). DOI: 10.1140/epja/s10050-020-00048-5

[45] Dennis Bonatsos et al. "Parameter-free predictions for the collective deformation variables beta and gamma within the pseudo-SU(3) scheme". In: *EPJ ST* 229 (Aug. 30, 2020), p. 2367. DOI: 10.1140/epjst/e2020-000034-3. arXiv: http://arxiv.org/abs/2009.00468v1 [nucl-th]

[46] J.P Draayer and K.J Weeks. "Towards a shell model description of the low-energy structure of deformed nuclei I. Even-even systems". In: *Annals of Physics* 156.1 (Aug. 1984), pp. 41–67.

publication is the follow-up of Refs. [47] and actually established that the filling order of the orbitals by nucleons should be the one of the highest weight SU(3) irreps, in every fermionic, algebraic Nuclear Model, not only in the proxy-SU(3) symmetry.

The collaboration with the experimentalists, whose findings gave rise to the proxy-SU(3) symmetry, resulted to the publication of Ref. [48]. In this work an experimental signature was proposed, in order to distinguish the axial γ rigidity from the γ softness in axially asymmetric nuclei. In simple words the γ rigid nuclei have certain type of deformation (prolate, oblate, spherical), while the γ-soft are flexible among the three types of deformation. The signature, which has been introduced in the reference, is totally model independent and has a wide range of applicability.

Funding

The Nuclear Theory research group has been awarded with two grants during the year 2020. Both proposals had been written by Andriana Martinou.

The first has been awarded by the State Scholarships Foundation (I.K.Y.) to Andriana Martinou for Post Doctoral research. It has a duration of 24 months, a total budget of 26,400.00€, and MIS number 5033021. The research aims to investigate the "Magic Numbers of Exotic Nuclei" and especially the connection of the phenomenon of shape coexistence in nuclei to the nuclear magic numbers.

The second grant has been awarded through the Operational Program "Human Resources Development, Education and Lifelong Learning 2014-2020" in the context of the project "Nucleon Separation Energies" with MIS number 5047793. The program funds the Principal Investigator (Dennis Bonatsos), a Post Doctoral Researcher (Konstantinos Karakatsanis) and a Ph.D. candidate (Smaragda Sarantopoulou). The total budget is 41.451,50€ and the duration is 15 months.

A third grant with MIS number KP-06-PN48/3 has been awarded by the National Science Fund of Bulgaria to N. Minkov in the I.N.R.N.E. in Sofia, Bulgaria. Three members (D. Bonatsos, A. Martinou and S. Sarantopoulou) of the Nuclear Theory group of the I.N.P.P. in Demokritos have participated in the proposal. The research aims to investigate the " Evolution of nuclear structure, shapes and symmetries in the standard and extreme regions of nuclear masses and energy". The three members of the Nuclear Theory group in the I.N.P.P. use the fund to cover travel expenses and fees for conferences.

DOI: 10.1016/0003-4916(84)90210-0

[47] Dennis Bonatsos et al. "Analytic predictions for nuclear shapes, prolate dominance, and the prolate-oblate shape transition in the proxy-SU(3) model". In: *Physical Review C* 95.6 (June 2017). DOI: 10.1103/physrevc.95.064326; Dennis Bonatsos. "Prolate over oblate dominance in deformed nuclei as a consequence of the SU(3) symmetry and the Pauli principle". In: *European Physical Journal A* 53.7 (July 2017), p. 148. DOI: 10.1140/epja/i2017-12346-x

[48] R. F. Casten et al. "Simple new signature of structure in deformed nuclei: Distinguishing the nature of axial asymmetry". In: *Physical Review C* 102.5 (Nov. 2020). DOI: 10.1103/physrevc.102.054310

Table 11: Grants awarded to the Nuclear Theory group of the I.N.P.P. Demokritos in 2020.

Prog. ID	Title	Host Institution	Principal Investigator	Starting date	Finishing date	Budget (€)
5033021	Magic numbers of exotic nuclei	I.N.P.P. Demokritos	A. Martinou	01/01/2020	31/12/2021	26,400.00
5047793	Nucleon separation energies	I.N.P.P. Demokritos	D. Bonatsos	27/04/2020	26/08/2021	41,541.50
KP-06-N48/1	Evolution of nuclear structure, shapes and symmetries in the standard and extreme regions of nuclear masses and energy	INRNE-BAS	N. Minkov	26/11/2020	26/11/2023	86,920.00

Outreach

Unfortunately all the scheduled workshops and visits for the year 2020 were canceled due to the pandemic of covid-19. Nevertheless the research group of the Nuclear Theory in the I.N.P.P had been working remotely with the following network of international collaborators:

Klaus Blaum[1], **R. Burcu Cakirli**[2], **Richard F. Casten**[3]
[1] Max Planck Institute for Nuclear Physics, Heidelberg, Germany, [2] Istanbul University, Turkey, [3] Yale University, USA

Proxy –SU(3) has been discovered in collaboration with the above-mentioned experimentalists, who were the first to notice the importance of the Nilsson pairs of orbitals in creating nuclear deformation.

Jozsef Cseh[4]
[4] Institute for Nuclear Research, Debrecen, Hungary

Collaboration on the connection of proxy-SU(3) to the shell model through the Elliott model.

Jerry P. Draayer[5], **Feng Pan**[6], **Ziwei Feng**[6], **Sai Cui**[6]
[5] Louisiana State University, USA, [6] Liaoning Normal University, Dalian, P.R. China

Collaboration on special solutions of the Bohr collective Hamiltonian triggered through an extended visit of H. Sobhani to Liaoning Normal University and extended to a starting collaboration on microscopic fermionic nuclear models taking advantage of symmetries.

Hassan Hassanabadi[7], **Hadi Sobhani**[7]
[7] Shahrood University of Technology, Iran

Collaboration on the connection of proxy-SU(3) to the shell model through the Nilsson model, as part of H. Sobhani's Ph.D. thesis.

Nikolay Minkov[8]
[8] INRNE, Bulgarian Academy of Sciences, Sofia, Bulgaria

Close collaboration on all group theoretical and numerical aspects of the development of the proxy-SU(3) model from its very beginning, as part of a long term collaboration going on for 30 years.

T. J. Mertzimekis[9], **K. Zyriliou**[9], **P. Vasileiou**[9], **S. Pelonis**[9], **V. Lagaki**[9], **G. Siltzovalis**[9], **M. Efstathiou**[9], **A. Chalil**[10], **P. Koseoglou**[11]
[9] Physics Department, National Kapodistrian University of Athens, Athens, Greece
[10] Institute of Research into the Fundamental Laws of the Universe, CEA, Saclay, France, [11] Technische Universität Darmstadt, Darmstadt, Germany

Collaboration on two experimental proposals at the Horia Hulubei National Institute for R&D in Physics and Nuclear Engineering. The experiments aim to measure the spectrum and the lifetimes of the ^{178}Yb and ^{180}Hf isotopes. The research group has been given 3 days beam time for ^{178}Yb and 14 days for ^{180}Hf. The theory group at the I.N.P.P. in Demokritos participated in the proposal and will deliver theoretical predictions about the lifetimes and the electric transition probabilities among the the nuclear states.

Overview

The Nuclear Theory group in the I.N.P.P. Demokritos has developed its own theory, the proxy-SU(3) symmetry. Thus, a unique in the world expertise on this model has been created in the Institute. The Master class, the Ph.D. students and the Post-Doctoral Fellows of the Nuclear Theory group have a valuable know-how on the Shell Model SU(3) and the proxy-SU(3) symmetry.

The group has expanded its network of collaborators despite the transportation difficulties due to the pandemic. Nuclear theorists from the East to the West are by now familiar with the proxy-SU(3) symmetry. Collaborations with colleagues from China, Iran, Bulgaria, Hungary, U.S.A., Turkey, Germany and Greece resulted to 6 peer-review publications and may result to many more in the future.

The support from two funding agencies was decisive and valuable for the evolution of the group. The group received 67.941,50€ to cover the scholarships of two Post Doctoral fellows and one Ph.D. student. Without this support the above achievements would not have been possible.

By now the proxy-SU(3) symmetry is a model, which is of interest only to those working on the basic research in Nuclear Structure Theory. But this model has the future potential to be linked to various new a) technologies, such as nuclear medicines, nuclear batteries and quantum computers, b) physics beyond the Standard Model, through calculations concerning the neutrino-nucleus reactions, c) Nuclear Physics, by unifying the Nuclear Models, or by investigating the phe-

nomenon of shape coexistence in nuclei, d) cosmological models, since one may use the proxy-SU(3) symmetry to calculate the nucleon capture cross sections, the nuclear level densities and the nuclear binding energies, all of them being valuable in nuclear astrophysics and in cosmology.

Experimental Nuclear Physics

Researchers:	Sotirios. V. Harissopoulos
	Anastasios Lagoyannis
	Michail Axiotis
Research Associates:	Zoi Kotsina
	Eleni Vagena
PhD students:	Aggelos Laoutaris
	Ioannis Madesis
	Eleni Ntemou
	Kostas Preketes-Sigalas
	Achment Chalil
Master students:	Maria Peoviti
	Stefanos Nanos
Diploma students:	Artemis Tsantiri
Practical work students:	Anastasia Kotsovolou
	Christos Andrikopoulos
Employees:	Stefanos Papagiannis

Introduction

The Experimental Nuclear Physics group runs the in-house TANDEM Accelerator, where it's main activities are implemented. The research program of the team is focused mainly on applications of Ion Beam Analysis (IBA) techniques and nuclear astrophysics, along with studies in the field of nuclear structure. Additionally, the group in collaboration with other Greek institutions participates at the European Space Agency's (ESA) G4G program.

Moreover, the group has supported to prepare and conduct the experiments of all the external users of the accelerator of the lab.

Unfortunately, due to the COVID-19 pandemic and the movement restrictions the opportunities of performing experiments were limited and consequently the scientific output of the group.

Activities

In the following sections the scientific output of the group for year 2020 is briefly presented.

IBA

The group is active in the field of IBA techniques. In this context, during the last year the differential cross-sections of deuteron induced reactions on beryllium were reported for an energy range between 1.0 to 2.2 MeV for several detection angles (120°, 140°, 150°, 160° and 170°) appropriate for NRA technique. Beryllium, is a light weight metal used in many industrial applications and also is considered as a candidate material for the plasma facing walls of the fusion reactors. Thus the reliable determination of Beryllium content in a sample is of imperative importance for the FUSION community.

Furthermore, towards the goal of facilitating the applicability of the PIGE technique, the group has developed an open source computer code (PiGreCo) for the analysis of experimental data. During the last year a detailed inter-comparison of the different available codes was published by the International Atomic Energy Agency (IAEA), in order to determine their correct applicability for analyzing PIGE experimental data. The conclusion of the study was that all the codes are in good agreement between them (better than the accuracy of the available cross-sections) and thus they are fit for their purpose.

Finally, the well established recognition of the group's contribution to IBA techniques, is demonstrated by it's participation to IAEA's technical meeting on the 'Advanced Methodologies for the Analysis of Materials in Energy Applications Using Ion Beam Accelerators'. The conclusions of the meeting were published, in order to prepare the IBA community for the challenges that arise from the application of IBA techniques to the fusion research.

Nuclear Structure

In the field of nuclear structure, the group in collaboration with the UoI and NTUA has measured and published the cross-sections of the $^{165}Ho(n, 2n)$ reaction for the population of ^{164}Ho to the ground and the isomeric state for the energy range from the reaction's threshold up to 20 MeV. This was a tedious work because of the low energy gamma-ray (37.3 keV) that had to be detected through the activation method. In order to establish the detector efficiency for such low energy, detailed Geant4 simulations had to be performed. The cross-sections for energies near the threshold were reported for the first time. The experimental data were compared to statistical calculations of the TALYS code and the impact of different models was investigated.

G4G

The activities of the group in the context of the G4G ESA's project mainly involve the porting of the GRAS Geant4 based code to multi-threading and the newest version of Geant4. In this framework the group has almost completed the task of implementing multi-threading capabilities to the code. The code will be handed to ESA and is probable to be released during next year or early 2022.

Funding

- Calibra
- G4G
- Fusion

Outreach

PhD Thesis

1. **E. Ntemou:** "Cross-section studies of deuteron reactions and application in light element ion beam analysis techniques"; Lagoyannis (member of Advisory and Examination committee), NTUA, 2020
2. **Khaliel Ahmed:** "Nuclear structure of the neutron-rich nuclei ^{140}Ba and ^{180}Hf"; Axiotis (member of Examination committee), NKUA, 2020

PhD Thesis - Ongoing

1. **S. Chasapoglou:** Lagoyannis, NTUA
2. **E. Georgali:** Axiotis and Lagoyannis, UoI
3. **A. Laoutaris:** Lagoyannis, ???
4. **I. Madesis:** Charisopoulos, UoC
5. **S. Nanos:** Axiotis, UoI
6. **K. Preketes - Sigalas:** Lagoyannis, NTUA
7. **P. Tsavalas:** Lagoyannis, NTUA
8. **A. Zyriliou:** Lagoyannis, NKUA

MSc Thesis

1. **N. Dimitrakopoulos:** "Title"; Lagoyannis, NTUA, 2020
2. **S. Nanos:** "Title"; Axiotis, UoI, 2019
3. **P. Vasiliou:** "Title"; Lagoyannis, NKUA, 2020

MSc Thesis - Ongoing

1. **M. Peoviti:** Axiotis and Lagoyannis, UoI

Diploma Thesis

1. **A. Biniskos:** "Title"; Axiotis, UoI, 2020
2. **A. Tsantiri:** "Cross-section measurement of the fission reaction $^{232}Th(n, f)$ with MicroMegas detectors"; Axiotis and Lagoyannis (members of the Examination committee), NTUA, 2020

Overview

X-ray Spectrometry

Researchers:	Dr. Andreas-Germanos Karydas
	Maria Kaparou (extrernal part time collaborator)
PhD students:	Kalliopi Tsampa
	Nikoletta-Kanella Kladouri
Master students:	Evangelia Eleftheriou
	Dimitra Tsakou
Practical work students:	Zoe Bari

Introduction

The research interests of the x-ray spectrometry group (INPP-XRS), include three basic directions:

1. the use of synchrotron radiation for basic and applied research. The basic research activities refer to the measurement of fundamental x-ray and atomic parameters related to the interaction of X-rays with matter and atom de-excitation processes, whereas applications involve the characterization of advanced new materials, but also technological (production) aspects of archaeological ones.
2. the development of laboratory or/and portable x-ray fluorescence methodologies and applications in the fields of cultural heritage and environmental monitoring, including the design, realization and characterization of new spectrometers.
3. the development of cultural heritage and environment- related applications using x-rays induced through the inner shell atoms ionization by energetic proton beams with micrometer or millimeter size (micro-PIXE and external beam PIXE).

During 2020, the INPP-XRS research program related with the aforementioned multi-thematic areas, succeeded in generating substantial results and scientific contributions. Moreover, previous years' momentum, academic output and recognition driven the establishment of sustained external partnerships, but also the creation of new ones in line with the prioritized subjects of interest. The main pillar for the sustainability and further deepening of the established collaborations relied on the fact that four new PhD programs were initiated in 2020 for which the XRS group is to have either the main implementation responsibility (Kalliopi Tsampa with the School of Applied Mathematics and Physical Science, National Technical University of Athens), or key co-supervising role (three remaining ones; with the Department of Materials Science & Engineering of the University of Ioannina, Greece -Stefanos Papayannis and Anastasios Asvestas- and with the Department of History, Archaeology and Cultural Resources Management, University of the Peloponnese -Eleni Triantafyllidi).

The internal collaborations – within N.C.S.R. "Demokritos" – were further

expanded including two colleagues from the Institute of Nanoscience and Nanotechnology (INN), E. Makarona (Energy Harvesting and Autonomous Sensors Group) and A. Hein (Ceramics and Composite Materials Group), in addition to the previously established with E. Filippaki (Paleoenvironment an Ancient Metal Studies Group). The fruitful long-standing collaboration with the Environmental Radioactivity Laboratory (ERL) of the Institute of Nuclear and Radiological Sciences and Technology, Energy and Safety (INRASTES) was further strengthened regarding the joined utilization and research exploitation of the benchtop EDXRF spectrometer operated at the XRF laboratory premises.

New collaborations were also initiated at national and international level focused on developing XRF methodologies and applications in the fields of environmental monitoring (School of Chemical and Environmental Engineering, Technical University of Crete), and biology/biomedicine (Physics Department, NOVA School of Science and Technology, Caparica, Portugal). The already established (since 2016) collaboration with the Istituto di Scienze per il Patrimonio Culturale – Consiglio Nazionale delle Ricerche (ISPC-CNR) in Catania in multiple XRS thematics was further enhanced and as a recognition A. Karydas was officially granted by the ISPC-CNR branch in Catania with a Research Association.

The year 2020 marked the potential to upgrade significantly the INPP-XRS instrumentation resources through two different funding opportunities, the project "PROTEAS" (Advanced System for collection and management of analytical data for documentation and conservation of large-scale paintings in an open laboratory, ΕΡΕΥΝΩ-ΔΗΜΙΟΥΡΓΩ-ΚΑΙΝΟΤΟΜΩ Β' ΚΥΚΛΟΣ, 2020-2023) and CALIBRA infrastructure project, the latter thanks to the re-allocation of project funds proposed by the scientific responsible (S. Harissopulos) and further supported and approved by the INPP-Director (Ch. Markou) and funding authority. Thus, during the last quarter of 2020, significant effort was placed in defining the needs and instrumentation specifications, but also in running administrative issues.

Activities

XRS at Synchrotron

Due to the pandemic it was not possible to access a synchrotron radiation facility for new experiments, thus, effort was made to complete analyses on data acquired during previous years' beam times and proceed with relevant publications. This effort resulted to four (4) peer-review publications with the two of them together with Greek collaborators from the National Technical University of Athens, Aristotle University of Thessaloniki and the University of Peloponnese.

Material Sciences

1)In collaboration with colleagues from the National Technical University of Athens and AGH University of Science and Technology, Poland, a mathematical model for deep ion implantation depth profiling by synchrotron radiation grazing incidence

X-ray fluorescence (GIXRF) spectrometry was proposed. GIXRF spectrometry is usually applied to obtain shallow depth distributions (less than 25 nm) using information from the X-ray standing wave (XSW). Thus, the new XSW-free mathematical model fairly extended the applicability of GIXRF spectrometry. An indisputable advantage of the model is the absence of any requirement for the absolute calibration of the X-ray instrument with respect to the beam flux and the solid angle of detection. All that is needed to determine the ion retained doses and their in-depth distribution are the efficiencies of the X-ray detector used for XRF spectra acquisition and specific X-ray fundamental parameters (Fig.58). Although the proposed model is a basic and ideal approximation of real and complex ion implanted systems, it provides the robust quantitative characterization of ion depth distribution profiles with the uncertainty budget held at a modest level. The model was validated with three test Si(111) wafers deeply implanted with 200 keV argon ions of nominal doses of 10^{15} to 10^{16} at. per cm^2. Ar ion retained doses determined with the new XSW-free GIXRF model agreed well with nominal quantities, whereas additionally cross-check by ion beam analysis (IBA) techniques was performed for the highest Ar retained dose found to be in decent agreement.

The deduced depth profiles of Ar ions are critically discussed in comparison with the Monte Carlo simulation of Ar ion transport in amorphous silicon (Fig.59). A binary collision approximation adopted in the latter assumes only the existence of a 'random' target, which excludes all the channeling perturbations leading to increased implantation depths, due to the corresponding change in the electronic stopping power. This may be very important during the implantation process, due to the implemented Si crystalline wafer substrate. Moreover, the Monte Carlo simulation in the SRIM software is limited to a rather small (10^6) number of impinging ions and by no means can it incorporate the dynamic mobility of noble gas Ar ions within the Si matrix close to the implantation area, especially at high doses, which may lead to significantly broadened distributions.

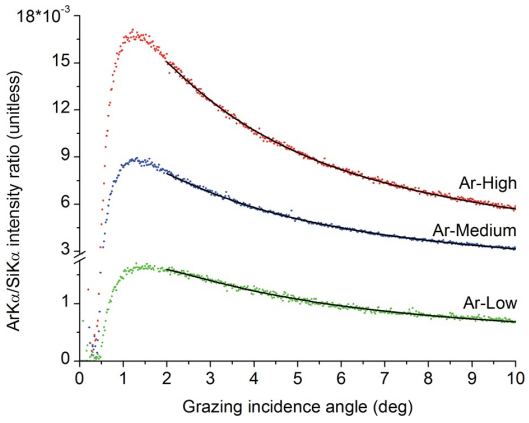

Figure 58: Experimental ratios (coloured dots) of Ar-Ka to Si-Ka net line intensities were fitted (black continuous lines) in the angular range from 2 to 10 degrees with the analytical function deduced from the XSW-free GIXRF model.

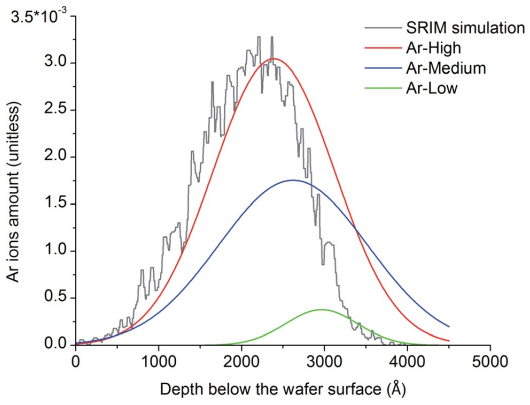

Figure 59: Depth distributions of Ar ions deep implantation in Ar-high, Ar-medium and Ar-low wafers determined with the XSW-free GIXRF quantification model and simulated by SRIM software (normalized to the Ar-high distribution).

2)With colleagues from the Bhabha Atomic Research Centre in India and Elettra Sincrotrone Trieste in Italy, the development of a direct non-destructive synchrotron-radiation-based total reflection X-ray fluorescence (TXRF) analytical methodology for elemental determinations in zirconium alloy samples was reported for the first time. Discs, of diameter 30 mm and about 1.6 mm thickness, of the zirconium alloys Zr-2.5%Nb and Zircalloy-4 were cut from plates of these alloys, mirror polished and presented for TXRF measurements at the XRF beamline at Elettra synchrotron light source, Trieste, Italy, at two different excitation energies, 1.9 keV and 14 keV, for the determinations of low- and high-Z elements, respectively. The developed analytical methodology involves two complementary quantification schemes, i.e. using either the fundamental parameter method or relative sensitivity- based method, allowing quantification of fifteen minor and trace elements with respect to Zr with very good precision and accuracy. In order to countercheck the TXRF analytical results, some samples were analyzed using the DC arc carrier distillation atomic emission spectrometry technique also, showing an excellent agreement with the results of the TXRF-based methodology developed in this work.

The present work resulted in a nondestructive TXRF elemental characterization methodology of metal and alloy samples avoiding the cumbersome dissolution and matrix separation which are normally required in other techniques and traditional methods of TXRF determination. Further on, the proposed methodology improves the detection limits significantly compared with normal XRF determinations, whereas it simplifies and improves the accuracy of such quantitative analysis by eliminating matrix corrections. In addition, the production of analytical waste could also be avoided to a great extent. Although the work was carried out for specific applications in the nuclear industry, it is equally suitable for other such samples in different industrial applications. For example, it can be further extended to the elemental determinations of alloy materials like steel, inconel, etc., which hold high technological importance. Although for this study we have used a synchrotron light source, not easily available for routine sample analysis, the method developed can be also used for routine sample analysis in the laboratory with different suitable tube sources, detectors and vacuum sample chambers optimized for such applications.

Cultural Heritage

In collaboration with colleagues from the Aristotle University of Thessaloniki and University of Peloponnese, synchrotron based X-Ray Absorption Fine Structure (XAFS) spectroscopies were applied for the study of the structural and colouring/decolouring role of transition metals (TM) chromophores (Mn, Fe, Co, Cu) in blue and green-blue soda-lime beads from Thebes, central Greece dated back to the Classical and Hellenistic period. Concerning the TMs redox and their consequent influence on colour, it was established that the major blue colourants are Co2+ and Cu2+, colourless Cu+ dominates the blue beads (Fig.60a), whereas chromophores Fe3+ and Cu2+ give rise to a green-blue hue (Fig.60b). The Mn2+ content in the blue beads, whose occurrence is attributed to unintentional addition via the Co- rich mineral colourant, counteracts the effect of the moderately higher

content of Fe2+ in the raw materials. Based on the XAFS analysis results, it was proposed that the fractions of all TM under question (Mn, Fe, Co and Cu) were chosen and adjusted properly not only to control the desired colour, but also to ensure the stability of the glass matrix. Indeed, the integrity of the silica matrix should be further enhanced, due to the presence of intermediate Fe oxides linking to Cu ions in either planar or linear geometry, while Mn and Co act as typical network formers.

To conclude, besides the quantitative determination of key structural parameters of certain TMs (Mn, Fe, Co and Cu) within the glass silica network, the present combined XANES and EXAFS study has generated the following results of archaeological and technological importance: (a) the quantitative determination of Cu+ and Cu2+ fractions; (b) the presence of ferrous ions in the Co+Cu blue beads that counteracts the elevated Mn content, the latter being unintentionally added in the glass via the cobaltiferous alum; (c) the identification of the dominant share of Cu2+cations in the green blue bead, whereas significant portion was added as azurite; (d) the Co ions contained in the Co+Cu blue beads are divalent in the form of smalt (CoO).

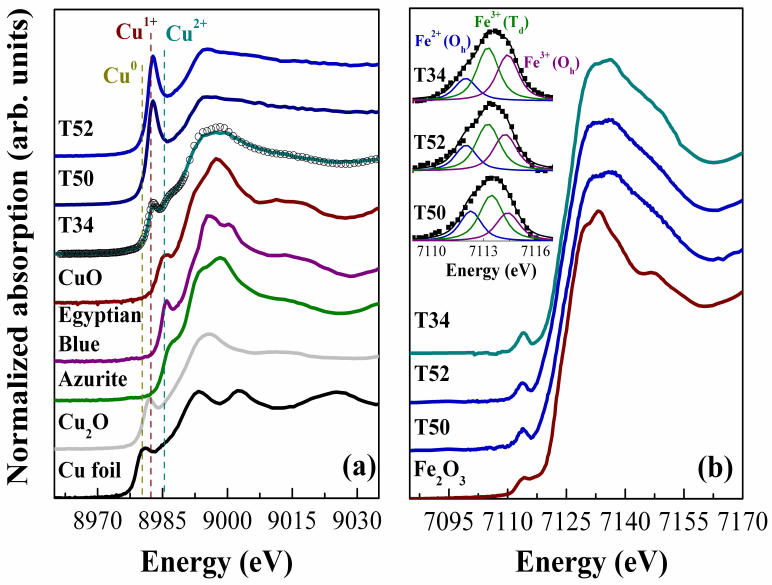

Figure 60: (a) Cu-K-XANES spectra of the blue (T50 and T52) and green-blue (T34) beads and reference Cu oxides and metal Cu foil. The linear combination fitting curve of the XANES spectrum of bead T34, using the spectra of azurite and bead T50 is shown in circles. (b) Fe-K-XANES spectra of the studied beads and reference hematite (Fe_2O_3) powder. The inset is a magnification of the pre-edge absorption region (squares), the number of functions (coloured solid lines) used for the fitting (black solid line) accounting for the deferent Fe valence and site occupation are also depicted.

X-ray Fundamental Parameters

Within the long-standing collaboration with the Department of Basic and Applied Sciences, Punjabi University, India (Prof. Sanjiv Puri group) and M. Czyzycki from the AGH University of Science and Technology, Poland, the X-ray mass attenuation coefficients for Sb (Z=51) have been measured at forty energies across its Li (i = 1–3) sub-shell absorption edges covering an extended energy region within 4.0 keV – 14.0 keV. The aim of this study is to experimentally determine the key X-ray fundamental parameters for Sb with improved accuracy by using tunable energy synchrotron radiation. From the present measured mass attenuation coefficients, the Li (i=1–3) sub-shell photoionization cross sections have been deduced at twenty-four energies across the Li (i = 1–3) edge-energies of Sb covering the region 4.150 keV–5.0 keV by using experimentally deduced Li edge jump ratios. Two theoretical datasets of X-ray mass attenuation coefficients and total photoionization cross sections were served to evaluate their consistency with the present experimental values and reveal possible discrepancies, in particular, across the Li edge-energies of Sb. The present measured mass attenuation coefficients for the Sb were found to be higher by up to 11% than the two sets of theoretical values, (μ/ρ) XCOM (Berger et al., 2010) and the (μ/ρ)) Chant by (Chantler, 1995) over the energy region 4.0 keV $\leq$ E $\leq$ 5.0 keV, except at energies in the vicinity (few eV) of the Li sub-shell absorption edge energies, where the measured values are found to be considerably higher than both the sets of theoretical values. Further, in the energy region 5.0 keV $<$ E $\leq$ 14.0 keV, the difference between measured and two sets of tabulated values, (μ/ρ))XCOM and (μ/ρ))Chant, increases up to 14% and 23%, respectively. The Li sub-shell photoionization cross sections for Sb at energies across its Li edge energies over the region 4.150 keV–5.0 keV deduced from the present measured mass attenuation coefficients and edge jump ratios are found to agree within 10% with both the sets of theoretical values. It may be mentioned that both the tabulations of theoretical photoionization cross sections are based on the independent particle approximation (IPA) models, where the many body effects) including electron correlations are completely ignored. These many body effects are particularly important at photon energies in vicinity of the absorption edges of a given element. Therefore, theoretical calculations of photoionization cross sections including many body effects along with solid-state effects are required to understand the observed differences between measured and theoretical photoionization cross sections. Further inclusion of contribution of near-edge processes such as the resonant Raman scattering (RRS) at energies just below the absorption edges is needed to explain the significant differences between tabulated and measured mass attenuation coefficients.

XRS at XRF Laboratory

During 2020 a significant part of the XRS group research work has been directed to further exploiting and developing the imaging capabilities of the so-called macroscopic XRF analysis, when applied to archaeological materials (one publication and one MSc thesis awarded), but also to utilizing the laboratory experience and available spectrometers in new investigations of materials with strong archaeological interest (two publications). Moreover, the interest and involvement in

environmental monitoring studies is reflected in two other publications, whereas the established in 2020 close collaboration with the Institute of Nanoscience and Nanotechnology (INN) and Eleni Makarona (Energy Harvesting and Autonomous Sensors Group) resulted in our first common publication supported by measurements performed in the XRF laboratory.

Cultural Heritage

1)The MSc student Kalliopi Tsampa supported in July 2020 her thesis diploma entitled: *"Macroscopic X-ray fluorescence characterization of Platinum Group Mineral (PGM) inclusions in archaeological gold"*. This work included a detailed analytical investigation of PGM inclusions discovered on two signet gold rings amongst the four recently excavated (May 2015) by a team from the University of Cincinnati from an unlooted Mycenaean tomb near the Palace of Nestor in Pylos Messenia. The holistic macro-XRF (MA-XRF) imaging analysis of the external surface of the rings offered the unique possibility of identifying non-destructively the presence of PGM inclusions containing elements, such as Osmium (Os), Iridium (Ir) and Ruthenium (Ru). As an example, Fig.61 demonstrates an example of the MA-XRF imaging distribution of Cu, Ir and Os elements within the bezel of the ring SN24-7 (left), together with the central pixel XRF spectrum of PGM inclusion R4B1 (right). The measurements were carried in-situ at Chora Archaeological Museum, in Messenia using the state of art LANDIS-X mobile X-ray scanner, developed by Laboratori Nazionali del Sud (INFN-LNS) and Istituto di Scienze per il Patrimonio Culturale – Consiglio Nazionale delle Ricerche (ISPC-CNR) in Catania, Italy. The presence of PGM inclusions in ancient gold objects is considered a clear indication that the gold and the PGM inclusions became associated as a result of fluvial transport. A detailed characterization of the PGM inclusions in terms of their morphological features and compositional profile was carried out within the MSc thesis work, with the results planned to be submitted for publication within 2021.

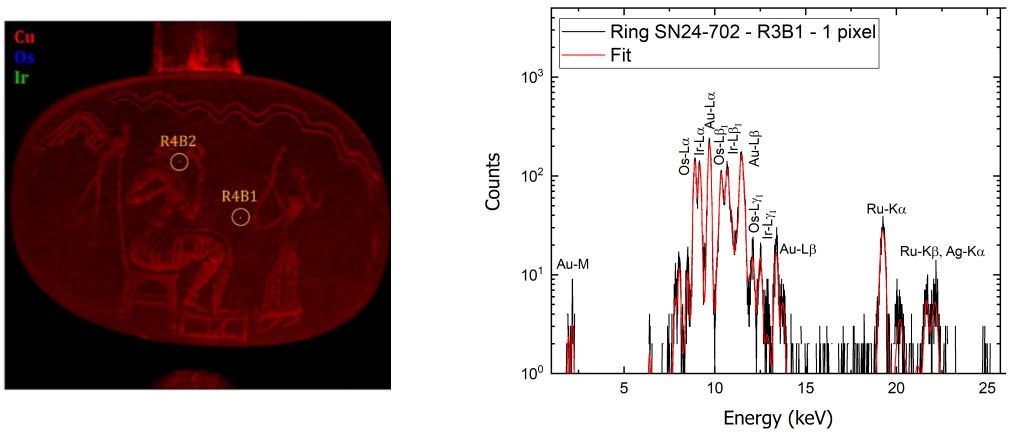

Figure 61: MA-XRF imaging distribution of Cu, Ir and Os elements within the bezel of the ring SN24-7 (left), together with the central pixel XRF spectrum of PGM inclusion R4B1 (right)

2)The unprecedented application of MA-XRF imaging in the study of heavily deteriorated Late Bronze Age wall-paintings at the Mycenaean Palace of Nestor, in Pylos Greece, unraveled hidden iconographic elements and polychromy, thus, allowing to integrate the iconography and perform an objective, scientifically based re-assessment of the accuracy of previously executed wall-painting reconstructions. Moreover, painting materials and artistic techniques of their application were also uncovered, enhancing and further re-confirming the results obtained via other analytical techniques.

3)The analytical study of 19 silver decorations of six Archaic bronze helmets from the archaeological site of Olympia, Greece using micro-X-ray fluorescence (XRF) spectrometry was performed within the MSc thesis diploma of Rebeca Grethe (Culttech MSc program) in collaboration with the University of Peloponnese (Fig.62). The principal aim of the study was to investigate technological aspects of the smelting process that influence the composition of Ag, reveal possible elemental correlations and shed light on its source, assigning a likely provenance. The XRF results revealed that all decorations contain high amounts of Ag $> 95\%$. The quantitative determination of several fingerprint minor elements, such as Au, Pb and Bi, provided interesting insights related to the efficiency of the cupellation process, the ore type used for the silver extraction and the geological origin of the ores.

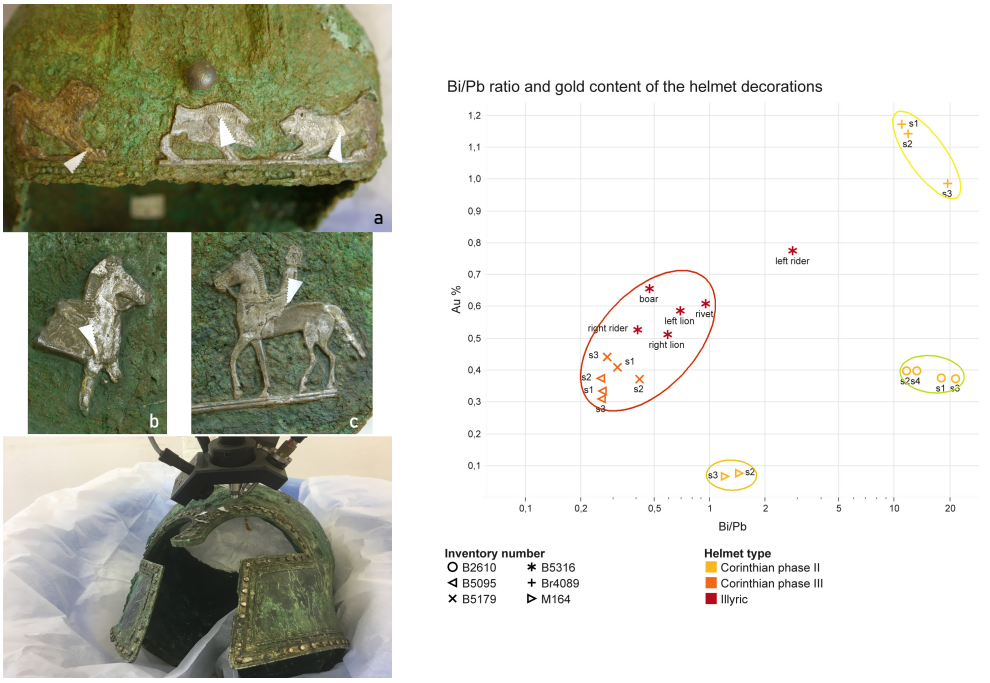

Figure 62: Overview of the analysed spots on B5316, an Illyric helmet using the INPP Micro-X-ray fluorescence (XRF) portable spectrometer in the storage room of the Archaeological Museum of Olympia (left). Identified groups regarding the Bi/Pb ratio (logarithmic scale) and Au content (right). The Au content within the range 0.01–0.1% suggests silver extraction from galena or native Ag, whereas less than <0.5% from chlorargyrite, acanthite or oxidized phase of silver such as cerussite and anglesite. Gold concentration more than >0.5% may originate from recycled gilded silver. The weight ratio Bi/Pb can be employed as fingerprint of the raw minerals used for the silver extraction.

4)Within a broad National collaboration led by Prof. Liritzis a ceramic assemblage selected from a recently excavated Late Helladic settlement at Kastrouli (Central Greece) has been chemically analyzed and statistically elaborated, to add new information and contribution to understanding Mycenaean culture in the wider studied area. The chemical composition of 142 ceramic sherds represented by a wide range of household typologies was measured using a hand-held XRF (HHXRF) analyzer.

The specific role of the XRS group was to evaluate and validate the calibration procedure of the HHXRF analyzer, in view of the lack of free-available software packages. Fired briquettes prepared from 8 local clay sources and several mixtures of them were similarly analyzed. A robust statistical analysis was applied based on 15 major and minor/trace elements employing hierarchical cluster analysis with several linkages, descriptive statistics, biplots and boxplots, principal component analysis (PCA), as well as, Euclidean and Mahalanobis distances on standardized ratio transformed data. The chemical characterization and the statistical evaluation were coupled by petrographic analysis. The results obtained revealed that some local clay sources and their mixtures are placed within the archaeologically identified broad ceramics group, providing, thus, evidence for a local production of the studied pottery, and artisan's skills employed a variety of manufacture technologies.

Environmental monitoring

The XRS group was involved in 2019-2020 in two international collaborations related with air-quality studies, having resulted in two publications within 2020. In the first study, elemental composition and source apportionment of atmospheric aerosols (Particulate Matter-PM2.5) collected from urban and residential areas of Jordan using multi-secondary targets energy dispersive XRF analysis was reported, whereas in the second one, ambient particulate matter source apportionment using receptor modelling in European and Central Asia urban areas was carried out. Both studies relied on the quality of the analytical data on PM2.5 analyses collected using different XRF instrumentation, a subject where the XRS group of INPP significantly contributed, together with the role of A.G. Karydas as project coordinator in large scale projects of the International Atomic Energy Agency (IAEA).

Material Sciences

In this work, performed in collaboration with Institute of Nanoscience and Nanotechnology of NCSR "Demokritos", a comprehensive study on how to combine purely chemical, bottom-up solution-based synthesis with advanced e-beam lithography for the controllable production of ZnO-nanostructure periodic arrays on Si and SiO_2 substrates is presented. The study was complemented with micro-XRF spectrometry demonstrating the latter's great potential as a rapid, non-destructive and enabling nanometrology technique that can leverage the development of novel nanofabrication processes.

The study resulted in a fabrication process framework that not only can help in relating the process parameters to the desired geometrical feature of the periodic nanoarchitectures, but that is also compatible with standard microfabrication techniques and largescale production. This preliminary study showed that it is possible to fuse EBL patterning and HG of metal oxides -at least for the case of ZnO- in order to produce uniform periodic arrays of sub-micron patterns filled with nanostructures over a wide dynamic range of sizes. The study also revealed the potential of micro-XRF to be used as a non-destructive screening method of the substrates to predict the uniformity of the of the hydrothermally-grown nanostructures (Fig.63).

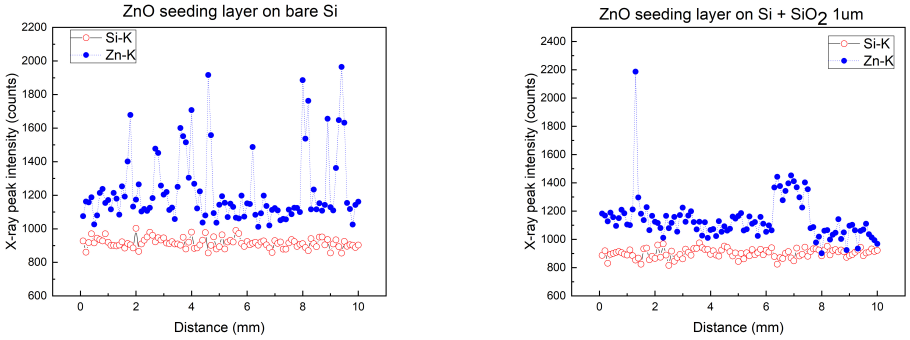

Figure 63: Variability of Zn-Ka peak intensity (circles) and of Si-K line used as reference (squares) during the line scan of the seeding layers on Si (left) and on a SiO_2/Si substrate (right)

XRS using Ion Beam Analysis

1)During 2020, the analysis of PIXE and RBS data acquired on Mycenaean gold foils towards technological characterization and provenance assignment was carried out and a draft report was prepared. The measurements were performed at the C2RMF Accélérateur Grand Louvre d'Analyses Elémentaires, AGLAE a located at the Louvre Museum, Paris, France with the support of the IPERION-CH project through the successful proposal submitted by Maria Kaparou, a close external collaborator of the XRS group, entitled: *"Provenance study of Mycenaean Gold"* with the acronym "Myc-GoldPro". The beamtime shifts (20-24 October 2019) were also attended by the MSc student K. Tsampa and the PhD student N. Kladouri.

In this work, PIXE and RBS measurements were conducted using an external 3 MeV, 2 nA proton micro- beam on 18 gold foils from prehistoric Paleokastro in Arcadia, Greece. Thanks to the improved beam optics, analytical and operational capabilities of the New AGLAE facility, an area of about 200 mm^2 of the surface, representing around 60% of their total mass, was scrutinized using a proton-microbeam with 40 μm spatial resolution (Fig.64 demonstrates the results of such a scanning measurement on a gold foil). The combined PIXE/RBS measurements render possible to apply independent methodologies for the gold foils' thickness characterization and deduce results of improved reliability, thus,

enlightening aspects of their manufacture, such as elemental composition and purification process and evaluation of its variability across their surface. Hence, the foils present a thickness of few micrometers (2.5 - 5 μm), low copper (<1.5%) and rather high Ag content (10.5%). Since the PIXE data did not reveal the presence of mineral inclusions associated with PGEs, origin of gold from primary mining can be suggested.

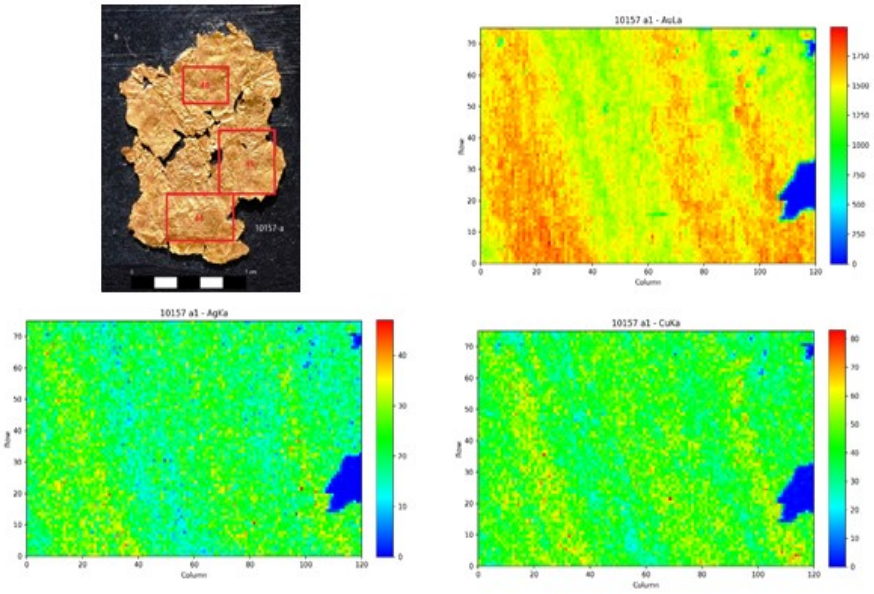

Figure 64: Photo of the gold sample 10157 a1 (scan no 44) and elemental spatial distribution maps of AuLa, AgKa and CuKa sum x-ray intensities extracted from two high energy silicon drift detectors.

2)Given the re-allocation of CALIBRA funds to provide significant support in the re-innovation of the external ion-bam analysis facility, effort was made to identify specific requirements for the needed x-ray instrumentation and at the same time to re-design the set-up. A preliminary sketch is shown in Fig.65.

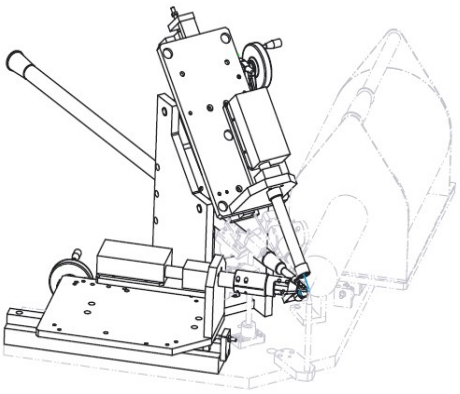

Figure 65: A preliminary re-design of the external ion beam analysis set-up including Silicon Drift Detectors in replacement of the obsolete liquid nitrogen Si(Li) detectors, previously used.

Funding

The Project “PROTEAS” entitled: Advanced System for collection and management of analytical data for documentation and conservation of large-scale paintings in an open laboratory, ΕΡΕΥΝΩ-ΔΗΜΙΟΥΡΓΩ-ΚΑΙΝΟΤΟΜΩ Β’ ΚΥΚΛΟΣ, 7/2020-7/2023, Τ2ΕΔΚ-02428/MIS: 5069984 was started in July 2020. Budget: 155.311,00 €. Participants: Two research institutes of the Foundation for Research and Technology - the Institute of Computer Science and the Institute of Electronic Structure and Laser, one research Institute of the National research center ”Demokritos” - the Institute of Nuclear and Particle Physics, the National Art Gallery, two companies up2metric, a new company located in Lefkippos Technological Park of ”Demokritos” and the Printec - a large automation company.

The underlying idea of the PROTEUS project is to introduce the public to the work of the art conservator and, through this, in the materials and techniques employed, the historical context of a work of art, as well as the message and the expression of the creator. Important for implementing this idea, is to establish an open communication channel between curators, conservators and researchers. Modern technology supports this communication through a) portable analytic devices b) flexible robotic arrangements and c) advanced information systems that allow an integrated, innovative approach to documentation, management and presentation of the information gathered during the conservation of artwork. In this context, the main objective of the project is the development of an Open-Access Workshop (OAW) within the premises of the National Gallery at Athens (NGA), where researchers from IESL-FORTH and INPP-NCSR Demokritos will install innovative analytical systems based on imaging and spectroscopic techniques which, via combined protocols for in-situ application, will integrate and upgrade the current documentation and conservation methodology used by NGA for the integrated study of paintings.

Outreach

Presentations at Conferences

1) 7th Balkan Symposium on Archaeometry, Athens, 22-25 September 2020
Study and conservation of a 19th century printed silk scarf from the collection of the National Historical Museum of Greece, Nikoleta Tasiouli, Stamatis Boyatzis, Anna Karatzani, Andreas G. Karydas
2) 6th ARCH_RNT Symposium-Archaeological Reasearch and New Technologies, 8-9 October 2020

1. EDXRF analysis of Rare Earth Elements in archaeological ceramics: Development and validation of the method, A. P. Panagopoulou, K. Tsampa, St. Papagiannis, K. Eleftheriadis, A. Hein, A. Karydas
2. Preliminary Investigation of an Archaic Bronze Double Axe from The Cemetery of Phaleron Delta, Attica, Aik. Panagopoulou, S. Chryssoulaki, A. G. Karydas, N. Zacharias

3. Technological and Chronological Study of Mortar samples from Varnakova Monastery in Fokida, N. Zacharias, P. Moska, K. Triantafyllopoulos, E. T. Delegou, M. Apostolopoulou, A. Karydas, A. Moropoulou

4. Preliminary Results of an Integrated Study on a Western Religious Canvas Painting from the series of the Station of the Cross, S. Kesidis, A. G. Karydas, D. Anglos, N. Zacharias, E. Kouloumpi

5. The Application of Micro-Beam X-Ray Fluorescence Spectrometry (Micro-Xrf) in the study of the Metal Artefacts of four Sanctuaries at Tegea, Arcadia, Greece (10th-7th C. Bce), N.K. Kladouri, A.G. Karydas, V. Orfanou, V. Kantarelou, N. Zacharias (Oral Presentation)

Highlighted pupblication

The publication by N. Kallithrakas-Kontos *et. al., Sci. Total Environ.* 697 (2019) 134099; entitled: *"X-ray absorption near edge structure (XANES) analysis provide insight on the behavior of mercury preconcentration on solid-state membranes"* with A.G. Karydas included amongst the authors, was selected to be included in **Elettra Highlights 2019-2020 volume**. Authors: N. Kallithrakas-Kontos, S. Foteinis, E. M. Vazgiouraki, A. G. Karydas, J. Osán, E. Chatzisymeon, pp. 34-35, (2020)

Overview

The research activities of the XRS group continued and were further corroborated within 2020 in prioritized basic and applied thematic areas, including cultural heritage, material sciences and environmental monitoring, utilizing synchrotron radiation techniques and laboratory benchtop and portable XRF spectrometers. The scientific output was remarkable (10 peer review journal publications) with several conference contributions, albeit few others with expected significant participation (relevant abstracts had been submitted in three different conferences) by the group were postponed due to the pandemic. It should be also highlighted that during 2020 and despite the access restrictions, 15 PhD/MSc students and collaborators have utilized effectively the XRF laboratory infrastructure. Importantly, the year 2020 marked the significant enhancement of the XRS group research potential through the active participation in new PhD programs, in close collaboration with the Universities of Ioannina and Peloponnese and the start of a new, nationally funded competitive project. The latter is to allow building state of the art portable XRF equipment for imaging purposes in the forthcoming years, whereas the additional support in X-ray instrumentation by the CALIBRA infrastructure program is to allow for considerable expansion of the analytical capabilities for elemental analyses of complex samples using Ion Beam Analysis techniques.

Activities of the XRF Laboratory

Given the particular restrictions imposed for accessing the laboratory, during the first semester of 2020 efforts were specifically directed to re-evaluate and validate new calibration protocols for the portable micro-XRF spectrometer, succeeding to build robust methodologies for performing accurate quantitative analysis of different sample matrices. The PhD students K. Tsampa and S. Papayiannis, but also the practical work of Zoe Bari, diploma student of SEMFE, contributed significantly towards this goal. As a result, the participation of the XRF laboratory in the IAEA inter-comparison exercise (PTNATIAEA/18, World Wide Open Proficiency Test, Soil) yielded very satisfactory results.

1) In January –February 2020, a collaboration with Portuguese colleagues from the Physics Department, NOVA School of Science and Technology, Caparica, Portugal was initiated and continued in 2021. The objective of this collaboration is two-fold: 1) to quantify trace elements in eco-innovative biofortified farmed fish and 2) to quantify trace elements in normal and tumour human tissues. In both case studies, the laboratory secondary target XRF spectrometer with polarized geometry (E5 model) was employed. About 100 fish and 30 tissue samples were measured and analyseds by developing new dedicated calibration protocols.

It should be noted that the transfer of essential nutrients to tailor-made farm fish using sustainable marine resources (biofortification) is one potential strategy to cope with dietary deficiencies observed in the human populations worldwide. In order to evaluate the efficacy of such a methodology, it is important to be able to quantify the accumulation of trace elements by farmed fish exposed to different diets that contain key nutrients and further understand the observed differences so that to optimize the biofortification process. The results allowed for a better understanding of trace elements accumulation by farmed fish exposed to different diets and have re-confirmed and further enhanced the attractive potential of polarized excited XRF analysis for trace elements analysis in biological matrices.

The trace element analysis of normal and tumour human tissues can help to establish possible correlations between variations of element concentrations and factors like age or sex, leading to a better understanding of carcinogenesis. However, most of the existing studies have a major drawback: the scarce number of analysed samples, resulting in statistical irrelevance. On the other hand, anatomical pathology services have at their disposal a vast collection of tissue samples, embedded in paraffin for long-term preservation, that can be used for histopathology and research purposes. Thus, the present study aimed to determine accurate trace element concentrations and compared with those obtained with paraffin embedded tissues, thus allowing the later samples to be used for routine analysis and screening.

2) Another in-house development was conducted in collaboration with A. Hein (Ceramics and Composite Materials Group of INN) and A. Panagopoulou, a PhD student. It was related to the development of a methodology to apply benchtop high-energy and polarized geometry EDXRF analysis for Rare Earth Elements in archaeological ceramics: The results of this work were presented as a poster contribution in the 6th `ARCH_RNT` Symposium - Archaeological Research and New

Technologies, Kalamata 8-9 October 2020. The results of this study confirmed that several REEs can determined with adequate accuracy, precision and limit of detection (1-2 ppm for La, Ce, Nd, Sm), so that they can be used for statistical data evaluations and formation of compositional groups in archaeological ceramic studies even though specific limitations have emerged. Moreover, and apart from the analytical performance of this EDXRF method, the comparably simple sample preparation in the form of pelletized powders proved to be an advantage as the material can be stored and reanalyzed in the future by complementary techniques. Fig.66,67 demonstrate the results from the quantitative determination of Lα.

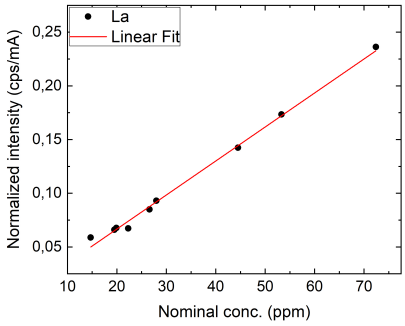

Figure 66: Calibration curves of normalized characteristic X-ray intensities versus the concentration of analyte.

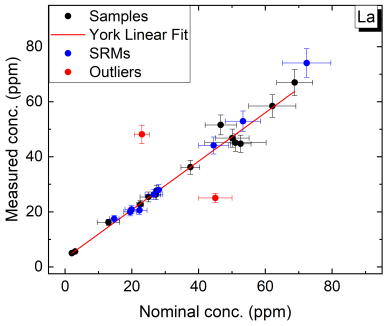

Figure 67: Validation of the calibration comparing measured and nominal concentrations of certified standards and clays.

3) In collaboration with the School of Chemical and Environmental Engineering, Technical University of Crete, and the research associate Dr Chatousidou Sofia-Eirini, the analytical capabilities of a HHXRF analyzer were exploited with the aim to attain reliable quantification of trace elements in Air Particulate Matter samples. In September 2020, systematic measurements were carried out at the XRF laboratory with the purpose to investigate and evaluate optimized analytical protocols. This work and collaboration was continued through 2021 as well.

4) In November 2020 a collaboration was started with Dr. Vana Orfanou, University College Dublin, Ireland, regarding protocols to evaluate the correctness of XRF quantification methodologies for the analysis copper corroded samples.

Support in student's work

About 15 PhD/MSc, Diploma students or external collaborators have accessed the XRF laboratory premises (see detailed list in Table 12). **Nelly Kladouri** conducted metal analysis on votive finds from various sanctuaries of Tegea, Arcadia, Greece dating between the 9th -7thc. B.C.E. In explicit, micro-XRF measurements were carried out from approximately 100 ancient artefacts from the sanctuaries of Alea Athena and of Athena Sotira and Poseidon. **Tatiana Panagopoulou** performed detailed micro-XRF study on approximately 200 metal artefacts from the Bronze Age Minoan Peak Sanctuary at Ayios Yeoryios sto Vouno, Kythera, Greece. MSc student **Philippos Kastanias** and PhD student **Panagiotis Tsamos** from the Aristotle University of Thessaloniki, Chemistry Department have conducted EDXRF measurements on ten plant and 21 soil samples.

Table 12: PhD/MSc, Diploma students and external collaborators of the XRF laboratory in the year 2020.

Student	**PhD/ MSc/ Diploma/ Practical**	**Thesis committee or supervisor**	**Start or duration of activity**	**Thesis title or/and Specific activity involved**
A. Asvestas	PhD	D. Anagnostopoulos, A. G. Karydas, M. Karakasides	2020	Development of portable XRF spectroscopy and applications in elemental analyses of materials
S. Papagiannis	PhD	D. Anagnostopoulos, A. G. Karydas, E. Diapouli	2020	X-ray spectrometry techniques applied for the characterization of atmospheric aerosol and pollution sources
N. Kladouri	PhD	N. Zacharias, E. Zymi, A.G Karydas	2018	The copper-based technology of votive offerings from the sanctuaries of Tegea, Arcadia, Greece, 9th-7th c. BCE
E. Triantafyllidi	PhD	N. Zacharias, E. Zymi, A.G Karydas	2020	Archaeometric Study of fine Hellenistic and Roman Ceramic ware from sites in Messene and Ileia
K. Tsampa	PhD	A. G. Karydas, M. Kokkoris, D. Anagnostopoulos	2020	Development and application of portable instrumentation of X-ray fluorescence imaging spectrometry in the analysis of archaeological gold alloys and study of the emission spectrum of the characteristic L and M rays of gold using Synchrotron radiation

Student	PhD/ MSc/ Diploma/ Practical	Thesis committee or supervisor	Start or duration of activity	Thesis title or/and Specific activity involved
Ch. Christofi	MSc	N. Zacharias, A. G. Karydas, V. Kassianidou	11/20	In-situ p-XRF analysis of Mycenaean swords at Patras archaeological museum within the thesis:The analysis of the swords Naue II type from Achaea-Greece and Enkomi – Cyprus (see Fig.68)
D. Tsakou	MSc	A. G. Karydas, M. Kokkoris	Since 9/2020	Study of the emission spectrum from end-window x-ray tubes
E. Eleftheriou	MSc	A. G. Karydas, M. Kokkoris	Since 9/2020	Advanced XRF Tools and Methodologies for the Study of Ancient Polychrome
Zoe Bari	BSc	A. G. Karydas	7-8/2020	Practical work
T. Panagopoulou	PhD	University of Peloponnese	2017	Copper Metallurgy, Metalwork and Trade of the Bronze Age in Aegean: The Bronze Finds from the Minoan Peak Sanctuary at Ayios Yeoryios sto Vouno, Kythera
P. Kastanias	MSc	Aristotle University of Thessaloniki	7/2020	XRF measurements of biological samples within the thesis entitled: Effect of phosphate fertilizers on the concentration of heavy metals and radionuclides on vegetables
P. Tsamos	PhD	Aristotle University of Thessaloniki	7/2020	XRF measurements of soil samples
M. Roggenbucke	PhD		11/20	Micro-XRF analysis of archaeological iron samples in support of PhD thesis

Student	PhD/ MSc/ Diploma/ Practical	Thesis committee or supervisor	Start or duration of activity	Thesis title or/and Specific activity involved
S.-E. Chatousidou	Post Doc	Technical University of Crete	9/20	Development of calibration procedures for Handheld XRF (HHXRF) analysis of Air Particulate Matter samples
E. Panagopoulou	PhD student		Autumn 2020	EDXRF analysis of Rare Earth Elements in archaeological ceramics: Development and validation of the method

Figure 68: In-situ portable XRF measurements conducted in November 2020 at the Patras Archaeological Museum in the frame of Master of Science diploma thesis of Christoforos Christofi with subject entitled: "The analysis of the swords Naue II type from Achaea-Greece and Enkomi – Cyprus", implemented within the MSc program ≪Cultural Heritage Materials and Technologies≫ of the University of Peloponnese.

Funding-Analytical Services

- University College Dublin
- Benaki museum

DAMA
DIL
OptoEL
Kalamata Annex
DOM
TANDEM Accelerator
XRF

This is a test

Education and Outreach Activities

Among the activities of the Institute of Nuclear and Particle Physics education is of great importance. In this context, the INPP offers opportunities to both university students and high school and primary school aged children. The main educational activities can be summarized below:

Graduate and PostGraduate Educational activities

INPP in collaboration with the National Technical University of Athens (NTUA) organize a program of postgraduate studies which leads to a MSc or a PhD degree. The researchers of the Institute along with professors of NTUA jointly teach classes in this program. Furthermore, researchers of the Institute supervise and guide graduate students for the completion of their degree. During 2020 the following PhD and MSc degrees have been awarded:

- Dimitrakopoulos Nikolaos, MSc, A. Lagoyannis
- Eleutheriou Eva, MSc, A. Karydas
- Nanos Stefanos, MSc, M. Axiotis
- Peroulis Spyridon, MSc, D. Bonatsos
- Trantou Foteini Faidra, MSc, T. Geralis
- Tsakou Dimitra, MSc, A. Karydas
- Vasiliou Polytimos, MSc, A. Lagoyannis
- Asenov Patrick, PhD, D. Loukas
- Khaliel Ahmed, PhD, M. Axiotis
- Ntemou Eleni, PhD, A. Lagoyannis
- Paspalaki Garyfallia, PhD, A. Kyriakis
- Sobhani Hadi, PhD, D. Bonatsos

The following PhD/MSc efforts are ongoing:

- Peoviti Maria, MSc, M. Axiotis
- Assiouras Panagiotis, PhD, D. Loukas
- Asvestas Anastasios, PhD, A. Karydas
- Canko Dhimiter, PhD, K. Papadopoulos
- Chasapoglou Sotirios, PhD, A. Lagoyannis
- Georgali Eustathia, PhD, A. Lagoyannis & M. Axiotis
- Kladouri Nikoletta-Kanella, PhD, A. Karydas
- Laoutaris Aggelos, PhD, A. Lagoyannis
- Madesis Ioannis, PhD, S. Charisopoulos
- Nanos Stefanos, PhD, M. Axiotis
- Panagopoulou Tatiana, PhD, A. Karydas
- Papagiannis Stefanos, PhD, A. Karydas
- Prapa Maria-Myrto, PhD, T. Geralis
- Preketes - Sigalas Konstantinos, PhD, A. Lagoyannis
- Sarantopoulou Smaragda, PhD, D. Bonatsos
- Sinopoulou Anna, PhD, E. Tzamariudaki
- Stakia Anna, PhD, G. Daskalakis

- Stavropoulos Dimitrios, PhD, E. Tzamariudaki
- Syrrakos Nikolaos, PhD, K. Papadopoulos
- Tsampa Kalliopi, PhD, A. Karydas
- Tsavalas Pavlos, PhD, A. Lagoyannis
- Tsourapis Vasileios, PhD, C. Markou
- Tzanetatos Dimitrios, PhD, C. Markou
- Zorba Olga, PhD, T. Geralis
- Zyriliou Ekaterini, PhD, A. Lagoyannis

INPP, through agreements with Universities in Greece, supervise and guide undergraduate students during their Diploma thesis as well as their practical training. Students are trained by participating to the research projects of the Institute in order to acquire a training certificate (about 1-3 months training) or a diploma thesis needed for their graduation (about 6 months training). During 2020 nine (17) undergraduate students were trained from the INPP researchers.

- Biniskos Andreas, Diploma thesis, M. Axiotis
- Blanas Vasilis, Diploma thesis, T. Geralis
- Dizis Aggelos, Diploma thesis, D. Loukas
- Tsantiri Artemis, Diploma thesis, A. Lagoyannis
- Agoritsis Georgios, Practical Training, G. Anagnostou
- Androutsou Eleni, Practical Training, G. Stavropoulos
- Iatridis Georgios, Practical Training, C. Markou
- Giannakopoulos Dimitrios, Practical Training, G. Stavropoulos
- Kalpakidou Eudoksia, Practical Training, G. Daskalakis
- Katsimalis Philippos, Practical Training, C. Markou
- Ligda Artemis, Practical Training, E. Tzamariudaki
- Moniaki Melina, Practical Training, E. Tzamariudaki
- Mpari Zoi, Practical Training, A. Karydas
- Papaphillipou Dimitris, Practical Training, D. Loukas
- Peza Aleksandra, Practical Training, C. Markou
- Remoundou Theodora, Practical Training, G. Stavropoulos
- Tsolis Nikolaos, Diploma thesis, C. Papadopoulos
- Velezioti Marilia, Practical Training, G. Anagnostou
- Zarpapis Georgios, Practical Training, E. Tzamariudaki

Cadet Researchers

"Cadet Researchers A life experience" is an educational activity held in NCSR DEMOKRITOS with the initiative of the Institute of Nuclear and Particle Physics.

TO BE FILLED (Christos)

Particle Physics Masterclasses

The Institute of Nuclear and Particle Physics of NCSR Demokritos, organizes every year the Particle Physics Masterclasses for high school students. The international particle physics masterclasses are workshops organized by the International Particle Physics Outreach Group (IPPOG, http://ippog.org/). The Masterclasses take place in more than 50 countries and more than 200 universities and research

institutes all over the world. In Greece, the participants are the universities of Athens, Thessaloniki, Crete, the National Technical University (NTUA), as well as NCSR Demokritos. During the day, high school students have the opportunity to work together with researchers in high energy physics and analyze particle physics data from the Large Hadron Collider (LHC). Initially, the students attend presentations for particle physics theory, accelerators, detectors and cosmology. Then, in the second part of the masterclass, the students are trained to analyze events from CMS experiment and "discover" by themselves the Higgs Boson. Finally, a teleconference takes place with other high schools around the world participating in the masterclass at the same day. During the conference, the students present and discuss their results and familiarize themselves with the international/multicultural tradition of research in fundamental physics. In 2020, INPP organized a virtual masterclass (due to Pandemic) at NCSR Demokritos.

www.physicsmasterclasses.org
https://physicsmasterclasses.org/index.php?cat=country&page=gr_athen3
www.facebook.com/InternationalParticlePhysicsMasterclasses
https://twitter.com/physicsIMC

NCSR Demokritos Summer School

INPP scientists have been members of the organizing committees and have participated as lecturers in Summer Schools for University graduate students and young scientists. The Summer School organized each year by NCSR Demokritos is a two-week course and aims to keep them up-to-date with the latest research developments at the Center and internationally. Speeches are given by Institute members and guest speakers, while participants visit the Institute's laboratory facilities. INPP speakers are ranked at the top positions based on students' evaluation.

Complex Systems and Applications (C.O.S.A.)

Our theory group research activity on Classical and Quantum Chaotic Dynamics is strengthened with the COSA Initiative. It was kicked off in 2006 by an act of the Council of institute Directors of NCSR Demokritos at the scientific recommendation of researchers from the center. Its purpose was to set up an interdisciplinary network of Greek researchers, with NCSR Demokritos as its cross-fertilizing hub. Its aim is to promote the study of the emerging new field of complexity research. It requires the synergy of a variety of concepts, methods and techniques from a variety of fields such as information Science, Nonlinear Sciences-deterministic chaos, nonequilibrium statistical mechanics and Fractal geometry. It equally touches through its insights a wide range of the human scientific endeavor ranging from particle and nuclear physics, cosmology and astrophysics, nanotechnology and mesoscopic physics as well as biology, economics and social sciences.

COSA's activities are educational and outreach through

- a semester course offered for credit in collaboration with the National Technical University of Athens on "Special Topics on Complex Systems"
- Cosa seminars on "Nonlinear Science and Complexity"

High Energy Physics - ATLAS

[Aab+20a] Morad Aaboud et al. "Fluctuations of anisotropic flow in Pb+Pb collisions at $\sqrt{s_{\mathrm{NN}}} = 5.02$ TeV with the ATLAS detector". In: *JHEP* 01 (2020), p. 051. DOI: 10.1007/JHEP01(2020)051. arXiv: 1904.04808 [nucl-ex].

[Aab+20b] Morad Aaboud et al. "Measurements of top-quark pair spin correlations in the $e\mu$ channel at $\sqrt{s} = 13$ TeV using pp collisions in the ATLAS detector". In: *Eur. Phys. J. C* 80.8 (2020), p. 754. DOI: 10.1140/epjc/s10052-020-8181-6. arXiv: 1903.07570 [hep-ex].

[Aad+20a] Georges Aad et al. "A search for the $Z\gamma$ decay mode of the Higgs boson in pp collisions at $\sqrt{s} = 13$ TeV with the ATLAS detector". In: *Phys. Lett. B* 809 (2020), p. 135754. DOI: 10.1016/j.physletb.2020.135754. arXiv: 2005.05382 [hep-ex].

[Aad+20b] Georges Aad et al. "Alignment of the ATLAS Inner Detector in Run-2". In: *Eur. Phys. J. C* 80.12 (2020), p. 1194. DOI: 10.1140/epjc/s10052-020-08700-6. arXiv: 2007.07624 [hep-ex].

[Aad+20c] Georges Aad et al. "ATLAS data quality operations and performance for 2015–2018 data-taking". In: *JINST* 15.04 (2020), P04003. DOI: 10.1088/1748-0221/15/04/P04003. arXiv: 1911.04632 [physics.ins-det].

[Aad+20d] Georges Aad et al. "Combination of searches for Higgs boson pairs in pp collisions at $\sqrt{s}$ =13 TeV with the ATLAS detector". In: *Phys. Lett. B* 800 (2020), p. 135103. DOI: 10.1016/j.physletb.2019.135103. arXiv: 1906.02025 [hep-ex].

[Aad+20e] Georges Aad et al. "Combination of the W boson polarization measurements in top quark decays using ATLAS and CMS data at $\sqrt{s} = 8$ TeV". In: *JHEP* 08.08 (2020), p. 051. DOI: 10.1007/JHEP08(2020)051. arXiv: 2005.03799 [hep-ex].

[Aad+20f] Georges Aad et al. "Combined measurements of Higgs boson production and decay using up to 80 fb^{-1} of proton-proton collision data at $\sqrt{s} = 13$ TeV collected with the ATLAS experiment". In: *Phys. Rev. D* 101.1 (2020), p. 012002. DOI: 10.1103/PhysRevD.101.012002. arXiv: 1909.02845 [hep-ex].

[Aad+20g] Georges Aad et al. "CP Properties of Higgs Boson Interactions with Top Quarks in the $t\bar{t}H$ and tH Processes Using $H \to \gamma\gamma$ with the ATLAS Detector". In: *Phys. Rev. Lett.* 125.6 (2020), p. 061802. DOI: 10.1103/PhysRevLett.125.061802. arXiv: 2004.04545 [hep-ex].

[Aad+20h] Georges Aad et al. "Dijet resonance search with weak supervision using $\sqrt{s} = 13$ TeV pp collisions in the ATLAS detector". In: *Phys. Rev. Lett.* 125.13 (2020), p. 131801. DOI: 10.1103/PhysRevLett.125.131801. arXiv: 2005.02983 [hep-ex].

[Aad+20i] Georges Aad et al. "Evidence for electroweak production of two jets in association with a $Z\gamma$ pair in pp collisions at $\sqrt{s} = 13$ TeV with the ATLAS detector". In: *Phys. Lett. B* 803 (2020), p. 135341. DOI: 10.1016/j.physletb.2020.135341. arXiv: 1910.09503 [hep-ex].

[Aad+20j] Georges Aad et al. "Evidence for $t\bar{t}t\bar{t}$ production in the multilepton final state in proton–proton collisions at $\sqrt{s} = 13\ TeV$ with the ATLAS detector". In: *Eur. Phys. J. C* 80.11 (2020), p. 1085. DOI: 10.1140/epjc/s10052-020-08509-3. arXiv: 2007.14858 [hep-ex].

[Aad+20k] Georges Aad et al. "Higgs boson production cross-section measurements and their EFT interpretation in the 4ℓ decay channel at $\sqrt{s}$ =13 TeV with the ATLAS detector". In: *Eur. Phys. J. C* 80.10 (2020). [Erratum: Eur.Phys.J.C 81, 29 (2021), Erratum: Eur.Phys.J.C 81, 398 (2021)], p. 957. DOI: 10.1140/epjc/s10052-020-8227-9. arXiv: 2004.03447 [hep-ex].

[Aad+20l] Georges Aad et al. "Measurement of azimuthal anisotropy of muons from charm and bottom hadrons in Pb+Pb collisions at $\sqrt{s_{NN}} =$ 5.02 TeV with the ATLAS detector". In: *Phys. Lett. B* 807 (2020), p. 135595. DOI: 10.1016/j.physletb.2020.135595. arXiv: 2003.03565 [nucl-ex].

[Aad+20m] Georges Aad et al. "Measurement of azimuthal anisotropy of muons from charm and bottom hadrons in pp collisions at $\sqrt{s} = 13$ TeV with the ATLAS detector". In: *Phys. Rev. Lett.* 124.8 (2020), p. 082301. DOI: 10.1103/PhysRevLett.124.082301. arXiv: 1909.01650 [nucl-ex].

[Aad+20n] Georges Aad et al. "Measurement of differential cross sections for single diffractive dissociation in $\sqrt{s} = 8$ TeV pp collisions using the ATLAS ALFA spectrometer". In: *JHEP* 02 (2020). [Erratum: JHEP 10, 182 (2020)], p. 042. DOI: 10.1007/JHEP02(2020)042. arXiv: 1911.00453 [hep-ex].

[Aad+20o] Georges Aad et al. "Measurement of isolated-photon plus two-jet production in pp collisions at $\sqrt{s} = 13$ TeV with the ATLAS detector". In: *JHEP* 03 (2020), p. 179. DOI: 10.1007/JHEP03(2020)179. arXiv: 1912.09866 [hep-ex].

[Aad+20p] Georges Aad et al. "Measurement of soft-drop jet observables in pp collisions with the ATLAS detector at $\sqrt{s}$ =13 TeV". In: *Phys. Rev. D* 101.5 (2020), p. 052007. DOI: 10.1103/PhysRevD.101.052007. arXiv: 1912.09837 [hep-ex].

[Aad+20q] Georges Aad et al. "Measurement of the azimuthal anisotropy of charged-particle production in $Xe + Xe$ collisions at $\sqrt{s_{\mathrm{NN}}} = 5.44$ TeV with the ATLAS detector". In: *Phys. Rev. C* 101.2 (2020), p. 024906. DOI: 10.1103/PhysRevC.101.024906. arXiv: 1911.04812 [nucl-ex].

[Aad+20r] Georges Aad et al. "Measurement of the Lund Jet Plane Using Charged Particles in 13 TeV Proton-Proton Collisions with the ATLAS Detector". In: *Phys. Rev. Lett.* 124.22 (2020), p. 222002. DOI: 10.1103/PhysRevLett.124.222002. arXiv: 2004.03540 [hep-ex].

[Aad+20s] Georges Aad et al. "Measurement of the transverse momentum distribution of Drell–Yan lepton pairs in proton–proton collisions at $\sqrt{s} = 13$ TeV with the ATLAS detector". In: *Eur. Phys. J. C* 80.7 (2020), p. 616. DOI: 10.1140/epjc/s10052-020-8001-z. arXiv: 1912.02844 [hep-ex].

[Aad+20t] Georges Aad et al. "Measurement of the $t\bar{t}$ production cross-section and lepton differential distributions in $e\mu$ dilepton events from pp collisions at $\sqrt{s} = 13\,TeV$ with the ATLAS detector". In: *Eur. Phys. J. C* 80.6 (2020), p. 528. DOI: 10.1140/epjc/s10052-020-7907-9. arXiv: 1910.08819 [hep-ex].

[Aad+20u] Georges Aad et al. "Measurement of the $t\bar{t}$ production cross-section in the lepton+jets channel at $\sqrt{s} = 13$ TeV with the ATLAS experiment". In: *Phys. Lett. B* 810 (2020), p. 135797. DOI: 10.1016/j.physletb.2020.135797. arXiv: 2006.13076 [hep-ex].

[Aad+20v] Georges Aad et al. "Measurement of the $Z(\to \ell^+\ell^-)\gamma$ production cross-section in pp collisions at $\sqrt{s} = 13$ TeV with the ATLAS detector". In: *JHEP* 03 (2020), p. 054. DOI: 10.1007/JHEP03(2020)054. arXiv: 1911.04813 [hep-ex].

[Aad+20w] Georges Aad et al. "Measurements of inclusive and differential cross-sections of combined $t\bar{t}\gamma$ and $tW\gamma$ production in the eμ channel at 13 TeV with the ATLAS detector". In: *JHEP* 09 (2020), p. 049. DOI: 10.1007/JHEP09(2020)049. arXiv: 2007.06946 [hep-ex].

[Aad+20x] Georges Aad et al. "Measurements of the Higgs boson inclusive and differential fiducial cross sections in the 4ℓ decay channel at $\sqrt{s} = 13$ TeV". In: *Eur. Phys. J. C* 80.10 (2020), p. 942. DOI: 10.1140/epjc/s10052-020-8223-0. arXiv: 2004.03969 [hep-ex].

[Aad+20y] Georges Aad et al. "Measurements of the production cross-section for a Z boson in association with b-jets in proton-proton collisions at $\sqrt{s} = 13$ TeV with the ATLAS detector". In: *JHEP* 07 (2020), p. 044. DOI: 10.1007/JHEP07(2020)044. arXiv: 2003.11960 [hep-ex].

[Aad+20z] Georges Aad et al. "Observation and Measurement of Forward Proton Scattering in Association with Lepton Pairs Produced via the Photon Fusion Mechanism at ATLAS". In: *Phys. Rev. Lett.* 125.26 (2020), p. 261801. DOI: 10.1103/PhysRevLett.125.261801. arXiv: 2009.14537 [hep-ex].

[Aad+20aa] Georges Aad et al. "Observation of the associated production of a top quark and a Z boson in pp collisions at $\sqrt{s} = 13$ TeV with the ATLAS detector". In: *JHEP* 07 (2020), p. 124. DOI: 10.1007/JHEP07(2020)124. arXiv: 2002.07546 [hep-ex].

[Aad+20ab] Georges Aad et al. "Operation of the ATLAS trigger system in Run 2". In: *JINST* 15.10 (2020), P10004. DOI: 10.1088/1748-0221/15/10/P10004. arXiv: 2007.12539 [physics.ins-det].

[Aad+20ac] Georges Aad et al. "Performance of electron and photon triggers in ATLAS during LHC Run 2". In: *Eur. Phys. J. C* 80.1 (2020), p. 47. DOI: 10.1140/epjc/s10052-019-7500-2. arXiv: 1909.00761 [hep-ex].

[Aad+20ad] Georges Aad et al. "Performance of the ATLAS muon triggers in Run 2". In: *JINST* 15.09 (2020), P09015. DOI: 10.1088/1748-0221/15/09/p09015. arXiv: 2004.13447 [physics.ins-det].

[Aad+20ae] Georges Aad et al. "Performance of the missing transverse momentum triggers for the ATLAS detector during Run-2 data taking". In: *JHEP* 08 (2020), p. 080. DOI: 10.1007/JHEP08(2020)080. arXiv: 2005.09554 [hep-ex].

[Aad+20af] Georges Aad et al. "Performance of the upgraded PreProcessor of the ATLAS Level-1 Calorimeter Trigger". In: *JINST* 15.11 (2020), P11016. DOI: 10.1088/1748-0221/15/11/P11016. arXiv: 2005.04179 [physics.ins-det].

[Aad+20ag] Georges Aad et al. "Reconstruction and identification of boosted di-τ systems in a search for Higgs boson pairs using 13 TeV proton-proton collision data in ATLAS". In: *JHEP* 11 (2020), p. 163. DOI: 10.1007/JHEP11(2020)163. arXiv: 2007.14811 [hep-ex].

[Aad+20ah] Georges Aad et al. "Search for a scalar partner of the top quark in the all-hadronic $t\bar{t}$ plus missing transverse momentum final state at $\sqrt{s} = 13$ TeV with the ATLAS detector". In: *Eur. Phys. J. C* 80.8 (2020), p. 737. DOI: 10.1140/epjc/s10052-020-8102-8. arXiv: 2004.14060 [hep-ex].

[Aad+20ai] Georges Aad et al. "Search for chargino-neutralino production with mass splittings near the electroweak scale in three-lepton final states in $\sqrt{s}$=13 TeV pp collisions with the ATLAS detector". In: *Phys. Rev. D* 101.7 (2020), p. 072001. DOI: 10.1103/PhysRevD.101.072001. arXiv: 1912.08479 [hep-ex].

[Aad+20aj] Georges Aad et al. "Search for dijet resonances in events with an isolated charged lepton using $\sqrt{s} = 13$ TeV proton-proton collision data collected by the ATLAS detector". In: *JHEP* 06 (2020), p. 151. DOI: 10.1007/JHEP06(2020)151. arXiv: 2002.11325 [hep-ex].

[Aad+20ak] Georges Aad et al. "Search for direct production of electroweakinos in final states with missing transverse momentum and a Higgs boson decaying into photons in pp collisions at $\sqrt{s} = 13$ TeV with the ATLAS detector". In: *JHEP* 10 (2020), p. 005. DOI: 10.1007/JHEP10(2020)005. arXiv: 2004.10894 [hep-ex].

[Aad+20al] Georges Aad et al. "Search for direct production of electroweakinos in final states with one lepton, missing transverse momentum and a Higgs boson decaying into two b-jets in pp collisions at $\sqrt{s} = 13$ TeV with the ATLAS detector". In: *Eur. Phys. J. C* 80.8 (2020), p. 691. DOI: 10.1140/epjc/s10052-020-8050-3. arXiv: 1909.09226 [hep-ex].

[Aad+20am] Georges Aad et al. "Search for direct stau production in events with two hadronic τ-leptons in $\sqrt{s} = 13$ TeV pp collisions with the ATLAS detector". In: *Phys. Rev. D* 101.3 (2020), p. 032009. DOI: 10.1103/PhysRevD.101.032009. arXiv: 1911.06660 [hep-ex].

[Aad+20an] Georges Aad et al. "Search for displaced vertices of oppositely charged leptons from decays of long-lived particles in pp collisions at $\sqrt{s}$ =13 TeV with the ATLAS detector". In: *Phys. Lett. B* 801 (2020), p. 135114. DOI: 10.1016/j.physletb.2019.135114. arXiv: 1907.10037 [hep-ex].

[Aad+20ao] Georges Aad et al. "Search for electroweak production of charginos and sleptons decaying into final states with two leptons and missing transverse momentum in $\sqrt{s} = 13$ TeV pp collisions using the ATLAS detector". In: *Eur. Phys. J. C* 80.2 (2020), p. 123. DOI: 10.1140/epjc/s10052-019-7594-6. arXiv: 1908.08215 [hep-ex].

[Aad+20ap] Georges Aad et al. "Search for flavour-changing neutral currents in processes with one top quark and a photon using 81 fb^{-1} of pp collisions at $\sqrt{s} = 13$ TeV with the ATLAS experiment". In: *Phys. Lett. B* 800 (2020), p. 135082. DOI: 10.1016/j.physletb.2019.135082. arXiv: 1908.08461 [hep-ex].

[Aad+20aq] Georges Aad et al. "Search for heavy diboson resonances in semileptonic final states in pp collisions at $\sqrt{s} = 13$ TeV with the ATLAS detector". In: *Eur. Phys. J. C* 80.12 (2020), p. 1165. DOI: 10.1140/epjc/s10052-020-08554-y. arXiv: 2004.14636 [hep-ex].

[Aad+20ar] Georges Aad et al. "Search for heavy Higgs bosons decaying into two tau leptons with the ATLAS detector using pp collisions at $\sqrt{s} = 13$ TeV". In: *Phys. Rev. Lett.* 125.5 (2020), p. 051801. DOI: 10.1103/PhysRevLett.125.051801. arXiv: 2002.12223 [hep-ex].

[Aad+20as] Georges Aad et al. "Search for heavy resonances decaying into a photon and a hadronically decaying Higgs boson in pp collisions at $\sqrt{s} = 13$ TeV with the ATLAS detector". In: *Phys. Rev. Lett.* 125 (2020), p. 251802. DOI: 10.1103/PhysRevLett.125.251802. arXiv: 2008.05928 [hep-ex].

[Aad+20at] Georges Aad et al. "Search for Higgs Boson Decays into a Z Boson and a Light Hadronically Decaying Resonance Using 13 TeV pp Collision Data from the ATLAS Detector". In: *Phys. Rev. Lett.* 125.22 (2020), p. 221802. DOI: 10.1103/PhysRevLett.125.221802. arXiv: 2004.01678 [hep-ex].

[Aad+20au] Georges Aad et al. "Search for Higgs boson decays into two new low-mass spin-0 particles in the $4b$ channel with the ATLAS detector using pp collisions at $\sqrt{s} = 13$ TeV". In: *Phys. Rev. D* 102.11 (2020), p. 112006. DOI: 10.1103/PhysRevD.102.112006. arXiv: 2005.12236 [hep-ex].

[Aad+20av] Georges Aad et al. "Search for light long-lived neutral particles produced in pp collisions at $\sqrt{s} = 13$ TeV and decaying into collimated leptons or light hadrons with the ATLAS detector". In: *Eur. Phys. J. C* 80.5 (2020), p. 450. DOI: 10.1140/epjc/s10052-020-7997-4. arXiv: 1909.01246 [hep-ex].

[Aad+20aw] Georges Aad et al. "Search for long-lived, massive particles in events with a displaced vertex and a muon with large impact parameter in pp collisions at $\sqrt{s} = 13$ TeV with the ATLAS detector". In: *Phys. Rev. D* 102.3 (2020), p. 032006. DOI: 10.1103/PhysRevD.102.032006. arXiv: 2003.11956 [hep-ex].

[Aad+20ax] Georges Aad et al. "Search for long-lived neutral particles produced in pp collisions at $\sqrt{s} = 13$ TeV decaying into displaced hadronic jets in the ATLAS inner detector and muon spectrometer". In: *Phys. Rev. D* 101.5 (2020), p. 052013. DOI: 10.1103/PhysRevD.101.052013. arXiv: 1911.12575 [hep-ex].

[Aad+20ay] Georges Aad et al. "Search for Magnetic Monopoles and Stable High-Electric-Charge Objects in 13 Tev Proton-Proton Collisions with the ATLAS Detector". In: *Phys. Rev. Lett.* 124.3 (2020), p. 031802. DOI: 10.1103/PhysRevLett.124.031802. arXiv: 1905.10130 [hep-ex].

[Aad+20az] Georges Aad et al. "Search for new non-resonant phenomena in high-mass dilepton final states with the ATLAS detector". In: *JHEP* 11 (2020). [Erratum: JHEP 04, 142 (2021)], p. 005. DOI: 10.1007/JHEP11(2020)005. arXiv: 2006.12946 [hep-ex].

[Aad+20ba] Georges Aad et al. "Search for new phenomena in final states with large jet multiplicities and missing transverse momentum using $\sqrt{s} = 13$ TeV proton-proton collisions recorded by ATLAS in Run 2 of the LHC". In: *JHEP* 10 (2020), p. 062. DOI: 10.1007/JHEP10(2020)062. arXiv: 2008.06032 [hep-ex].

[Aad+20bb] Georges Aad et al. "Search for new resonances in mass distributions of jet pairs using 139 fb^{-1} of pp collisions at $\sqrt{s} = 13$ TeV with the ATLAS detector". In: *JHEP* 03 (2020), p. 145. DOI: 10.1007/JHEP03(2020)145. arXiv: 1910.08447 [hep-ex].

[Aad+20bc] Georges Aad et al. "Search for non-resonant Higgs boson pair production in the $bb\ell\nu\ell\nu$ final state with the ATLAS detector in pp collisions at $\sqrt{s} = 13$ TeV". In: *Phys. Lett. B* 801 (2020), p. 135145. DOI: 10.1016/j.physletb.2019.135145. arXiv: 1908.06765 [hep-ex].

[Aad+20bd] Georges Aad et al. "Search for pairs of scalar leptoquarks decaying into quarks and electrons or muons in $\sqrt{s} = 13$ TeV pp collisions with the ATLAS detector". In: *JHEP* 10 (2020), p. 112. DOI: 10.1007/JHEP10(2020)112. arXiv: 2006.05872 [hep-ex].

[Aad+20be] Georges Aad et al. "Search for resonances decaying into a weak vector boson and a Higgs boson in the fully hadronic final state produced in proton−proton collisions at $\sqrt{s} = 13$ TeV with the ATLAS detector". In: *Phys. Rev. D* 102.11 (2020), p. 112008. DOI: 10.1103/PhysRevD.102.112008. arXiv: 2007.05293 [hep-ex].

[Aad+20bf] Georges Aad et al. "Search for squarks and gluinos in final states with same-sign leptons and jets using 139 fb^{-1} of data collected with the ATLAS detector". In: *JHEP* 06 (2020), p. 046. DOI: 10.1007/JHEP06(2020)046. arXiv: 1909.08457 [hep-ex].

[Aad+20bg] Georges Aad et al. "Search for the $HH \to b\bar{b}b\bar{b}$ process via vector-boson fusion production using proton-proton collisions at $\sqrt{s} = 13$ TeV with the ATLAS detector". In: *JHEP* 07 (2020). [Erratum: JHEP 01, 145 (2021), Erratum: JHEP 05, 207 (2021)], p. 108. DOI: 10.1007/JHEP07(2020)108. arXiv: 2001.05178 [hep-ex].

[Aad+20bh] Georges Aad et al. "Search for the Higgs boson decays $H \to ee$ and $H \to e\mu$ in pp collisions at $\sqrt{s} = 13$ TeV with the ATLAS detector". In: *Phys. Lett. B* 801 (2020), p. 135148. DOI: 10.1016/j.physletb.2019.135148. arXiv: 1909.10235 [hep-ex].

[Aad+20bi] Georges Aad et al. "Search for top squarks in events with a Higgs or Z boson using 139 fb^{-1} of pp collision data at $\sqrt{s} = 13$ TeV with the ATLAS detector". In: *Eur. Phys. J. C* 80.11 (2020), p. 1080. DOI: 10.1140/epjc/s10052-020-08469-8. arXiv: 2006.05880 [hep-ex].

[Aad+20bj] Georges Aad et al. "Search for $t\bar{t}$ resonances in fully hadronic final states in pp collisions at $\sqrt{s} = 13$ TeV with the ATLAS detector". In: *JHEP* 10 (2020), p. 061. DOI: 10.1007/JHEP10(2020)061. arXiv: 2005.05138 [hep-ex].

[Aad+20bk] Georges Aad et al. "Searches for electroweak production of supersymmetric particles with compressed mass spectra in $\sqrt{s} = 13$ TeV pp collisions with the ATLAS detector". In: *Phys. Rev. D* 101.5 (2020), p. 052005. DOI: 10.1103/PhysRevD.101.052005. arXiv: 1911.12606 [hep-ex].

[Aad+20bl] Georges Aad et al. "Searches for lepton-flavour-violating decays of the Higgs boson in $\sqrt{s} = 13$ TeV pp collisions with the ATLAS detector". In: *Phys. Lett. B* 800 (2020), p. 135069. DOI: 10.1016/j.physletb.2019.135069. arXiv: 1907.06131 [hep-ex].

[Aad+20bm] Georges Aad et al. "Test of CP invariance in vector-boson fusion production of the Higgs boson in the H $\to \tau\tau$ channel in proton–proton collisions at s=13TeV with the ATLAS detector". In: *Phys. Lett. B* 805 (2020), p. 135426. DOI: 10.1016/j.physletb.2020.135426. arXiv: 2002.05315 [hep-ex].

[Aad+20bn] Georges Aad et al. "Transverse momentum and process dependent azimuthal anisotropies in $\sqrt{s_{\mathrm{NN}}} = 8.16$ TeV p+Pb collisions with the ATLAS detector". In: *Eur. Phys. J. C* 80.1 (2020), p. 73. DOI: 10.1140/epjc/s10052-020-7624-4. arXiv: 1910.13978 [nucl-ex].

[Aad+20bo] Georges Aad et al. "Z boson production in Pb+Pb collisions at $\sqrt{s_{\mathrm{NN}}}$= 5.02 TeV measured by the ATLAS experiment". In: *Phys. Lett. B* 802 (2020), p. 135262. DOI: 10.1016/j.physletb.2020.135262. arXiv: 1910.13396 [nucl-ex].

High Energy Physics - ESSnuSB

[Ced+20] Joakim Cederkall et al. "The ESSnuSB project". In: *PoS* EPS-HEP2019 (2020), p. 392. DOI: 10.22323/1.364.0392.

[Par+20] Joochun Park et al. "Status of the detector design studies for ESSνSB". In: *PoS* NuFact2019 (2020), p. 041. DOI: 10.22323/1.369.0041.

High Energy Physics - CMS

[al20] W. Adam et al. "Beam test performance of prototype silicon detectors for the outer tracker for the phase-2 upgrade of CMS," in: *JINST 15 (03) P03014.* (2020). DOI: https://doi:10.1088/1748-0221/15/03/p03014.

[Col20a] CMS Collaboration. "A Deep Neural Network for Simultaneous Estimation of b Jet Energy and Resolution". In: *Comput. Softw. Big Sci* 4.1 (2020), p. 10. DOI: 10.1007/s41781-020-00041-z. eprint: 1912.06046.

[Col20b] CMS Collaboration. "A deep neural network to search for new long-lived particles decaying to jets". In: *MLST* (2020). DOI: https://doi.org/10.1088/2632-2153/ab9023.

[Col20c] CMS Collaboration. "A measurement of the Higgs boson mass in the diphoton decay channel". In: *PLB* (2020). DOI: https://doi.org/10.1016/j.physletb.2020.135425.

[Col20d] CMS Collaboration. "A search for the standard model Higgs boson decaying to charm quarks". In: *Journal of High Energy Physics* 2020.3 (Mar. 2020). ISSN: 1029-8479. DOI: 10.1007/jhep03(2020)131. URL: http://dx.doi.org/10.1007/JHEP03(2020)131.

[Col20e] CMS Collaboration. "Beam test performance of prototype silicon detectors for the Outer Tracker for the Phase-2 Upgrade of CMS". In: *JINST* (2020). DOI: 10.1088/1748-0221/15/03/P03014.

[Col20f] CMS Collaboration. "Bose-Einstein correlations of charged hadrons in proton-proton collisions s at $\sqrt{s} = 13\ TeV$". In: *JHEP 03 (2020) 014* (2020). DOI: https://10.1007/JHEP03(2020)014,arXiv:1910.08815.

[Col20g] CMS Collaboration. "Calibration of the CMS hadron calorimeters using proton-proton collision data at $\sqrt{s} = 13\ TeV$". In: *JINST 15 (2020) P05002* (2020). DOI: https://doi:10.1088/1748-0221/15/05/P05002,arXiv:1910.00079.

[Col20h] CMS Collaboration. "Combination of the W boson polarization measurements in top quark decays using ATLAS and CMS data at $\sqrt{s} = 8\ TeV$". In: *JHEP* (2020). DOI: https://doi.org/10.1007/JHEP08(2020)051.

[Col20i] CMS Collaboration. "Constraints on the χ_{c1} versus χ_{c2} Polarizations in Proton-Proton Collisions at $\sqrt{s} = 8\ TeV$". In: *Physical Review Letters* 124.16 (Apr. 2020). ISSN: 1079-7114. DOI: 10.1103/physrevlett.124.162002. URL: http://dx.doi.org/10.1103/PhysRevLett.124.162002.

[Col20j] CMS Collaboration. "Dependence of inclusive jet production on the anti- distance parameter in pp collisions at $\sqrt{s} = 13\ TeV$". In: *JHEP* (2020). DOI: https://doi:10.1007/JHEP12(2020)082.

[Col20k] CMS Collaboration. "Determination of the strong coupling constant αS(mZ) from measurements of inclusive W$\pm$ and Z boson production cross sections in proton-proton collisions at $\sqrt{s} = 7\ and\ 8\ TeV$". In: *Journal of High Energy Physics* 2020.6 (June 2020). ISSN: 1029-8479. DOI: 10.1007/jhep06(2020)018. URL: http://dx.doi.org/10.1007/JHEP06(2020)018.

[Col20l] CMS Collaboration. "Evidence for WW production from double-parton interactions in proton-proton collisions at $\sqrt{s} = 13\ TeV$". In: *EPJC 80 (2020) 41* (2020). DOI: https://doi:10.1140/epjc/s10052-019-7541-6,arXiv:1909.06265.

[Col20m] CMS Collaboration. "Experimental study of different silicon sensor options for the upgrade of the CMS Outer Tracker". In: *JINST* (2020). DOI: 10.1088/1748-0221/15/04/P04017.

[Col20n] CMS Collaboration. "Identification of heavy, energetic, hadronically decaying particles using machine-learning techniques". In: *JINST* (2020). DOI: https://doi:10.1088/1748-0221/15/06/P06005.

[Col20o] CMS Collaboration. "Measurement of b jet shapes in proton-proton collisions at $\sqrt{s} = 5.02\ TeV$". In: *JHEP* (2020). DOI: https://doi:10.1007/JHEP05(2021)054.

[Col20p] CMS Collaboration. "Measurement of CKM matrix elements in single top quark -channel production in proton-proton collisions at $\sqrt{s} = 13\ TeV$". In: *PLB* (2020). DOI: https://doi:10.1016/j.physletb.2020.135609.

[Col20q] CMS Collaboration. "Measurement of properties of B_s^0ß$\mu^+\mu^-$ decays and search for B^0ß$\mu^+\mu^-$with the CMS experiment". In: *JHEP 04 (2020) 188* (2020). DOI: https://doi:10.1007/JHEP04(2020)188,arXiv:1910.12127.

[Col20r] CMS Collaboration. "Measurement of quark- and gluon-like jet fractions using jet charge in PbPb and pp collisions at $\sqrt{s}$ = 5.02 TeV". In: *JHEP* (2020). DOI: https://doi:10.1007/JHEP07(2020)115.

[Col20s] CMS Collaboration. "Measurement of single-diffractive dijet production in proton-proton collisions at $\sqrt{(s)} = 13\ TeV$". In: *EPJC* (2020). DOI: https://doi.org/10.1140/epjc/s10052-020-08562-y.

[Col20t] CMS Collaboration. "Measurement of the associated production of a Z boson with charm or bottom quark jets in proton-proton collisions at $\sqrt{(s)} = 13\ TeV$". In: *PRD* (2020). DOI: https://doi.org/10.1103/PhysRevD.102.032007.

[Col20u] CMS Collaboration. "Measurement of the cross section for electroweak production of a Z boson, a photon and two jets in proton-proton collisions at $\sqrt{(s)} = 13\ TeV$". In: *JHEP* (2020). DOI: https://doi.org/10.1007/JHEP06(2020)076.

[Col20v] CMS Collaboration. "Measurement of the cross section for production with additional jets and b jets in pp collisions at $\sqrt{s}$ = 13 TeV". In: *JHEP* (2020). DOI: doi:10.1007/JHEP07(2020)125.

[Col20w] CMS Collaboration. "Measurement of the Jet Mass Distribution and Top Quark Mass in Hadronic Decays of Boosted Top Quarks in pp Collisions at $\sqrt{s}$ = 13 TeV". In: *Physical Review Letters* 124.20 (May 2020). ISSN: 1079-7114. DOI: 10.1103/physrevlett.124.202001. URL: http://dx.doi.org/10.1103/PhysRevLett.124.202001.

[Col20x] CMS Collaboration. "Measurement of the top quark forward-backward production asymmetry and the anomalous chromoelectric and chromomagnetic moments in pp collisions at $\sqrt{(s)}$ = 13 TeV". In: *JHEP* (2020). DOI: https://doi.org/10.1007/JHEP06(2020)146.

[Col20y] CMS Collaboration. "Measurement of the top quark pair production cross section in dilepton final states containing one τ lepton in pp collisions at $\sqrt{s} = 13\ TeV$". In: *Journal of High Energy Physics* 2020.2 (Feb. 2020). ISSN: 1029-8479. DOI: 10.1007/jhep02(2020)191. URL: http://dx.doi.org/10.1007/JHEP02(2020)191.

[Col20z] CMS Collaboration. "Measurement of the Y(1S) pair production cross section and search for resonances decaying to Y(1S) mu+ mu- in proton-proton collisions at $\sqrt{(s)}$ = 13 TeV". In: *PLB* (2020). DOI: https://doi.org/10.1016/j.physletb.2020.135578.

[Col20aa] CMS Collaboration. "Measurements of dose-rate effects in the radiation damage of plastic scintillator tiles using silicon photomultipliers". In: *JINST* (2020). DOI: https://doi.org/10.1088/1748-0221/15/06/P06009.

[Col20ab] CMS Collaboration. "Measurements of production cross sections of WZ and same-sign WW boson pairs in association with two jets in proton-proton collisions at $\sqrt{s} = 13\ TeV$". In: *PLB* (2020). DOI: https://doi:10.1016/j.physletb.2020.135710.

[Col20ac] CMS Collaboration. "Measurements of ttH production and the CP structure of the Yukawa interaction between the Higgs boson and top quark in the diphoton decay channel". In: *PRL* (2020). DOI: doi:10.1103/PhysRevLett.125.061801.

[Col20ad] CMS Collaboration. "Mixed higher-order anisotropic flow and nonlinear response coefficients of charged particles in PbPb collisions at $\sqrt{S_{NN}} = 5.02\ TeV$". In: *EPJC 80 (2020) 534* (2020). DOI: https://doi:10.1140/epjc/s10052-020-7834-9,arXiv:1910.08789.

[Col20ae] CMS Collaboration. "Observation of the Λ_b^0ß$J/\psi\Lambda\phi$ decay in proton-proton collisions at $\sqrt{s} = 13\ TeV$". In: *Physics Letters B* 802 (Mar. 2020), p. 135203. ISSN: 0370-2693. DOI: 10.1016/j.physletb.2020.135203. URL: http://dx.doi.org/10.1016/j.physletb.2020.135203.

[Col20af] CMS Collaboration. "Observation of the Bs0 to X(3872) decay". In: *PRL* (2020). DOI: https://doi:10.1103/PhysRevLett.125.15200.

[Col20ag] CMS Collaboration. "Performance of the CMS Level-1 trigger in proton-proton collisions at $\sqrt{s} = 13\ TeV$". In: *JINST* (2020). DOI: https://10.1088/1748-0221/15/10/P10017.

[Col20ah] CMS Collaboration. "Performance of the reconstruction and identification of high-momentum muons in proton-proton collisions at $\sqrt{s} = 13\ TeV$". In: *Journal of Instrumentation* 15.02 (Feb. 2020), P02027–P02027. ISSN: 1748-0221. DOI: 10.1088/1748-0221/15/02/p02027. URL: http://dx.doi.org/10.1088/1748-0221/15/02/P02027.

[Col20ai] CMS Collaboration. "Pileup mitigation at CMS in 13 TeV data". In: *JINST* (2020). DOI: https://doi.org/10.1088/1748-0221/15/09/P09018.

[Col20aj] CMS Collaboration. "Reconstruction of signal amplitudes in the CMS electromagnetic calorimeter in the presence of overlapping proton-proton interactions". In: *JINST* (2020). DOI: https://10.1088/1748-0221/15/10/P10002.

[Col20ak] CMS Collaboration. "Running of the top quark mass from proton-proton collisions at $\sqrt{s} = 13\ TeV$". In: *PLB 803 (2020) 135263* (2020). DOI: https://doi:10.1016/j.physletb.2020.135263, arXiv:1909.09193.

[Col20al] CMS Collaboration. "Search for a heavy Higgs boson decaying to a pair of W bosons in proton-proton collisions at $\sqrt{s} = 13\ TeV$". In: *Journal of High Energy Physics* 2020.3 (Mar. 2020). ISSN: 1029-8479. DOI: 10.1007/jhep03(2020)034. URL: http://dx.doi.org/10.1007/JHEP03(2020)034.

[Col20am] CMS Collaboration. "Search for a heavy pseudoscalar Higgs boson decaying into a 125 GeV Higgs boson and a Z boson in final states with two tau and two light leptons at $\sqrt{s} = 13\ TeV$". In: *JHEP 03 (2020) 065* (2020). DOI: https://doi:10.1007/JHEP03(2020)065,arXiv:1910.11634.

[Col20an] CMS Collaboration. "Search for a light charged Higgs boson in the channel in proton-proton collisions at $\sqrt{s} = 13\ TeV$". In: *PRD* (2020). DOI: https://doi:10.1103/PhysRevD.102.072001.

[Col20ao] CMS Collaboration. "Search for a light pseudoscalar Higgs boson in the boosted final state in proton-proton collisions at $\sqrt{s} = 13\ TeV$". In: *JHEP* (2020). DOI: https://doi:10.1007/JHEP08(2020)139.

[Col20ap] CMS Collaboration. "Search for a Narrow Resonance Lighter than 200 GeV Decaying to a Pair of Muons in Proton-Proton Collisions at $\sqrt{s} = 13\ TeV$". In: *Physical Review Letters* 124.13 (Apr. 2020). ISSN: 1079-7114. DOI: 10.1103/physrevlett.124.131802. URL: http://dx.doi.org/10.1103/PhysRevLett.124.131802.

[Col20aq] CMS Collaboration. "Search for an excited lepton that decays via a contact interaction to a lepton and two jets in proton-proton collisions at $\sqrt{(s)} = 13\ TeV$". In: *JHEP* (2020). DOI: https://doi.org/10.1007/JHEP05(2020)052.

[Col20ar] CMS Collaboration. "Search for charged Higgs bosons decaying into a top and a bottom quark in the all-jet final state of pp collisions at $\sqrt{(s)} = 13\ TeV$". In: *JHEP* (2020). DOI: https://doi.org/10.1007/JHEP07(2020)126.

[Col20as] CMS Collaboration. "Search for dijet resonances using events with three jets in proton-proton collisions at $\sqrt{s} = 13\ TeV$". In: *PLB 805 (2020) 135448* (2020). DOI: https://doi:10.1016/j.physletb.2020.135448,arXiv:1911.03761.

[Col20at] CMS Collaboration. "Search for direct top squark pair production in events with one lepton, jets, and missing transverse momentum at 13 TeV with the CMS experiment". In: *JHEP* (2020). DOI: https://doi.org/10.1007/JHEP05(2020)032.

[Col20au] CMS Collaboration. "Search for disappearing tracks in proton-proton collisions at $\sqrt{s} = 13\ TeV$". In: *PLB* (2020). DOI: https://doi:10.1016/j.physletb.2020.135502.

[Col20av] CMS Collaboration. "Search for high mass dijet resonances with a new background prediction method in proton-proton collisions at $\sqrt{s} = 13\ TeV$". In: *Journal of High Energy Physics* 2020.5 (May 2020). ISSN: 1029-8479. DOI: 10.1007/jhep05(2020)033. URL: http://dx.doi.org/10.1007/JHEP05(2020)033.

[Col20aw] CMS Collaboration. "Search for lepton flavour violating decays of a neutral heavy Higgs boson to
$mu\tau$ and eτ in proton-proton collisions at $\sqrt{s} = 13\ TeV$". In: *Journal of High Energy Physics* 2020.3 (Mar. 2020). ISSN: 1029-8479. DOI: 10.1007/jhep03(2020)103. URL: http://dx.doi.org/10.1007/JHEP03(2020)103.

[Col20ax] CMS Collaboration. "Search for new neutral Higgs bosons through the $H \to ZA \to l^+l^-bb^-$ process in pp collisions at $\sqrt{s} = 13\ TeV$". In: *JHEP 03 (2020) 055* (2020). DOI: https://doi:10.1007/JHEP03(2020)055,arXiv:1911.03781.

[Col20ay] CMS Collaboration. "Search for physics beyond the standard model in events with jets and two same-sign or at least three charged leptons in proton-proton collisions at $\sqrt{(s)} = 13\ TeV$". In: *EPJC* (2020). DOI: https://doi.org/10.1140/epjc/s10052-020-8168-3.

[Col20az] CMS Collaboration. "Search for physics beyond the standard model in multilepton final states in proton-proton collisions at $\sqrt{s} = 13\ TeV$". In: *Journal of High Energy Physics* 2020.3 (Mar. 2020). ISSN: 1029-8479. DOI: 10.1007/jhep03(2020)051. URL: http://dx.doi.org/10.1007/JHEP03(2020)051.

[Col20ba] CMS Collaboration. "Search for resonant pair production of Higgs bosons in the bbZZ channel in proton-proton collisions at $\sqrt{s} = 13\ TeV$". In: *PRD* (2020). DOI: https://doi:10.1103/PhysRevD.102.032003.

[Col20bb] CMS Collaboration. "Search for supersymmetry in pp collisions at s=13TeV with $137 fb^{-1}$ in final states with a single lepton using the sum of masses of large-radius jets". In: *Physical Review D* 101.5 (Mar. 2020). ISSN: 2470-0029. DOI: 10.1103/physrevd.101.052010. URL: http://dx.doi.org/10.1103/PhysRevD.101.052010.

[Col20bc] CMS Collaboration. "Search for supersymmetry with a compressed mass spectrum in events with a soft τ lepton, a highly energetic jet, and large missing transverse momentum in proton-proton collisions at $\sqrt{s} = 13\ TeV$". In: *PRL 124 (2020) 041803* (2020). DOI: https://doi:10.1103/PhysRevLett.124.041803,arXiv:1910.01185.

[Col20bd] CMS Collaboration. "Search for top squark pair production in a final state with two tau leptons in proton-proton collisions at $\sqrt{s} = 13\ TeV$". In: *JHEP 02 (2020) 015* (2020). DOI: https://doi:10.1007/JHEP02(2020)015,arXiv:1910.12932.

[Col20be] CMS Collaboration. "Strange hadron production in pp and pPb collisions at $\sqrt{S_{NN}} = 5.02\ TeV$". In: *PRC 101 (2020) 064906* (2020). DOI: https://doi.10.1103/PhysRevC.101.064906, arXiv:1910.04812.

[Col20bf] CMS Collaboration. "Studies of charm quark diffusion inside jets using PbPb and pp collisions at $\sqrt{S_{NN}} = 5.02\ TeV$". In: *PRL 125 (2020) 102001* (2020). DOI: https://doi:10.1103/PhysRevLett.125.102001,arXiv:1911.01461.

[Col20bg] CMS Collaboration. "Study of excited Λ_b^0 states decaying to $\Lambda_b^0\pi^+\pi^-$ in proton-proton collisions at $\sqrt{(s)} = 13\ TeV$". In: *PLB* (2020). DOI: https://doi.org/10.1016/j.physletb.2020.135345.

[Col20bh] CMS Collaboration. "Study of J/ψ meson production from jet fragmentation in pp collisions at $\sqrt{s} = 8\ TeV$". In: *PLB 804 (2020) 135409* (2020). DOI: https://doi:10.1016/j.physletb.2020.135409,arXiv:1910.01686.

[Col20bi] CMS Collaboration. "The production of isolated photons in PbPb and pp collisions at $\sqrt{s} = 5.02\ TeV$". In: *JHEP* (2020). DOI: https://doi:10.1007/JHEP07(2020)116.

[PL20] A. Kyriakis P. Assiouras P. Asenov and D. Loukas. "Fast calculation of capacitances in silicon sensors with 3D and 2D numerical solutions of the Laplace's equation and comparison with experimental data and TCAD simulations". In: *J. Inst. 15 P11034* (2020). DOI: https://doi.org/10.1088/1748-0221/15/11/P11034.

High Energy Physics - Theory

[Axe+20] Minos Axenides et al. "M-theory as a dynamical system generator". In: July 2020. DOI: 10.1007/978-3-030-70795-8. arXiv: 2007.07028 [hep-th].

[BPS20] Hrachya Babujian, Rubik Poghossian, and George Savvidy. "Correlation Functions of Quantum Artin System". In: *Universe* 6.7 (2020), p. 91. DOI: 10.3390/universe6070091.

[De +20] Marius De Leeuw et al. "Spin Chain Overlaps and the Twisted Yangian". In: *JHEP* 01 (2020), p. 176. DOI: 10.1007/JHEP01(2020)176. arXiv: 1912.09338 [hep-th].

[KMP20] Dimitrios Katsinis, Ioannis Mitsoulas, and Georgios Pastras. "Geometric flow description of minimal surfaces". In: *Phys. Rev. D* 101.8 (2020), p. 086015. DOI: 10.1103/PhysRevD.101.086015. arXiv: 1910.06680 [hep-th].

[KP20] Dimitrios Katsinis and Georgios Pastras. "An Inverse Mass Expansion for the Mutual Information in Free Scalar QFT at Finite Temperature". In: *JHEP* 02 (2020), p. 091. DOI: 10.1007/JHEP02(2020)091. arXiv: 1907.08508 [hep-th].

[Kat+20] Dimitrios Katsinis et al. "Dressed minimal surfaces in AdS_4". In: *JHEP* 11 (2020), p. 128. DOI: 10.1007/JHEP11(2020)128. arXiv: 2007.10922 [hep-th].

[KS20a] Roland Kirschner and George Savvidy. "Parton Distribution Functions and Tensor Gluons". In: (May 2020). arXiv: 2005.09700 [hep-ph].

[KS20b] Roland Kirschner and George Savvidy. "Parton Distribution Functions and Tensorgluons". In: *Universe* 6.7 (2020), p. 88. DOI: 10.3390/universe6070088.

[Lin20] Georgios Linardopoulos. "Solving holographic defects". In: *PoS* CORFU2019 (2020), p. 141. DOI: 10.22323/1.376.0141. arXiv: 2005.02117 [hep-th].

[Sav20a] George Savvidy. "Discovery of Chromomagnetic Gluon Condensation". In: *PoS* CORFU2019 (2020), p. 162. DOI: 10.22323/1.376.0162.

[Sav20b] George Savvidy. "Extended Kolmogorov Entropy". In: (Apr. 2020). arXiv: 2004.13528 [math.DS].

[Sav20c] George Savvidy. "From Heisenberg–Euler Lagrangian to the discovery of Chromomagnetic Gluon Condensation". In: *Eur. Phys. J. C* 80.2 (2020), p. 165. DOI: 10.1140/epjc/s10052-020-7711-6. arXiv: 1910.00654 [hep-th].

[Sav20d] George Savvidy. "Maximally chaotic dynamical systems". In: *Annals Phys.* 421 (2020), p. 168274. DOI: 10.1016/j.aop.2020.168274.

[Sav20e] George Savvidy. "Maximally Chaotic Dynamical Systems of Anosov–Kolmogorov". In: *Phys. Part. Nucl.* 51.4 (2020), pp. 410–418. DOI: 10.1134/S1063779620040644. arXiv: 2001.01785 [hep-th].

[Sav20f] George Savvidy. "Yang-Mills Classical and Quantum Mechanics and Maximally Chaotic Dynamical Systems". In: (Jan. 2020). arXiv: 2001.04902 [hep-th].

Astroparticle Physics

[Aie+20a] S. Aiello et al. "Deep-sea deployment of the KM3NeT neutrino telescope detection units by self-unrolling". In: *JINST* 15.11 (2020), P11027. DOI: 10.1088/1748-0221/15/11/P11027. arXiv: 2007.16090 [astro-ph.IM].

[Aie+20b] S. Aiello et al. "Event reconstruction for KM3NeT/ORCA using convolutional neural networks". In: *JINST* 15.10 (2020), P10005. DOI: 10.1088/1748-0221/15/10/P10005. arXiv: 2004.08254 [astro-ph.IM].

[Aie+20c] S. Aiello et al. "gSeaGen: The KM3NeT GENIE-based code for neutrino telescopes". In: *Comput. Phys. Commun.* 256 (2020), p. 107477. DOI: 10.1016/j.cpc.2020.107477. arXiv: 2003.14040 [astro-ph.IM].

[Aie+20d] S. Aiello et al. "The Control Unit of the KM3NeT Data Acquisition System". In: *Comput. Phys. Commun.* 256 (2020), p. 107433. DOI: 10.1016/j.cpc.2020.107433. arXiv: 1910.00112 [astro-ph.IM].

[Hof+20] Jannik Hofestädt et al. “Atmospheric Neutrinos Detected with the First KM3NeT Detection Units of ARCA and ORCA”. In: *PoS* ICRC2019 (2020), p. 910. DOI: 10.22323/1.358.0910.

Nuclear Physics - Theory

[BSH20] Dennis Bonatsos, Hadi Sobhani, and Hassan Hassanabadi. “Shell model structure of proxy-SU(3) pairs of orbitals”. In: *The European Physical Journal Plus* 135.9 (Sept. 2020). DOI: 10.1140/epjp/s13360-020-00749-2.

[Bon+20] Dennis Bonatsos et al. “Parameter-free predictions for the collective deformation variables beta and gamma within the pseudo-SU(3) scheme”. In: *EPJ ST* 229 (Aug. 30, 2020), p. 2367. DOI: 10.1140/epjst/e2020-000034-3. arXiv: http://arxiv.org/abs/2009.00468v1 [nucl-th].

[Cas+20] R. F. Casten et al. “Simple new signature of structure in deformed nuclei: Distinguishing the nature of axial asymmetry”. In: *Physical Review C* 102.5 (Nov. 2020). DOI: 10.1103/physrevc.102.054310.

[Mar+20] Andriana Martinou et al. “Proxy SU(3) symmetry in the Shell Model basis”. In: *European Physical Journal A* 56.9 (2020), p. 239. DOI: 10.1140/epja/s10050-020-00239-0.

[Sob+20a] Hadi Sobhani et al. “Analytical study of the γ-unstable Bohr Hamiltonian with quasi-exactly solvable decatic potential”. In: *The European Physical Journal A* 56.2 (Feb. 2020). DOI: 10.1140/epja/s10050-020-00048-5.

[Sob+20b] Hadi Sobhani et al. “γ-Unstable Bohr Hamiltonian with sextic potential for odd-A nuclei”. In: *Nuclear Physics A* 1002 (Oct. 2020), p. 121956. DOI: 10.1016/j.nuclphysa.2020.121956.

Nuclear Physics - Experimental

[Bar+20] N. Pessoa Barradas et al. “International Atomic Energy Agency inter-comparison of particle induced gamma-ray emission codes for bulk samples”. English. In: *NUCLEAR INSTRUMENTS & METHODS IN PHYSICS RESEARCH SECTION B-BEAM INTERACTIONS WITH MATERIALS AND ATOMS* 468 (Apr. 2020), pp. 37–47. ISSN: 0168-583X. DOI: 10.1016/j.nimb.2020.02.019.

[Geo+20] E. Georgali et al. “Experimental study of the Ho-165(n, 2n) reaction: Cross section measurements for the population of the Ho-164 ground state and isomeric state from the threshold up to 20 MeV”. English. In: *PHYSICAL REVIEW C* 102.3 (Sept. 2020). ISSN: 0556-2813. DOI: 10.1103/PhysRevC.102.034610.

[May+20] M. Mayer et al. “Ion beam analysis of fusion plasma-facing materials and components: facilities and research challenges”. English. In: *NUCLEAR FUSION* 60.2 (Feb. 2020). ISSN: 0029-5515. DOI: 10.1088/1741-4326/ab5817.

[Tsa+20] P. Tsavalas et al. “Differential cross sections of the deuteron reactions on beryllium at energies and angles suitable for nuclear reaction analysis”. English. In: *NUCLEAR INSTRUMENTS & METHODS IN PHYSICS RESEARCH SECTION B-BEAM INTERACTIONS WITH MATERIALS AND ATOMS* 479 (Sept. 2020), pp. 205–210. ISSN: 0168-583X. DOI: 10.1016/j.nimb.2020.07.002.

X-Ray Spectrometry

[Alm+20] S.M. Almeida et al. “Ambient particulate matter source apportionment using receptor modelling in European and Central Asia urban areas”. In: *Environmental Pollution* 266 (2020). ISSN: 0269-7491. DOI: https://doi.org/10.1016/j.envpol.2020.115199.

[CKK20] Mateusz Czyzycki, Mike Kokkoris, and Andreas-Germanos Karydas. “A mathematical model for deep ion implantation depth profiling by synchrotron radiation grazing-incidence X-ray fluorescence spectrometry”. In: *Journal of Analytical Atomic Spectrometry* 35 (2020). DOI: 10.1039/D0JA00346H.

[Gre+20] Rebecca Grethe et al. “Micro-XRF analysis of silver decorations on Archaic helmets from Olympia”. In: *Archaeometry* 62 (2020). DOI: 10.1111/arcm.12561.

[Kau+20] Sandeep Kaur et al. “Measurements of mass attenuation coefficients for 51Sb over energy region 4 keV–14 keV using synchrotron radiation”. In: *Radiation Physics and Chemistry* 177 (2020). DOI: 10.1016/j.radphyschem.2020.109149.

[Kki+20] Eleni Kkiasmenou et al. “Macroscopic XRF imaging in unravelling polychromy on Mycenaean wallpaintings from the Palace of Nestor at Pylos”. In: *Journal of Archaeological Science: Reports* 29 (2020). DOI: 10.1016/j.jasrep.2019.102079.

[Lir+20] Ioannis Liritzis et al. “Characterization and provenance of ceramic artifacts and local clays from Late Mycenaean Kastrouli (Greece) by means of p-XRF screening and statistical analysis”. In: *Journal of Cultural Heritage* 46 (2020). DOI: 10.1016/j.culher.2020.06.004.

[Pap+20] G.P. Papageorgiou et al. “Controlled synthesis of periodic arrays of ZnO nanostructures combining e-beam lithography and solution-based processes leveraged by micro X-ray fluorescence spectroscopy”. In: *Micro and Nano Engineering* 8 (2020). DOI: 10.1016/j.mne.2020.100063.

[Pin+20] Fani Pinakidou et al. “Transition metal chromophores in glass beads of the classical and Hellenistic period: Bonding environment and colouring role”. In: *Spectrochimica Acta Part B: Atomic Spectroscopy* 171 (2020). DOI: 10.1016/j.sab.2020.105928.

[San+20] Kaushik Sanyal et al. “Direct non-destructive total reflection X-ray fluorescence elemental determinations in zirconium alloy samples”. In: *Journal of Synchrotron Radiation* 27 (2020). DOI: 10.1107/S1600577520009364.

[Sha+20] Abdallah Shaltout et al. “Elemental composition and source apportionment of atmospheric aerosols collected from urban and residential areas of Jordan using multi-secondary targets energy dispersive X-ray fluorescence”. In: *Spectrochimica Acta Part B: Atomic Spectroscopy* 170 (2020). DOI: 10.1016/j.sab.2020.105900.